INFORMATION TO USERS

Order Number 9222396

Analysis of air and sea physical properties and surface fluxes using a combination of *in situ* and SEASAT data

Legler, David M., Ph.D.

The Florida State University, 1992

U·M·I

THE FLORIDA STATE UNIVERSITY

COLLEGE OF ARTS AND SCIENCES

ANALYSIS OF AIR AND SEA PHYSICAL PROPERTIES AND SURFACE

FLUXES USING A COMBINATION OF IN-SITU AND SEASAT DATA
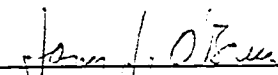
By

DAVID M. LEGLER
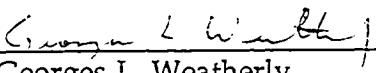
A Dissertation submitted to the Department of
Meteorology in partial fulfillment of the requirements
for the degree of Doctor of Philosophy

Degree Awarded:

Spring Semester, 1992
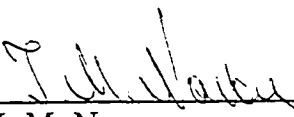
The members of the committee approve the dissertation of Mr. David

M. Legler defended on February 21, 1992.
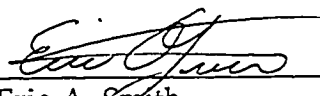
James J. O'Brien
Professor Directing Dissertation
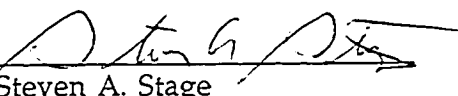
Georges L. Weatherly
Outside Committee Member

I. M. Navon
Committee Member

Eric A. Smith
Committee Member

Steven A. Stage
Committee Member

To Nan and Matthew

Acknowledgements

took interest in me 11 years ago and never gave up on convincing me of the importance of advanced degrees. He has given me unparalleled opportunities to develop and mature into a research scientist. I offer him my sincerest gratitude and admiration.

Finally, throughout this long and often difficult process, my family has always been there offering encouragement and support. They have been my most dedicated cheering section. To them I owe the greatest amount of thanks and love.

Table of Contents

List of Tables

List of Figures

Abstract

An objective technique which produces regularly spaced fields of winds, temperatures, humidity, wind stress and sensible and latent heat fluxes is developed. It combines in-situ Volunteer Observing Ship (VOS) data and remotely sensed data from SEASAT during the analysis period, July 7 - October 10, 1978 for the north Atlantic. The objective technique is a variational method which reduces a set of several constraints expressing closeness to input data, climatology and kinematics. Analysis results are presented for monthly and 5-day periods during the analysis period.

Seasonal (3 month) means of temperature, humidity, and flux determined by the monthly and 5-day results are comparable. However, 5-day wind results had much smaller errors than the monthly mean winds averaged over the 3-month period.

Variability of the 5-day results indicates high variability of temperatures, humidity, and heat fluxes in the vicinity of the Gulf Stream. Sea surface temperature (SST) variability is high in the eastern Atlantic and is coupled to wind driven ocean variability in the region.

Heat fluxes are coupled to and determined by various parameters. The variations for both sensible and latent heat fluxes in the extra-tropics are determined by the position and strength of the circulation of the semi-permanent high pressure system. Some evidence is also found to indicate

dependence of SST on latent heat. In the tropics, the heat fluxes are determined by a combination of factors, including zonal wind and SST.

Estimates of errors due to insufficient sampling and random data are presented for the monthly results. The sampling and random errors in wind stress are in the range of 10% - 20% of the mean values. For the sensible and latent heat fluxes, the sampling errors are about half of those attributable to random errors. Because of the difference operator used in diagnosing heat fluxes, these fluxes are found to be more sensitive to the accuracies of temperatures and humidity than accuracies of winds.

1. INTRODUCTION

The exchange of heat and momentum between the ocean and the atmosphere has been the subject of much study. Researchers have focused on estimating the amount of energy passing across this boundary in order to understand more fully the dynamic and thermodynamic variability of these fluids. In the summertime (July-August) the solar input into the oceans exceeds 200 W m^{-2} in northern extratropical regions. The ocean cools partly due to latent heat release (evaporation) on the order of 100 W m^{-2} with sensible heat flux adding or removing 10 W m^{-2}. Atmospheric wind forcing imparts enough momentum on the ocean to drive large upper-ocean currents such as the Gulf Stream and affects weather systems globally (El Niño for example). The question remains however: what are the spatial and temporal variability of these fluxes: wind stress, latent and sensible heat; on scales less than one season? Are there enough data to study successfully these time scales? How will the availability of remotely sensed data make an impact? These questions are the motivation behind this research. It is expected that by analyzing objectively all available data in the North Atlantic Ocean basin during a trial 95-day period, some insight can be obtained into these concerns.

Wind stress is the primary forcing mechanism for ocean dynamics. For the North Atlantic Ocean, the stress is dominated by an annual signal as suggested by Thompson, et al. (1983) and by a series of papers examining

1

derivative fields of the wind stress (Barnier (1986); Ehret and O'Brien (1989); Mac Veigh, et al. (1986); and Rienecker and Ehret (1988)). Good spatial resolution wind information is particularly important in the mid-latitudes where the internal radius of deformation is ~50 km. The role of the winds in formation of eddies remains unresolved (Schmitz, et al. (1983)).

Sensible and latent heat fluxes comprise a large part of the ocean-atmosphere heat exchange system, but models such as Semtner and Chervin (1989) are constrained by a lack of adequate surface heat flux information and instead constrain surface and interior model temperature and salinity values to climatological values (Levitus (1982)). We need better estimates of surface air-sea fluxes and some estimate of their uncertainty in order to better ascertain their role in upper ocean thermodynamics (as well as in atmospheric thermodynamics). The seasonal cycles of temperature and salinity are very large in the extratropics (Levitus (1984)), and because the thermocline is deep in mid-latitudes, variability in the mixed layer is more responsive to local atmosphere forcings. Frankignoul and Reynolds (1983) and Haney (1985) concluded that most SST anomalies in mid-latitudes are generated by local anomalous atmosphere forcings. However, in the tropics, where the thermocline is not as deep, remote forcing plays a more dominant role in mixed-layer characteristics (Schopf and Cane (1983)).

Some attempts have been made to examine the variability of the wind/heat flux fields on synoptic scales for short periods(Willebrand (1978)) and at high temporal resolution at single points (Bean and Reinking (1978) and Seguin and Kidwell (1979)), but until recently, there were no information on fields with sufficient resolution in space and time to address full temporal and spatial synoptic scale fluxes. Simonot and LeTreut (1987)

investigated the quality of daily surface heat fluxes produced by the European Centre for Medium range Weather Forecasting (ECMWF) prediction model for the period 1983-1985. Although these fluxes had several inconsistencies and a bias in the latent heat flux, the authors concluded the fluxes were useful as thermodynamic forcing for ocean models. An analysis of a more recent version of the ECMWF flux fields with higher resolution and improved parameterizations determined that there were indeed improvements in the latent and net heat flux, but that the short-wave flux was degraded (Barnier, et al. (1989)).

National meteorological center model produced fluxes, like the ECMWF fields, have large inter-model variations Lambert and Boer (1988) compared estimates of climatological winter and summer ocean-atmosphere fluxes from 12 meteorological centers' model results. Inter-comparison of twelve different products projected onto a common grid provided an estimate of how well the models as a whole replicate the known structure of climatology. Zonally averaged inter-model standard deviation of surface wind stress components and the climatology from Han and Lee (1981) indicate the model southern hemisphere stresses are weaker than climatology, especially in the southern summer. Variability in the tropics according to the models is too small. Spatial maps of inter-model stress variations show the climatological estimates and the model mean values differ widely in several locations and climate zones.

Trenberth and Olson (1988) found significant disagreement between NMC and ECMWF zonal averages of the east-west wind components over the oceans for 1979-1986. In the Northern Hemisphere wintertime, the RMS differences were 4-5 m s^{-1} while in the summertime these differences were

2 m s^{-1}. However, there was a marked improvement in the comparison during the last year of the analysis, 1986, possibly reflecting model improvements or perhaps an increase in similarity between the models.

Climatological fluxes for the North Atlantic have been established by several people (Hantel (1971); Esbensen and Kushnir (1981); Leetma and Bunker (1978); Bunker (1976); Han and Lee (1981); Hsiung (1986); Isemer and Hasse (1987); Oberhuber (1988); Hastenrath and Lamb (1977)). Each revision attempted an improvement in resolution or perhaps used a more sophisticated or more contemporary flux parameterization. For example, Isemer and Hasse (1987) updated the original Bunker atlas data by adjusting the bulk formula coefficients to achieve similarity of the net annual meridional oceanic heat transport as calculated from the fluxes and wind stress to that calculated by direct methods.

Each of these climatologies qualitatively agrees on the seasonal cycle of the North Atlantic fluxes, but differs (sometimes significantly) on the quantitative values. Each relies primarily on the same data base; the ship-of-opportunity or Volunteer Observing Ship (VOS) data collection.

The VOS data set is the only available set of in-situ surface marine observations that includes all standard meteorological variables. Since merchant shipping is still heavily used to transport goods across the oceans, most of the Northern Hemisphere is fairly well sampled (see section 2). It does not, however, readily lend itself for use in research of sub-monthly variability. There are errors of various types including instrument errors, measurement method errors, and transmission errors. Insufficient numbers of reports to calculate mean values can also lead to significant aliasing due to under-sampling the expected variability (Legler (1991)). Description of the

systematic errors in measurement, recording and other sources in VOS winds are delineated in Pierson (1990) who suggests that VOS data are vastly inferior to buoy data in determining synoptic scale wind fields. None the less, there have been VOS-based products (Goldenberg and O'Brien (1981); Legler and O'Brien (1985); Legler and O'Brien (1988); Picaut, et al. (1985)) which have been successfully used in numerous papers (Busalacchi and O'Brien (1980); Busalacchi and O'Brien (1981); Busalacchi, et al. (1983); Inoue and O'Brien (1984); Schott and Böning (1991)) indicating there is useful information in this type of data on monthly scales.

In addition to in-situ data from ships and buoys, surface winds and SST data are available from satellites for specific time periods. Surface air-temperature and surface humidity are not obtainable via remote sensing because vertical profiles of temperature and humidity returned by satellite instruments have insufficient vertical resolution in the boundary layer.

I will make use of surface wind speeds, vector winds, and SST available during the SEASAT mission: July 7 - October 10, 1978 (see special issues of Journal of Geophysical Research for collections of papers relating to SEASAT mission: Volume 87, April 30, 1982; and Volume 88, February 28, 1983).

The microwave scatterometer (hereafter referred to as SASS) on SEASAT was capable of determining vector winds at 19.5 meters height accurate to $\pm$ 2 m s^{-1} and $\pm20°$ (O'Brien, et al. (1982)). The SASS data have proven to be effective in enhancing NWP models (Anderson, et al. (1991)). Additionally, SASS data have also aided in analysis of intense cyclogenic storms such as the QE II storm in the N. Atlantic, September 9-11, 1978 (Harlan and O'Brien (1986)). Other instruments, such as the scanning

multichannel microwave radiometer (SMMR), and the microwave altimeter (ALT), provide estimates of wind speed but not direction (some efforts are underway to assign directions to these scalar values using model wind direction - Atlas, et al. (1991)).

SST values from infrared and microwave imagers such as the Advanced Very High Resolution Radiometer (AVHRR) or the SMMR on board SEASAT, are accurate to about 0.5° to 1.2°C but are biased due to atmospheric contaminants (Bernstein and Chelton (1985)). Additionally, remotely sensed SST are biased cold because they return essentially the skin temperatures which reflects evaporative cooling (Schluessel, et al. (1990)).

Direct determination of surface humidity (Q) has never been successfully accomplished using satellite data, but there have been alternative methods proposed. Liu and Niiler (1984) (and subsequently Liu (1986)) proposed and tested a method whereby an empirical correlation between total columnar water vapor W (precipitable water), which is available from satellite radiometers, and Q, was established using radiosonde reports from dozens of globally distributed locations. It allows for *monthly* mean Q from satellite W but does not hold for shorter time periods.

Remotely sensed data from SEASAT will supplement VOS data in an objective analysis technique to formulate monthly and 5-day mean fields of winds, temperatures, humidity, wind stress, and sensible and latent heat flux over the north Atlantic. By using this combination of VOS and remotely sensed data to augment the spatial coverage and data density, it will be demonstrated that it is possible to glean useful flux information on scales of one month or less.

It will be found that altimeter winds from SEASAT are detrimental to the analysis scheme; however, data from other instruments is beneficial. The monthly results are found to be only slightly better than the 5-day results for temperatures, humidity, and heat fluxes. The winds and wind stress are better in the 5-day results because of the nature of wind averaging. The results of the objective analysis compare favorably with evaluation data which include VOS means at locations that are well sampled, and an Ocean Weather Ship data set. Variability of the 5-day results agrees well with established patterns and also displays some intra-monthly variability patterns that have not been quantified before. Heat fluxes in the North Atlantic are correlated to the movement of the semi-permanent Bermuda High which advects air of one particular characteristic (i.e. wet, dry, cold, warm) into a regime of opposite conditions. In the tropics, the SST tends to drive the heat fluxes, but in the mid-latitudes off N. America and near Spain, there is evidence that latent heat plays some role in determining SST. Error fields are presented for the monthly results. Sampling errors are larger in wind stress than in heat flux.

Several data sets and the bulk method are described first in section 2. The variational objective analysis scheme is introduced in section 3. Sensitivity of the scheme and results of the objective analysis (section 4) are discussed, and a detailed look at the variability of the results offers insight into the intra-month variability of the surface fluxes (section 5). Uncertainties in the winds, temperatures, humidity, and fluxes due to random and sampling errors are shown to be different than previously thought(section 6). Finally, a summary and conclusions section will recap the findings (section 7).

2. DATA SETS

2.1 VOS and SEASAT Data

The period of July 7 - October 10, 1978 marked the advent of remote sensing for oceanography. SEASAT was launched June 27, 1978, and even though a short circuit rendered it inoperative after 100 days, this is the only time period when remotely sensed ocean wind vectors are available for analysis. There are also SST and wind speed data from additional instruments on board. In order to examine the possibility of using in-situ and remotely sensed data jointly to study flux variability, the North Atlantic (Equator to 60°N, 80°W to 0°E) region will be the focus of this study because of the higher density of VOS data. Data from the various sources and the method used to calculate the ocean-atmosphere surface fluxes will be described in this section.

The VOS data, as already described, are the set of all available surface meteorological observations for the period July 7 - October 10, 1978 in the N. Atlantic, Fig. 1. These number approximately 150,000 for this particular time period and reflect higher sampling in the dominant shipping lanes in the northern Atlantic basin (40°-60°N) and along the continental coasts as compared to the data coverage in the tropical region (Equator to 30°N). The VOS sea surface temperature (SST), air temperature (AT), dew point depression (DPD), and eastward and northward wind components (U, V) were obtained from the CMR5 COADS (Comprehensive Ocean Atmosphere

8
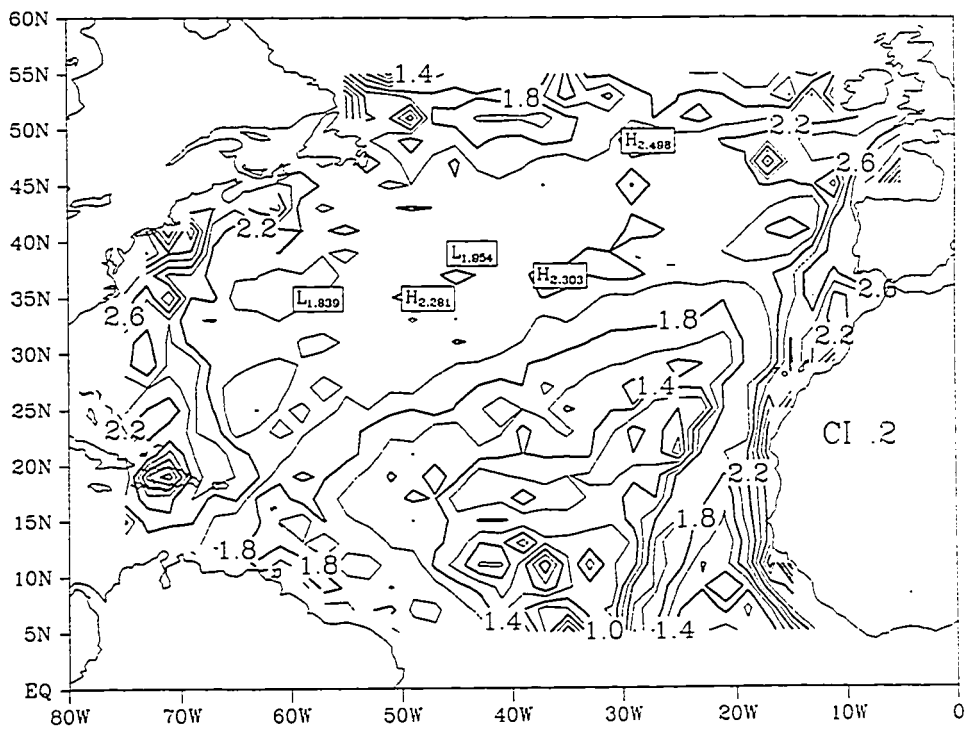
Figure 1.   Log 10 of the total number of VOS observations available for July 7 - October 10, 1978.

Data Set) (Slutz, et al. (1985)). All landlocked as well as flagged data outside a wide envelope of variability were eliminated (see Slutz, et al. (1985), Supplement C). Additionally, the VOS data were scanned to fall within the following guidelines: SST, -5° to 40° C; AT, -10° to 40° C; dew point temperature, -10° to 40° C; wind speed, 0 to 40 m s^{-1}; and U,V, -40 to 40 m s^{-1}. In 5 degree latitude-longitude boxes, values outside the 95-day mean ± 3σ were removed. Many VOS reports were not complete, and less than 100% of the reports had observations for any particular variable: SST - 81%, AT - 98%, DPD - 64%, U,V - 94%. Specific humidity for air at some height, Q, and at the sea surface, Qs, were calculated using standard thermodynamic approximations (see Liu, et al. (1979)). Summarizing, the total number of reports removed for each variable was generally less than 2%.

The remotely sensed data all originate from the various sensors on SEASAT. The SMMR instrument is described in Njoku, et al. (1980). SST values are on a 149-km. grid. Because of the sensitivity of specific frequency bands used on this instrument, rain in the field of view contaminates the SST values; likewise, problems exist for SMMR SST data within 600 km of land and for those values when the sun glint angle was less than 20° (Lipes (Ed.) (1980)) - all of these questionable data were not used. In a typical 30-day period, 15,000 SMMR SST observations are available, but are limited to those regions at least 600 km from land.

The SMMR instrument also returns 19.5 m height wind speed values (neutrally stable) on an 85 km. grid spacing. All data at least 600 km. from land with no sun glint angle less than 20° and no rain detection are used (same reasoning as previously discussed; see Wentz, et al. (1982)). Coverage

is better (due to increased resolution) with 50,000 observations in a typical 30-day period.

The SEASAT altimeter also has the capability of estimating the 19.5 m height neutral wind speed at the nadir location. The size of the cell is quite small: 3-30 km depending on sea state (see Townsend (1980) for a technical description). Coverage is 90 -150 thousand observations in a typical 30-day period.

Lastly, the SEASAT-A Satellite Scatterometer (SASS) provides neutrally stable wind *vectors* at 19.5 m height over the open ocean on a 100 km grid with dual swaths on either side of the satellite path: 200 - 800 km off-nadir. The original SASS vectors had a variety of systematic errors due to incorrect model parameterization and were biased high (Wentz, et al. (1984); Wentz (1986)). Additionally, the SASS vectors were actually a collection of up to four wind vectors for every SASS cell, each vector with nearly the same magnitude, but different directions, or 'aliases', with a recommended alias selection. Thus it was necessary to select the 'best' alias. The data used in this study are the reprocessed SASS data from Wentz (1986) with aliases chosen by the method presented in Kalnay and Atlas (1986).

Correlations between the SASS and VOS winds generally exceeded 0.75 except in the northwest Atlantic; 55°W, 40°N where the eastward wind correlations were considerably less than 0.5. No reason could be found for this regional discrepancy.

It is well documented that remotely sensed data tend to have errors in them that are not random in nature. SEASAT data are no exception. The SMMR SST was biased high by 0.5 to 0.75°C according to most reports (Lipes, et al. (1979); Bernstein (1982); Bernstein and Morris (1983); Njoku, et al.

(1980)). In reaffirming this, the SMMR SST values were scanned to match ship data within ±30 minutes and within 100 km. If more than one SMMR SST value were within this window, they were averaged together to form a super-observation; 890 such pairs of data were found and examined, Fig. 2. The mean bias (bias is hereafter defined as the in-situ mean - satellite mean) was -0.72°C and had a 1 standard deviation about this mean of 2.27°C. SMMR SST was particularly higher than comparable ship observations in the range cooler than 20°C. Correlations between the bias pair data and various atmospheric conditions as well as the distance between data pair points and time difference were low and did not explain any significant portion of the bias. There was some variation in time of the bias values - the maximum bias occurred in the middle third of the mission (bias=-1.2°C), which agrees with findings by Bernstein and Morris (1983) in which they attribute this temporal variation of SST bias to strong summertime surface warming which can be detected by the surface sensing SMMR, but not by ordinary ship intake temperature sensors which are located a few meters below the water line. SMMR SST comparison to co-located SST data from Ocean Weather Ship (OWS)-L at 57°N, 20°W (see Diaz, et al. (1987) for additional info on OWS data) gave a mean bias of -2.0°C; this location is an area of cooler SST, hence higher bias values as already mentioned.

SMMR wind speeds are also biased high, -2.1 m s⁻¹ with a 3.4 m s⁻¹ standard deviation about the mean. The bias is highest at low wind speeds, (less than 10 m s⁻¹), Fig. 3, which is similar to findings in Lipes (1982) particularly to their comparison of SMMR to JASIN data in the Gulf of Mexico. Additionally, there is a time dependency noted in the SMMR wind speed bias indicating a decreasing bias with mission duration. Explanation of
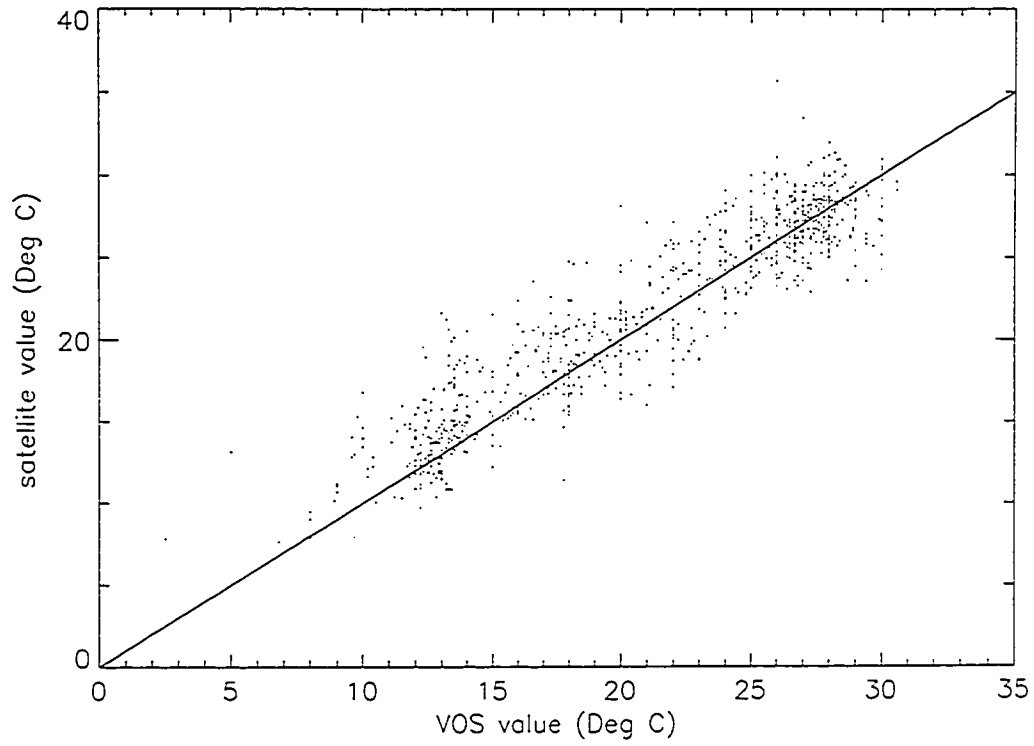
Figure 2.   Coincident VOS SST and SMMR SST superobservation values
            for the analysis period. The solid line indicates perfect
            agreement.
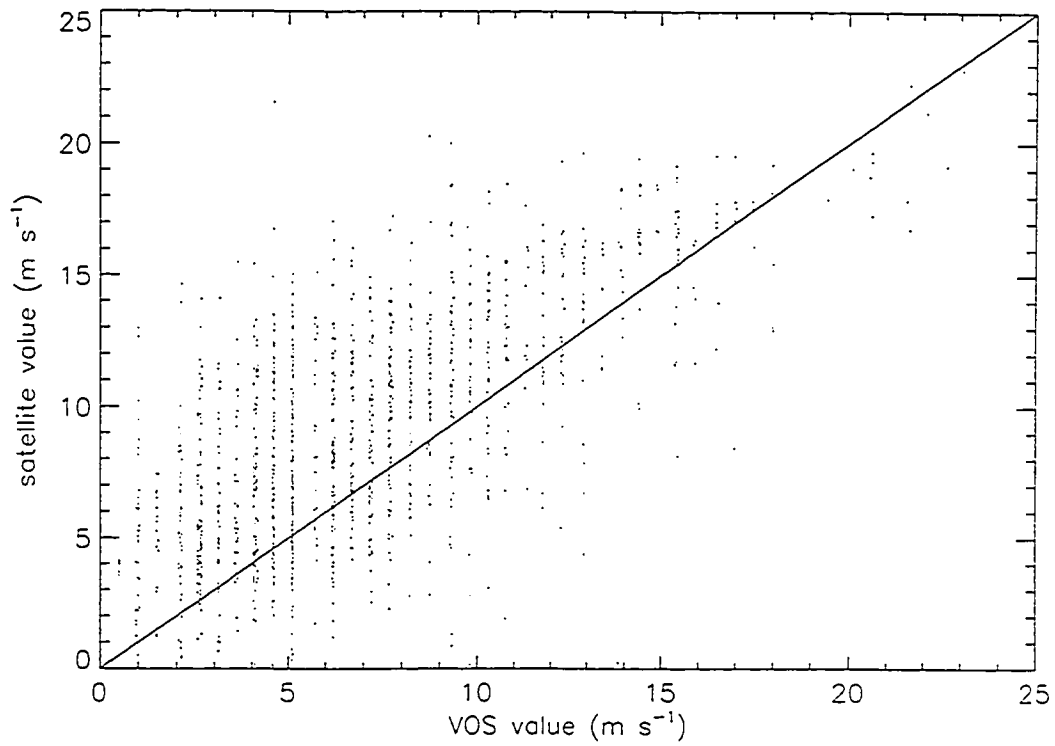
Figure 3. Coincident VOS wind speed and SMMR wind speed superobservation values for the analysis period. The solid line indicates perfect agreement.

this by an increase in mean wind speed and therefore a bias decrease is not possible since the mean wind speed increases only 0.5 m s⁻¹ - not enough to generate such a large improvement in the bias values.

Altimeter winds had the poorest quality of all the SEASAT wind products. The mean bias was 0.4 m s⁻¹ with a standard deviation of 2.7 m s⁻¹, but the bias is a very strong function of wind speed (Fig. 4) indicating overestimation of low wind speeds and underestimation of high wind speeds. The bias scatter increased with latitude due to the higher wind speeds at higher latitudes. Wentz, et al. (1982) found an ALT bias of about +1.6 m s⁻¹ to in-situ measurements and a 3.3 m s⁻¹ bias to SASS wind speeds (ALT wind speeds too low). Additionally Chelton and McCabe (1985) found similar results, but looked only at speeds greater than 4 m s⁻¹. As noted in Chelton, et al. (1981) and Chelton and McCabe (1985), the altimeter wind speed algorithm produced a non-physical histogram of wind speeds because of an incorrect processing algorithm. The SEASAT altimeter wind speed measurements are very suspect.

For the Wentz processed SASS data used in this study, the mean bias for both the U and V wind components was 0 with a standard deviation of 2.9 m s⁻¹, Fig. 5. There were no significant trends in the bias with time nor any correlation between the bias and the tested parameters such as temperature, humidity, etc., but there was a distinct difference noted when VOS reports indicated calm winds - SASS winds were sometimes remarkably different from calm.

For each of the satellite data sets, the mean bias for the entire time period, as detailed in Table 1, was subtracted from each satellite data value.
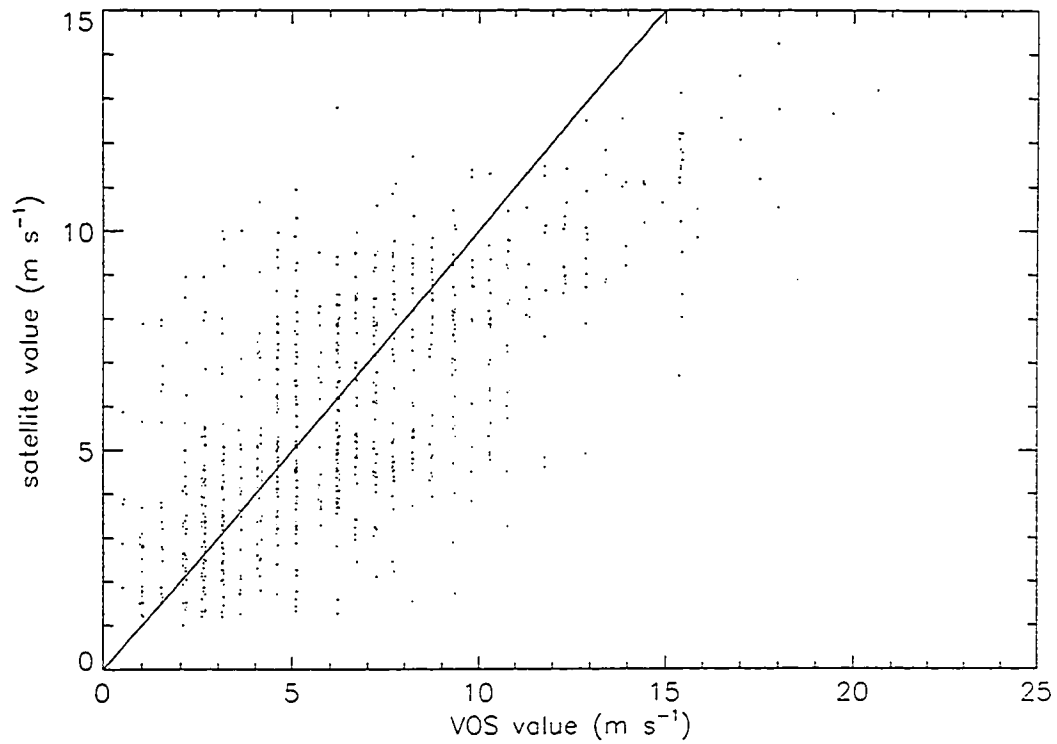
Figure 4.   Coincident VOS wind speed and ALT wind speed superobservation values for the analysis period. The solid line indicates perfect agreement.
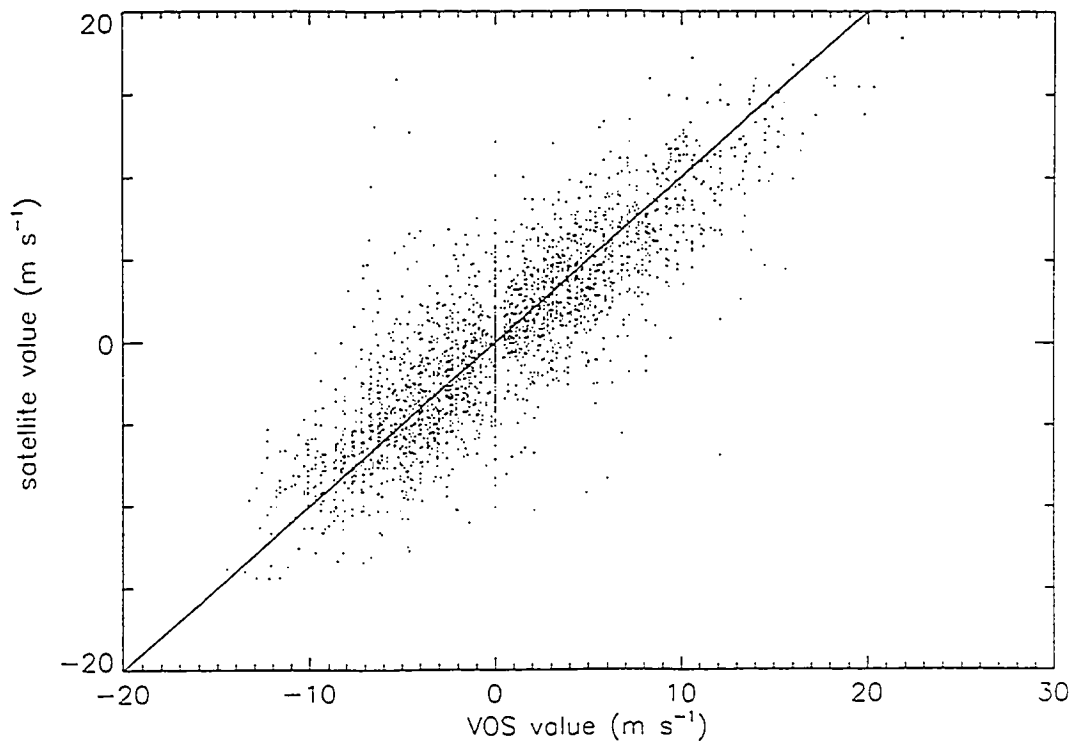
Figure 5.   Coincident VOS east-west wind component and SASS east-west wind component superobservation values for the analysis period. The solid line indicates perfect agreement.

Table 1.　Results of matching and mean bias calculation between remotely sensed and VOS data in the North Atlantic for the analysis period.

	Number of matches of VOS data within 100 km and ±30 minutes of remotely sensed superobservation	Mean bias correction added to each satellite value
SMMR SST	890	-0.72°C
SMMR Wind Speed	1394	-2.19 m s⁻¹
ALT Wind Speed	858	+0.40 m s⁻¹
SASS Wind Vector	2681	+0.00 m s⁻¹

For all vector wind data, individual winds were converted to pseudo-stress (wind component times the wind speed) before processing further.

2.2 Flux Calculation

It is most practical to use the bulk aerodynamic formula to calculate surface fluxes of momentum and sensible and latent heat. Other techniques such as the dissipation method are being examined, but cannot be used retroactively (Large and Businger (1988)). The bulk method is reviewed in Geernaert (1990) and can briefly be written as follows. The fluxes are a function of wind, temperature, and humidity as well as the bulk exchange coefficients. All are a strong function of height. The bulk formula are:

$$\tau_x = \rho C_d uW, \quad \tau_y = \rho C_d vW$$

$$H = \rho C_h C_P W (SST - AT)$$

$$E = \rho C_e LW (Q_s - Q)$$

τ_x	Eastward Wind Stress	Q	Specific Humidity
τ_y	Northward Wind Stress	Q_s	Specific Humidity
E	Latent Heat		at sea surface
H	Sensible Heat	ρ	Air Density
C_d, C_h, C_e	Bulk Coefficients	u, v	Wind components
W	Wind Speed	C_P	Specific Heat dry air
SST	Sea Surface Temperature	AT	Air Temperature
L	Latent Heat Vaporization		

where Q, AT, and the winds are measured at some height (taken here to be 10 - 20 meters). Negative values of H and E indicate stable conditions and a gain of thermal energy by the ocean. The bulk exchange coefficients, Cd, Ch, and Ce, are determined empirically from experimental data. These coefficients keenly govern the bulk formula relationships and are the subject of much discussion. They are parameterizations of conditions such as thermal and wet stratification, and wind speed. Blanc (1985) compared 10 different bulk flux formula coefficients applied to a single set of observations and found ranges of flux mean variation to be 20 - 40% about the mean for wind stress, sensible and latent heat fluxes.

Uncertainty in bulk flux calculations depends on how the bulk formula are applied. When monthly mean quantities of wind, temperature, and humidity are used to calculate fluxes, the results need to be compared to the average of the fluxes calculated from coincidental (simultaneous, coincident) observations. Esbensen and Reynolds (1981) and Hanawa and Toba (1987) both agree the averaging technique is of little or no consequence when calculating latent or sensible heat fluxes for averaging periods of 1-42 days. Wind stress from mean winds for 30-day periods represents only 70% of the stress calculated as the mean of coincident values of winds due to the importance of correlated wind component and wind speed (Hanawa and Toba (1987)). It is hoped that by using pseudo-stress components rather than wind components, the differences between means of coincident stress and stress from mean winds will be greatly reduced.

For this research, the values for Cd, Ch, Ce presented by Smith (1988) will be used in the bulk formula. These values were calculated using experimental data, a combination of the Businger-Dyer flux-gradient

relationships, and the Charnock wind stress formulation with the roughness length being the combination of the aerodynamic roughness length according to Charnock and the roughness length for a smooth surface. This generates an increase in Cd at wind speeds below 3 m s^{-1}. Cd and Ch are functions of wind speed and stability expressed as the difference between the virtual potential temperature at 10 m and the virtual temperature of saturated air at the surface temperature (assumed to be SST). As recommended by Smith (1988), Ce was approximated by multiplying Ch by 1.2. The winds are assumed to be measured at 20 m and AT, dewpoint are assumed to be measured at 10 m. These heights correspond to the tendency of VOS winds to be representative of winds at the highest point of the ship, whether it be from an anemometer or from a Beaufort estimate. The air temperature and humidity are usually measured on the deck level, 10 meters. Thus both temperature (dry) induced stability and humidity (wet) stability is considered in the determination of the bulk exchange coefficients.

2.3 Mean Conditions

The climatological conditions for the North Atlantic for July-September reflect the transition from summer-time to fall (see Esbensen and Kushnir (1981), Han and Lee (1981), and Oberhuber (1988) for detailed figures of climatology). Wind speeds and wind variability in the north portion of the Atlantic begin to increase towards their wintertime maximum. Wind speeds increase to 8-9 m s^{-1} by September. In the tropics, the reverse trend is observed as the mean wind speed decreases from 4-7 m s^{-1} in July to 4-5 m s^{-1} in September. Humidity increases in time in the tropics, but decreases in the

mid-latitudes. Wind stress trends follow closely those of the winds. Sensible heat flux plays a smaller role during this time of year since the ocean-atmosphere temperature difference is small: typically less than 2°C except in the Gulf Stream region where in September the difference exceeds 3°C. From July to September, the latent flux magnitude decreases in the tropics as Q becomes larger, but increases in the middle latitudes (Q decreases); but some of this variability is due to regional wind speed variability.

The overall mean conditions for the analysis period (Fig. 6) when compared to the Bunker Climatology (Bunker (1976)) indicate that the winds during the period were stronger than normal in the north, while in the tropics they were at or slightly less than normal magnitude. SST were near normal except north of 55°N where they were less than 1° cooler. Air temperature was warm, and moist conditions prevailed in the mid-east region; in the western region, it was dryer than usual. Sensible heat flux, H, for this period is similar in pattern to climatology but not in magnitude. The relatively cool air and warm Gulf Stream waters combine to form positive H off the coast of North America. A thin filament of negative H around the Brunswick/Newfoundland coast is generated by the cooler Labrador Current flowing southward into this region. Mean H is smaller than climatology in the Gulf Stream region and in general across most of the Atlantic. The latent flux is also generally smaller than normal but agreeing in characteristics: maximum E (> 130 W m-2) off the northeast coast of South America, extending into the area of the Gulf Stream; minimums in the northeast Atlantic, off northwest Africa and in the vicinity of the Labrador Current.
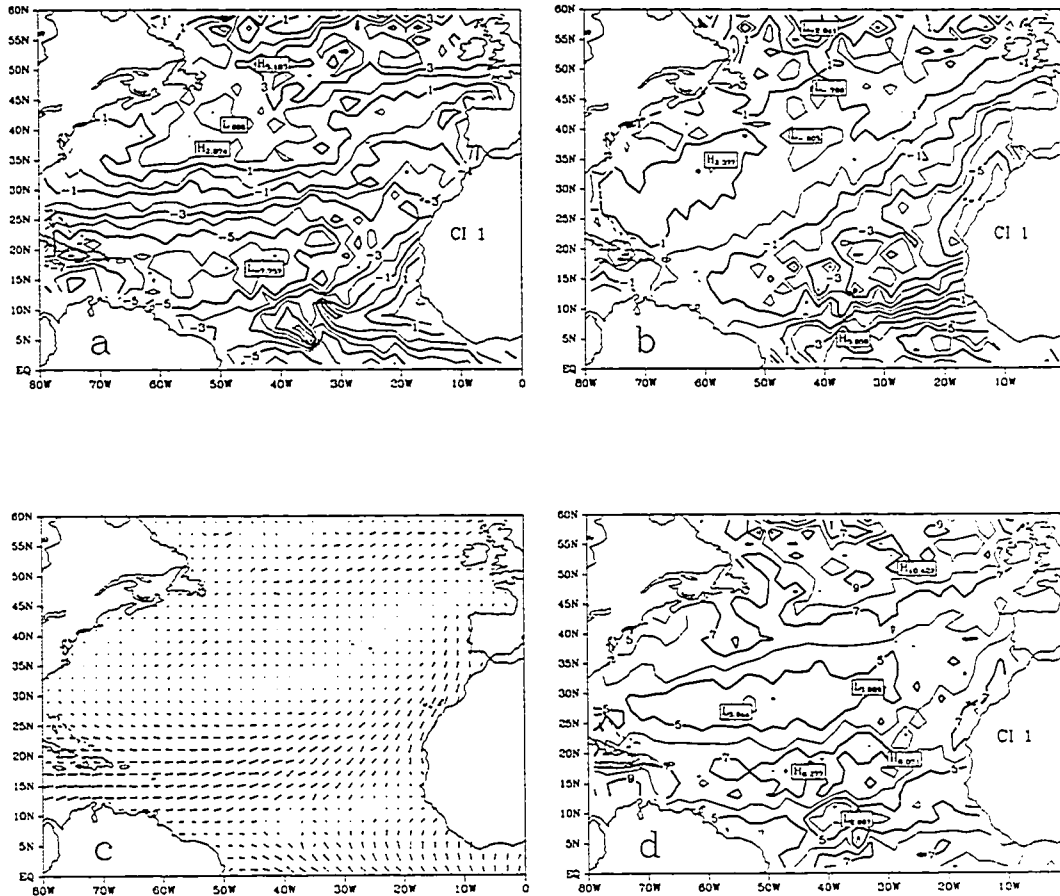
Figure 6. Mean fields of VOS measurements for the analysis period, July 7 - October 10, 1978: a) eastward wind (m s⁻¹), b) northward wind (m s⁻¹), c) wind vectors, d) wind speed (m s⁻¹), e) SST (°C), f) AT (°C), g) Q (kg kg⁻¹), h) Qs (kg kg⁻¹), i) Tx (N m⁻²), j) Ty (N m⁻²), k) Stress vectors and stress magnitude (N m-2), l) H (W m-2), m) E (W m-2). Contour intervals (CI) are as noted. Fluxes were calculated from coincident observations as described in text. Further plots of the above variables will be in same units.
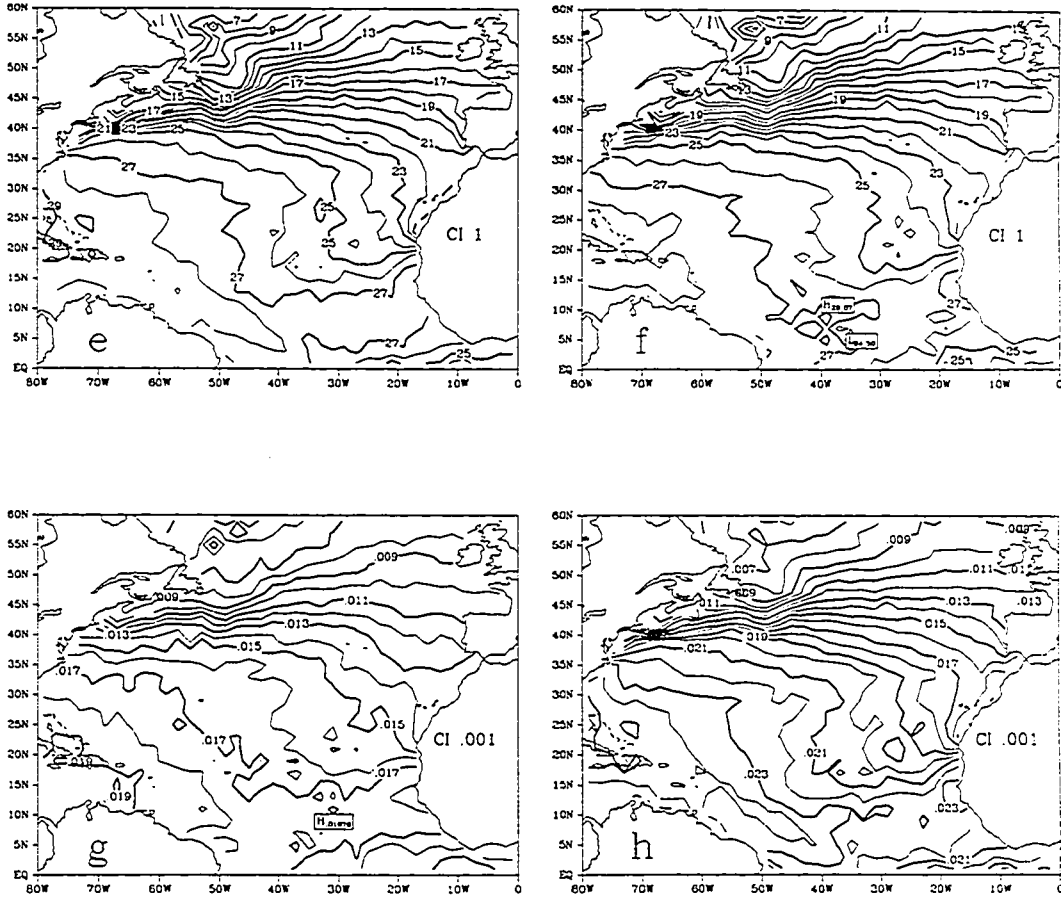
Figure 6.   (Continued)
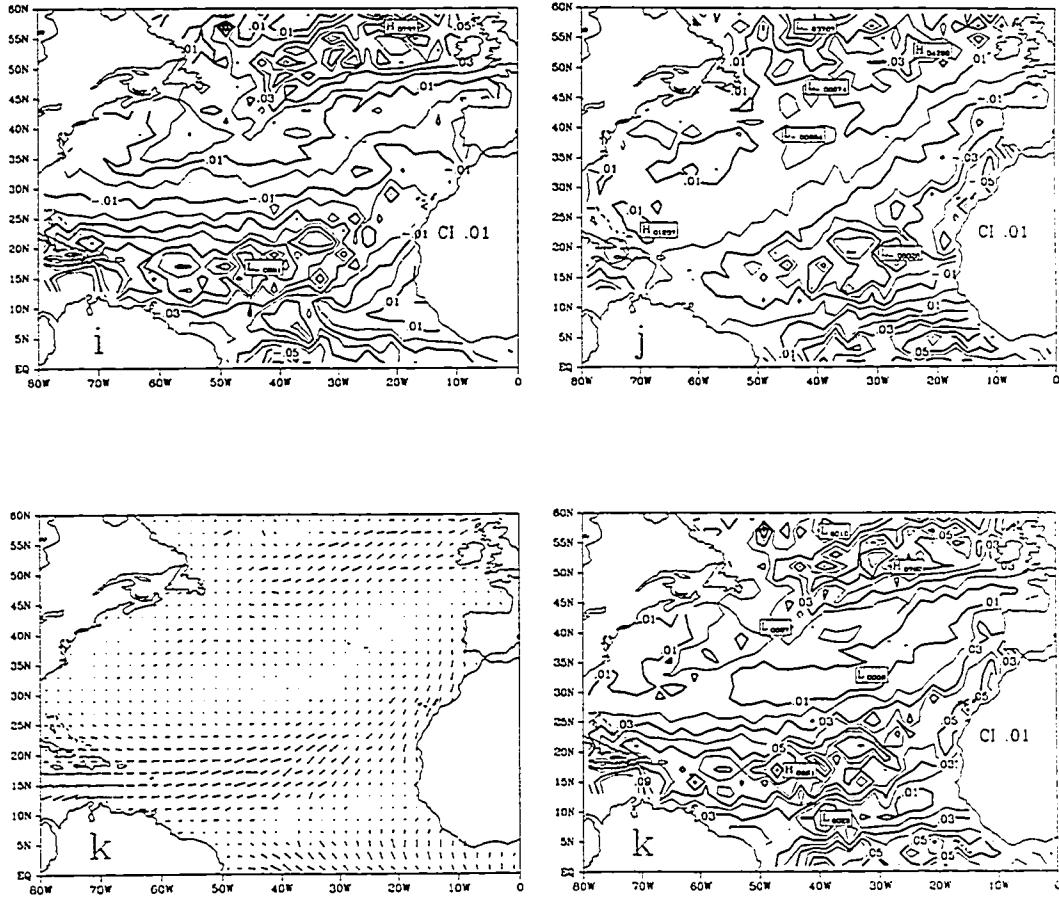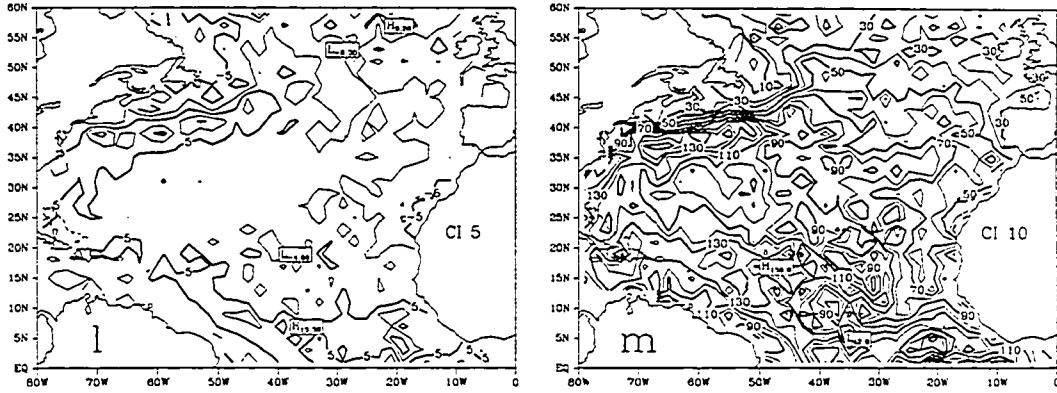
Figure 6.   (Continued)

Figure 6.   (Continued)

2.4 Auxiliary Data Sets

Included in the VOS data are reports from 2 Ocean Weather Ships (OWS) - semi-permanently located ships used for search and rescue missions as well as for routine meteorological and oceanographic observing. OWS R is located nominally at 17°W, 47°N, and OWS L is at 20°W, 57°N (see Diaz, et al. (1987) for further information). In the VOS data set, each had reports approximately every 3 hours. These OWS individual data records were often mysteriously split into 2 separate records; dew point in one report, and the remaining pieces of the observations in another. No changes or attempts at *gluing* together split reports was attempted in order to retain the original *flavor* of the VOS data. A separate, more complete set of OWS observations was obtained in which reports were complete and orderly. In this data set, reports were available each hour for both OWS R and L (Fig. 7, 8). Fluxes for each report were calculated using the method previously discussed. These OWS data and flux values will be used as independent validation information even though some of the OWS information is contained in the input VOS data.

An additional data set consisting of model ocean surface fluxes for the analysis period were also obtained. The GLAS fourth order GCM (Kalnay, et al. (1983)) surface sensible and latent heat fluxes for the SEASAT period were on a 5°-longitude by 4°-latitude grid, each 6 hours in time. These fluxes were calculated in the model with the bulk formula using model values of temperatures and humidity and also surface model winds. The effective drag coefficients have minimum values and otherwise are dependent on
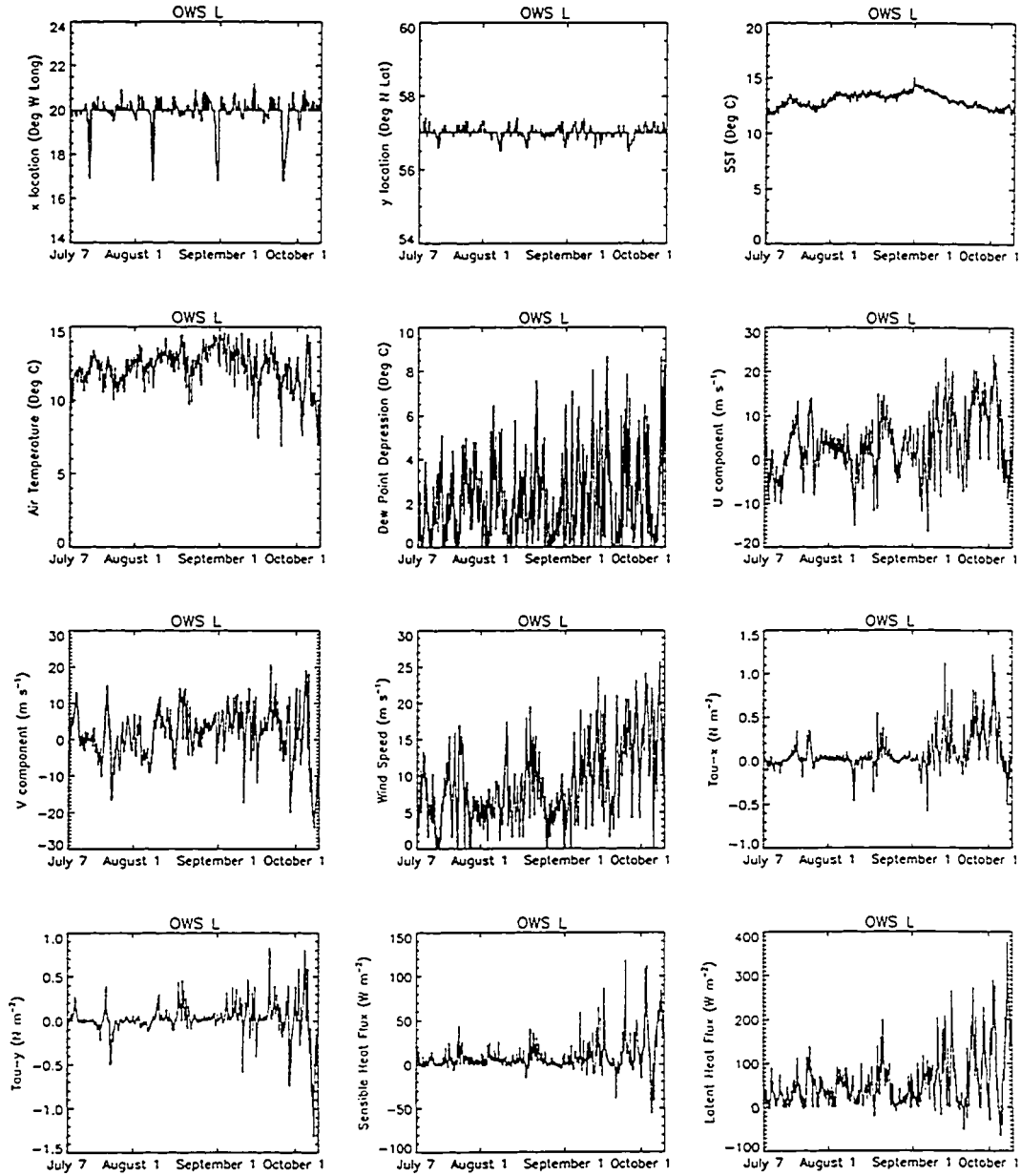
Figure 7.   OWS L measurements and calculated fluxes from the separate OWS data set for the analysis period. Units are as noted. Note that OWS is not necessarily stationary.
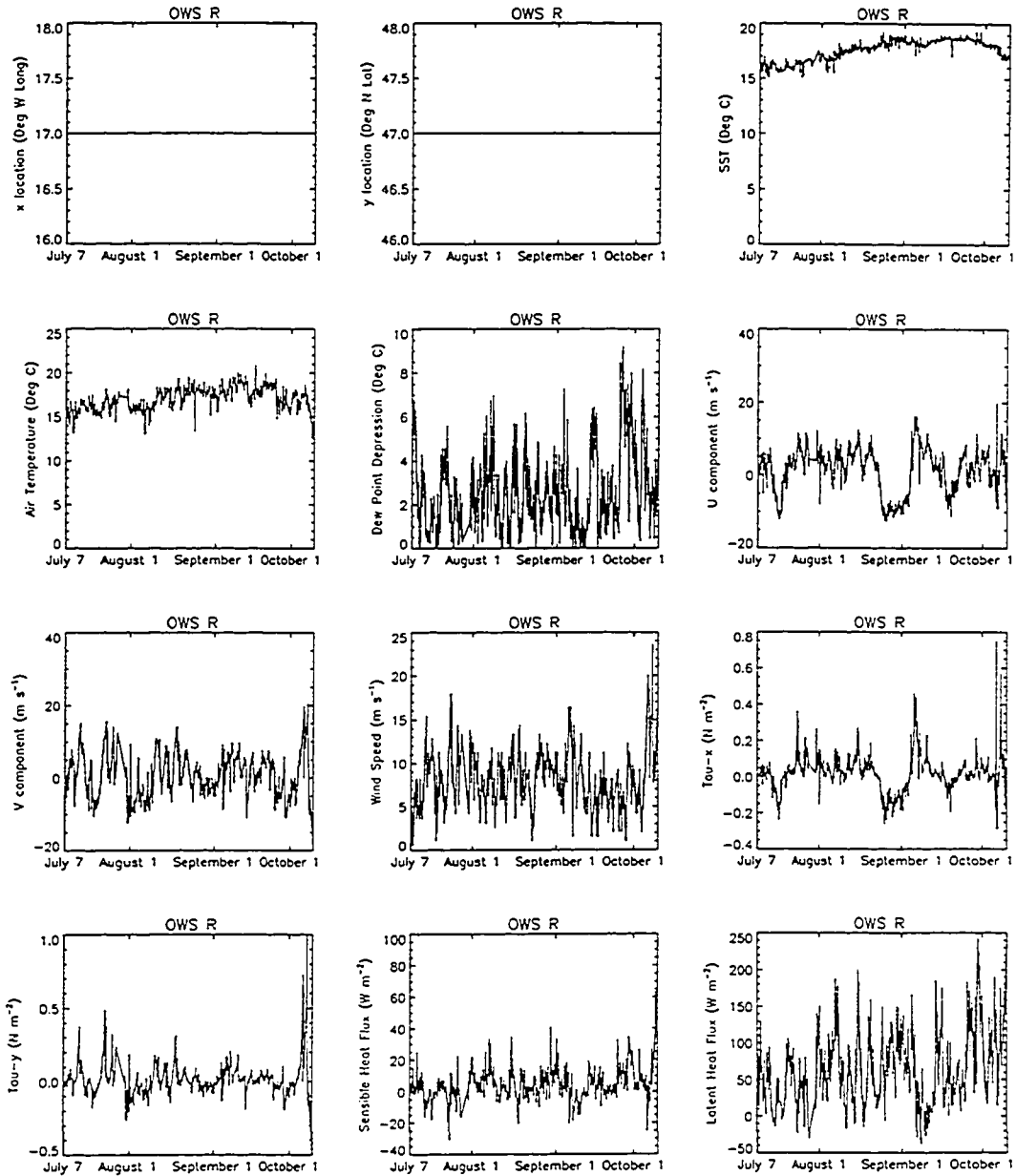
Figure 8.   OWS R measurements and calculated fluxes from the separate
OWS data set for the analyses period. Units are as noted. This
OWS was stationary during the analysis period. Data gap in the
last week of July is indicated by interpolated lines through data
gap period.

wind speed only. At OWS R and L locations, the GLAS fluxes weakly correspond to those values from OWS data; the correlation at OWS-L is only 0.53 and 0.64 for H and E respectively, while at OWS R, the H and E correlations are 0.45 and 0.46 respectively (see Fig. 9, 10).
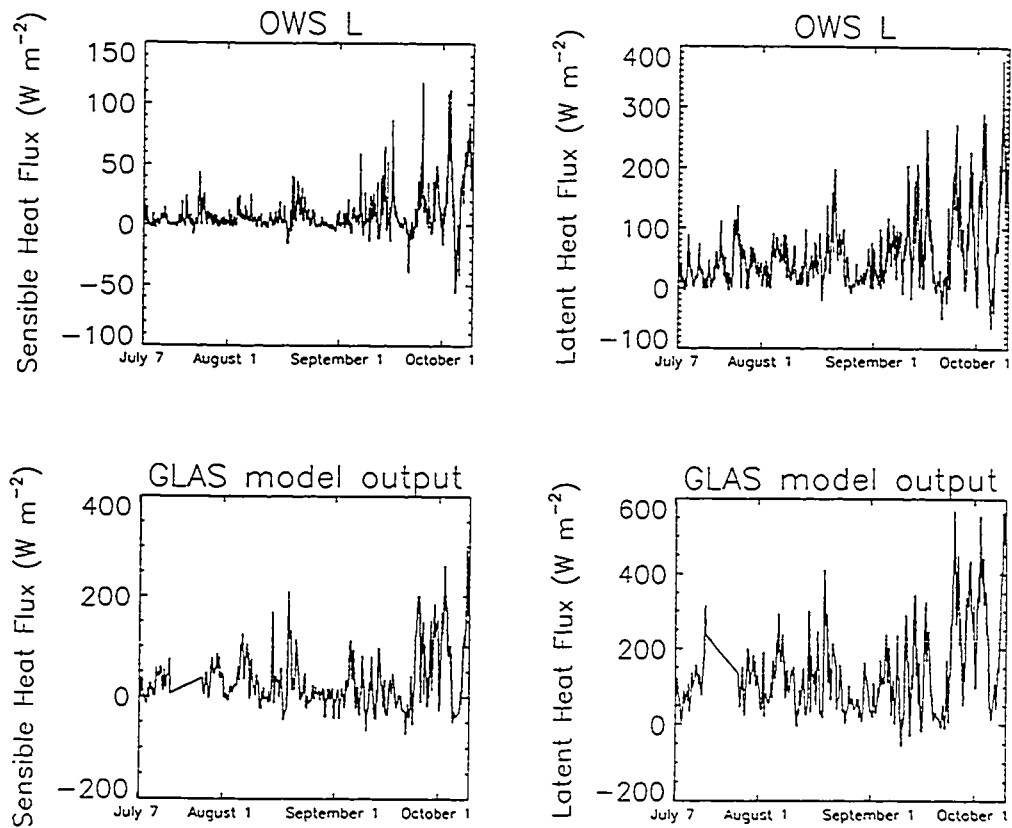
Figure 9.   Sensible (left) and latent (right) heat flux values from the GLAS model at OWS-L location and flux values from the separately obtained OWS-L data. GLAS model data are not available for a 2 week period in July.
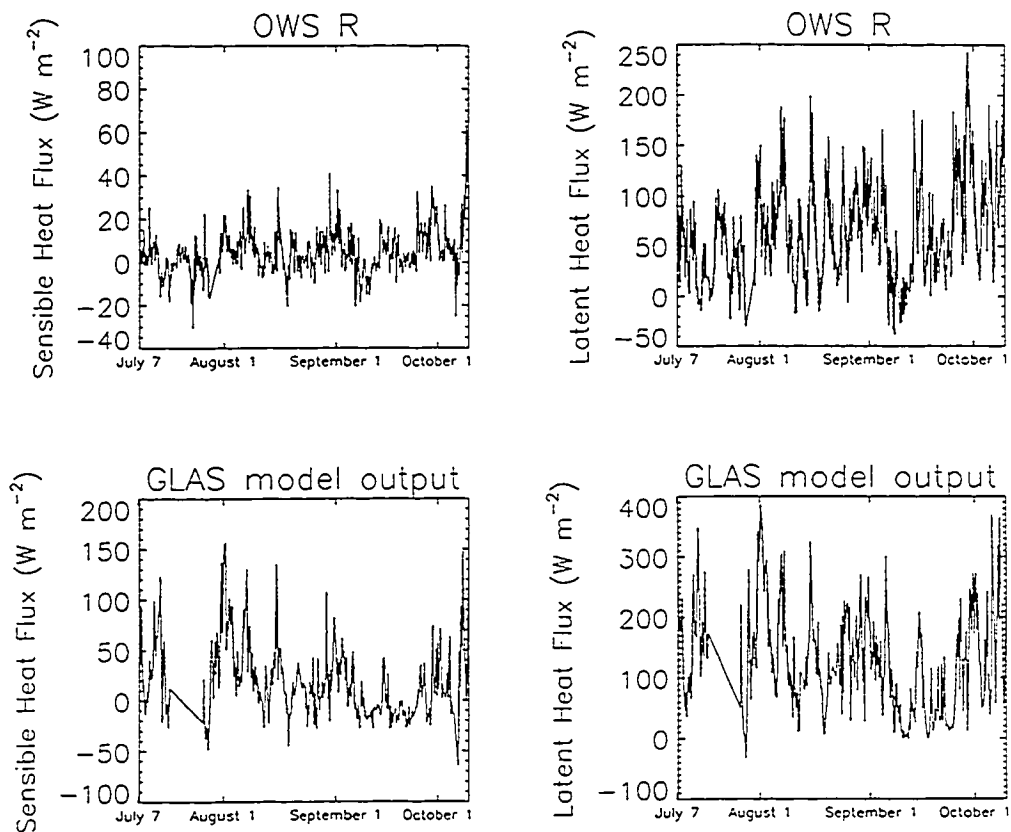
Figure 10.   Sensible(left) and latent (right) heat flux values from the GLAS
model at OWS-R location and flux values from the separately
obtained OWS-R data. GLAS model data are not available for a
2 week period in July. OWS-R data are not available during the
last week of July.

3. OBJECTIVE ANALYSIS METHOD

A variational approach is used for the objective analysis of the data. It involves direct minimization of a cost functional which consists of a number of terms - each expressing a lack of fit to a specific condition. Each constraint term is governed by an associated weight which will be set prior to minimization. This technique has been used successfully to de-alias SASS winds (Hoffman (1982); Hoffman (1984)) and to formulate surface pseudo-stress vectors in the Indian Ocean (Legler, et al. (1989)) and most recently in a scheme to assign direction to wind speed-only data from the DMSP SSM/I instrument (Atlas, et al. (1991)). The method is a form of non-linear least squares and must be solved by an iteration method.

The aim of the technique is to formulate not only the component fields of winds, temperatures, and humidity but also the derived fields of wind stress, and sensible and latent heat flux simultaneously according to a set of prescribed constraints.

The cost functional used in this study includes a series of expressions of misfits to input data sets (terms 1st - J); a sequence of terms that will smooth the results by forcing the resultant fields to resemble the smoothness of the climatology (terms N-R); a kinematic constraint forcing the curl of the wind field to be smooth (term S); and a series of constraints forcing the resultant fluxes to approximate the VOS flux fields (terms K-M).

$$F = \sum(\vec{VW} - \vec{VW}_{SH})^2 + B\sum(\vec{VW} - \vec{VW}_{SASS})^2 + C\sum(W - W_{SH})^2 +$$

$$D\sum(W - W_{ALT})^2 + E\sum(W - W_{SMMR})^2 +$$

$$F\sum(SST - SST_{SH})^2 + G\sum(SST - SST_{SMMR})^2 + H\sum(AT - AT_{SH})^2 +$$

$$I\sum(Q - Q_{SH})^2 + J\sum(Q_S - Q_{SSH})^2$$

$$K\sum(\vec{\tau} - \vec{\tau}_{SH})^2 + L\sum(H - H_{SH})^2 + M\sum(E - E_{SH})^2 +$$

$$Nl^4\sum(\nabla^2(\vec{VW} - \vec{VW}_C))^2 + Ol^4\sum(\nabla^2(SST - SST_C))^2 + Pl^4\sum(\nabla^2(AT - AT_C))^2 +$$

$$Ql^4\sum(\nabla^2(Q - Q_C))^2 + Rl^4\sum(\nabla^2(Q_S - Q_{SC}))^2 +$$

$$Sl^2\sum(\hat{k} \bullet \nabla \times(\vec{VW} - \vec{VW}_C))^2$$

$\vec{VW}_{SH}$	VOS Pseudo-Stress Vector	$\vec{VW}_{SASS}$	SASS Pseudo-Stress Vector
W_{SH}	VOS Scalar Wind Speed	W_{SMMR}	SMMR Wind Speed
W_{ALT}	Altimeter Wind Speed	SST_{SH}	VOS SST
SST_{SMMR}	SMMR SST	AT_{SH}	VOS Air Temp
Q_{SH}	VOS Spec Humid	Q_{SSH}	VOS Saturated Spec Humid
$\vec{\tau}_{SH}$	VOS Stress Vector	H_{SH}	VOS Sensible Heat
E_{SH}	VOS Latent Heat	l	Length scale

$\vec{VW}_C, SST_C, AT_C, Q_C, Q_{SC}$ 'Climatology'

The summation indicates over all points in space. In this case, the functional will operate on a regular 2° x 2° grid over the N. Atlantic. Each data set was mapped onto this grid by averaging over each grid box. The object is to iteratively solve for UW, VW, SST, AT, Q and hence indirectly, W, Tx, Ty, H, and E. Each input field is non-dimensionalized by its RMS basin-mean value in order to equalize the functional term magnitudes. Second-order finite differencing in spherical coordinates is used for all derivative calculations. It is necessary to non-dimensionalize the smoothing and curl constraint terms by multiplying them by an appropriate length factor, l, where l is based on the

distance term in the finite difference differential operator, here taken to be 2° in length, or ~ 222.2 km.

The unknown fields to be solved for are UW, VW, SST, AT, and Q (eastward and northward components of the pseudo-stress (pseudo stress is defined as the magnitude of the wind times its components), sea-surface temperature, air temperature, and the specific humidity respectively). All other fields are derived from these 5 variables. This method differs from previous objective analyses of fluxes in that this scheme operates in such a fashion that calculation of the fluxes is updated at each iteration, and any changes in the solution fields of pseudo-stress (or winds), temperatures, and humidity alter the fluxes which can then affect the other solution fields by the flux constraint terms. The implicit assumption here is that the flux formulation is deemed to be correct and any alterations in the flux constraint terms are the result of data inconsistencies or incorrect VOS flux fields, as opposed to incorrect flux formulation. The resulting solutions of UW,VW, SST, AT, and Q (and wind speed, wind stress, H, and E) will optimally be the best fit in a least squares sense not only to the input data fields, but also to some degree the input flux data fields.

This analysis method is run for each of the three monthly periods, and for each of the 19 5-day periods within the entire analysis period. For each monthly analysis, VOS mean UW, VW, SST, AT, and Q, are the first guess. If there are data voids, they are filled with the 95-day means. The filling of data voids was not sensitive to the particular data set selected for use as data void substitutes. For the 5-day analyses, data voids are filled with the results of the previous 5-day analysis results (or the results of the July monthly analysis results for the initial 5-day analysis). The grid size is 2° by 2°; and given the land

locations, the functional is evaluated at 891 locations. There are 5 variables for which to solve, thus the total number of points on which the functional operates is n=4455. At interior continental boundary locations, derivative constraint (i.e. smoothing and curl) terms are not considered since they cannot be evaluated. Additionally, there are two rows (and columns) of results along the perimeter of the analysis region that will not be considered results since the functional is not completely defined at those points.

There are various numerical techniques for minimizing non-linear functions of n variables. In practice, the conjugate-gradient method is the one of the best techniques when n is large (See Navon and Legler (1987)). The algorithm used here is Conmin (Shanno and Phua (1980)), which is a limited memory, quasi-Newton method which updates the Hessian matrix with a limited number of BFGS (Broyden-Fletcher-Goldfarb-Shanno) updates, but that reduces the needed memory by never storing the actual n x n Hessian - just the Hessian updates. The convergence criteria is such that the Euclidian norm of the gradient must be reduced by nearly 2 orders of magnitude. Convergence always occurred within 50 iterations, and often within 30 iterations.

4. RESULTS

4. 1 Sensitivity Analysis

Evaluation of the behavior of the functional under the effects of various weight selections is a necessary calculation before a successful selection of optimal weights can be made. There are 18 independent weights, each governing an implemented constraint. To test the sensitivity of the functional, over 100 cases were run for an example time period, each case with a different weight selection. Results from each case will not be presented since this would be of considerable length. In the sequence of cases presented here, a first case will show the results when all weights are unity. Then each weight in turn will be set to zero while the others remain at unity. This will highlight alterations to the results and indicate sensitivity to the loss of the term in the functional. A few additional cases are discussed that lead to the final weight selection.

The example analysis period is the 31-day period, July 7, 00Z - August 7, 00Z. Means of the VOS fields are shown in Fig. 11. The VOS wind data is generally noisy in the northern (high variability) and southern (few observations) regions. The effects of few VOS observations is also evident in the temperature data, especially between 10° and 15°N. Generally, the VOS fields adequately cover the analysis region for this month-long period and the satellite data provide only additional verification fields. Note the difference between wind vector magnitude and wind speed magnitude are large in the region north of 40°N due to high directional variability.
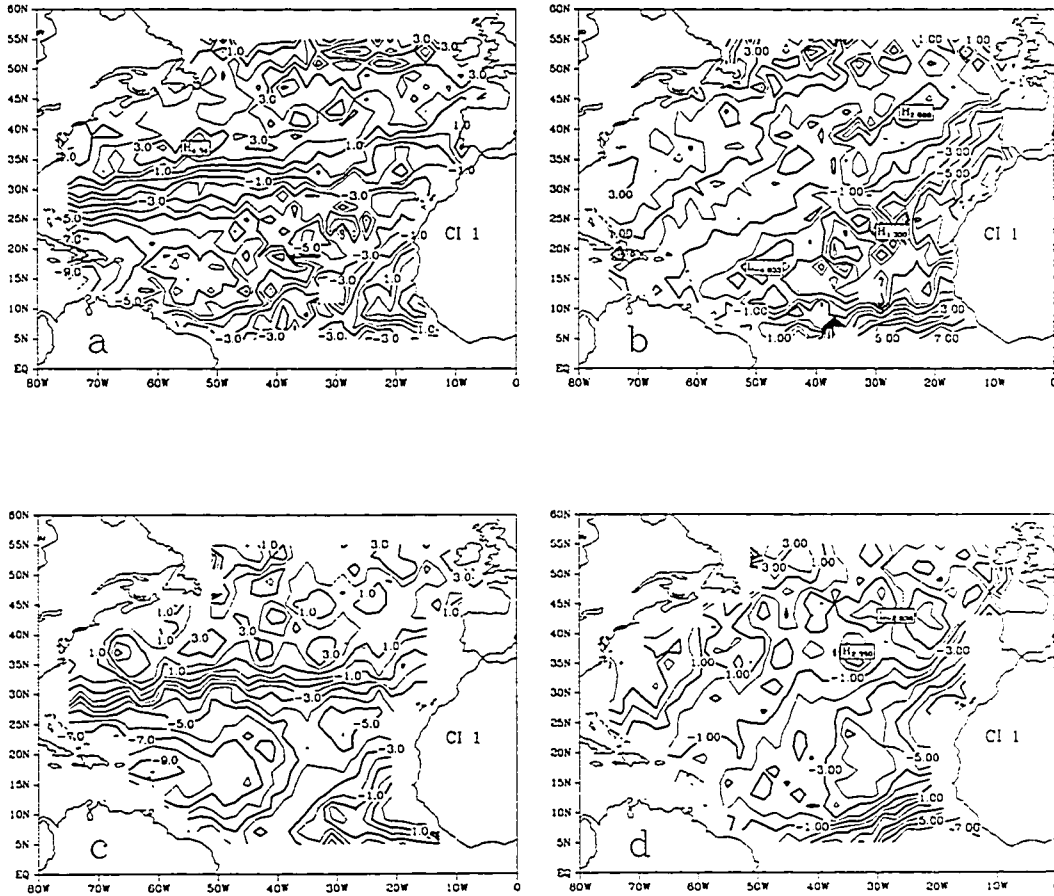
Figure 11.   Mean fields of VOS measurements for the period, July 7 - August
7, 1978: a) eastward VOS wind, b) northward VOS wind, c)
eastward SASS wind, d) northward SASS wind, e) VOS wind
speed, f) SMMR wind speed, g) ALT wind speed, h) VOS AT, i)
VOS SST, j) SMMR SST, k) VOS Q, l) VOS Qs, m) VOS eastward
stress (Tx), m) VOS northward stress (Ty), o) VOS H, and p) VOS
E. Contour intervals (CI) are as noted. Data voids indicate no data
available.
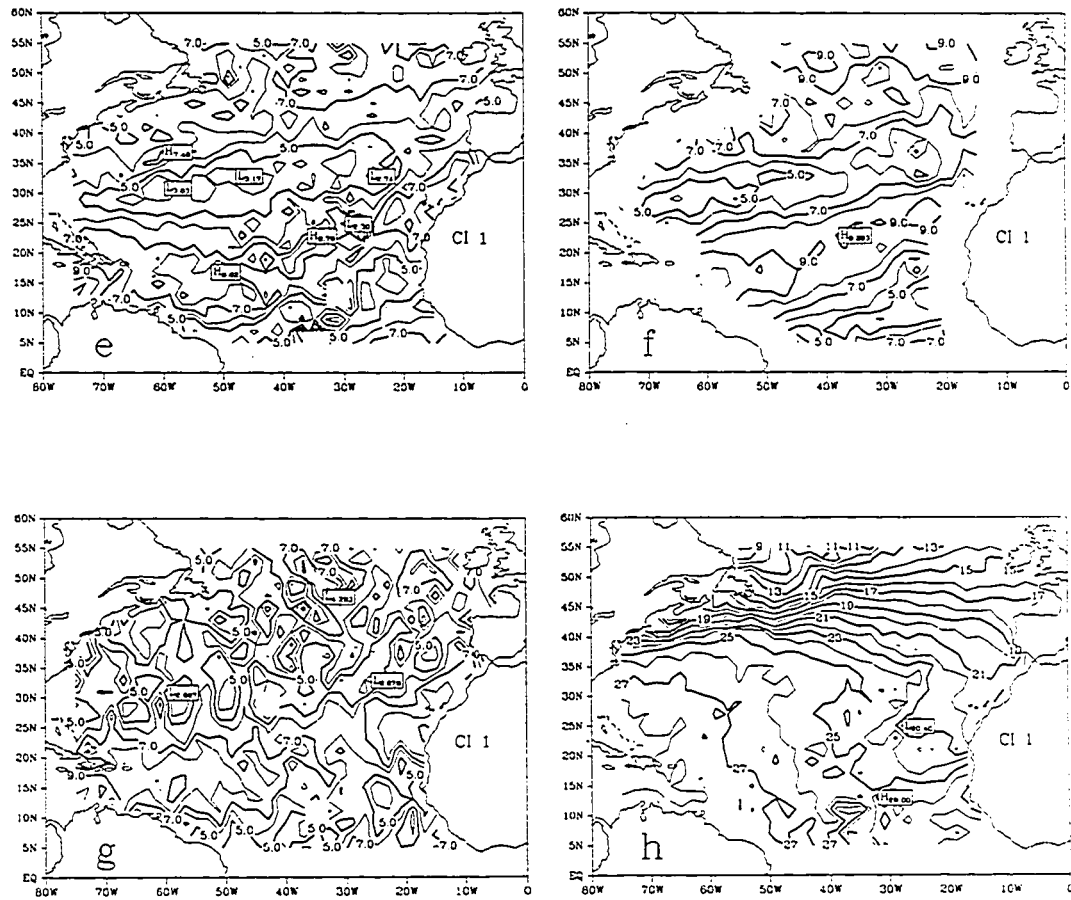
Figure 11.   (Continued)
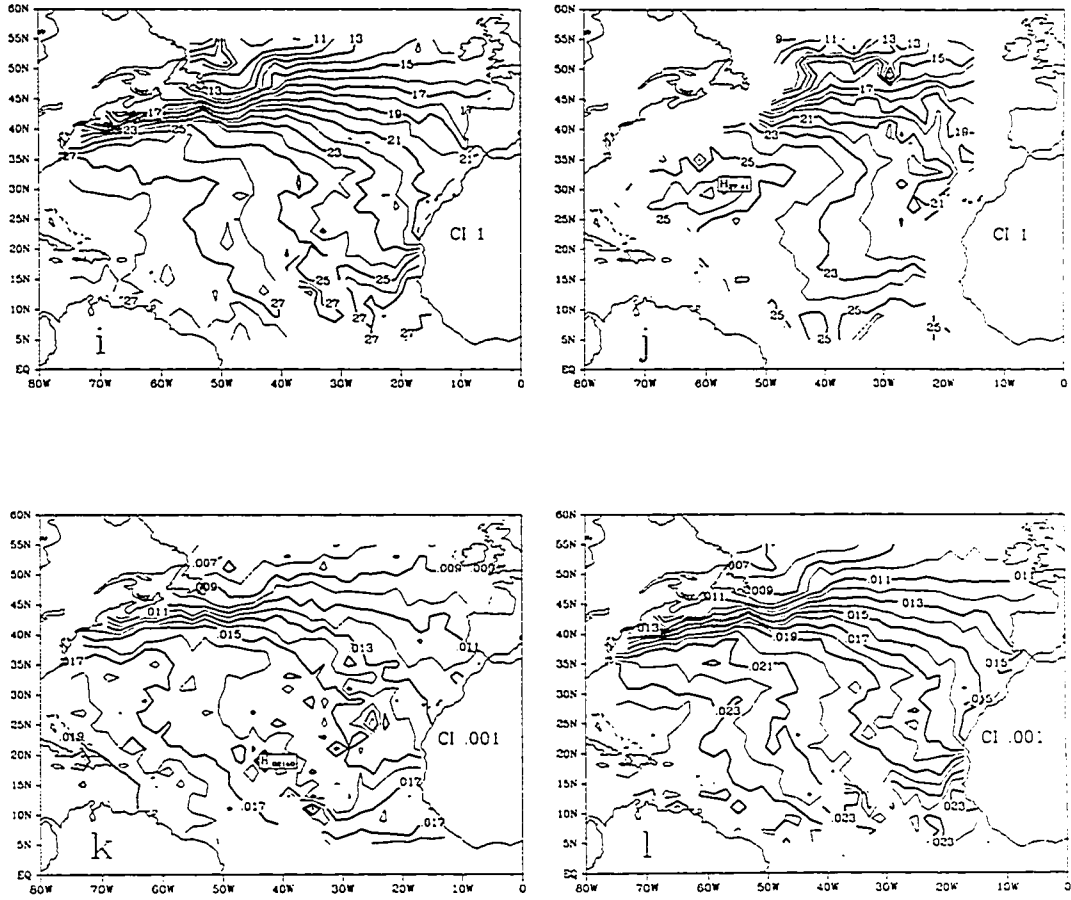
Figure 11.   (Continued)
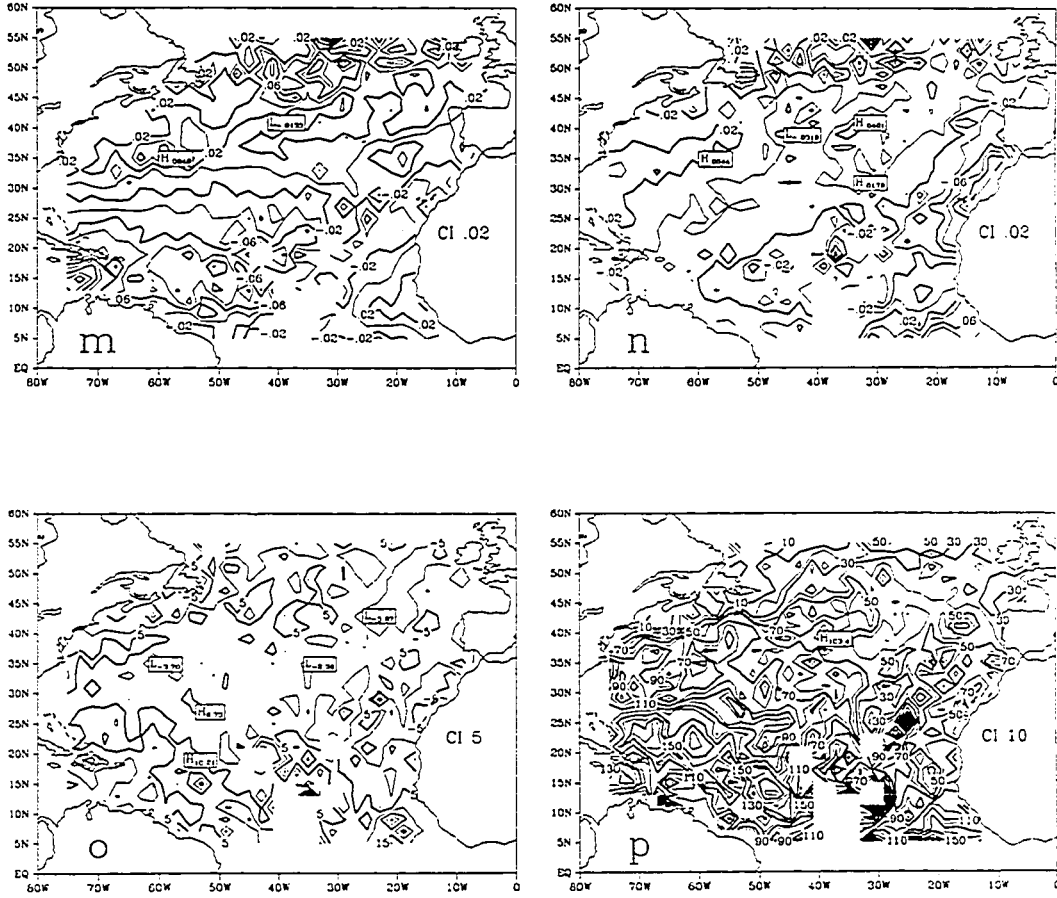
Figure 11. (Continued)

The first case, case 01, is the control case where all weights are set to 1.0. The behavior of the functional values demonstrate that although each constraint term is designed to be of the same order of magnitude, in fact, values span over a range of 3 orders of magnitude. None the less, the total functional value and gradient reduce quickly with each successive iteration and the criteria for convergence is met after approximately 30 iterations. Since the first guess fields are the VOS means, it is not unusual for some of the values of these constraint terms to increase. The smoothness terms for the winds are characteristically initially large, but reduce very rapidly due in part to their relative magnitude in comparison to the other terms in the functional.

The resultant fields for case 01 describe fairly well the VOS means. The anti-cyclonic Bermuda High dominates the wind circulation pattern and in the tropics, the Atlantic Inter-Tropical Convergence Zone (ITCZ) is clearly evident between 10°N at the eastern boundary and near 5°N near South America. Winds with unlikely gradients over 1 -2 grid points which occur primarily in the extreme north and in the tropics were filtered. The influence of the Gulf Stream and the tropical large-scale signature of the ocean circulation as the dominant dynamic features is shown in SST and AT. Results of SST are warmer than VOS estimates in the northwest quadrant and in the mid-tropics - by over 1.5° in some locations, and some questionable VOS SST were removed in other areas. For AT, the extreme northwest and coastal areas of northwest Africa were cooler. Q and Qs fields are smoother than VOS means with Qs alterations reflecting changes in SST. Stress results indicate a reduction in stress north of 45°N. H and E reflect changes in temperature and humidity fields; for example, in the region near 35°W, 10°N relatively weak initial values of E gave way to values exceeding 150 W m^{-2}.

The results for this case when compared to the mean condition at OWS-R (47°N, 17°W) are favorable, but not perfect; warmer than expected temperatures, higher wind components (but lower wind speed means) and a lower E value.

By setting the weight on the VOS pseudo-stress constraints term to zero, which is equivalent to removing the term from the functional, several minor changes in the resultant fields could be noted, and in general, OWS comparison improved, but improvements overall were typically very small.

Eliminating the SASS pseudo-stress components constraints, increased the wind magnitudes in all areas except within 500 km. of continental boundaries (no SASS data). This increase was more than in the case of no VOS pseudo-stress indicating a dominance of SASS on resulting winds. Additionally, SST and AT were closer in proximity to VOS values, but there were more instances of spurious small-scale temperature anomalies.

The lack of a stress vector constraint prompted a similar response; slightly higher wind magnitudes and better overall agreement with VOS SST and AT. Humidity and H were improved over case 01, but E was degraded; especially prevalent were numerous E extrema.

Removal of the VOS wind speed constraint induced minor variations in the wind field, but major detrimental variations in the temperature and flux fields due to the sensitivity of the fluxes to wind speed. The temperature field was affected in part due to the propensity of the technique to adjust the temperatures first when trying to enforce the H constraint. The results of the dropped SMMR and VOS wind speed constraint were similar, but the loss of the ALT constraint improved the results- leading credence to the information learned previously concerning the poor comparability of ALT and in-situ wind speeds.

The lack of SST constraints significantly degraded Qs and subsequently the E fields, but only in a few isolated locations. Similarly for the AT constraint; the H field was altered significantly more than the AT field. The fluxes degrade when the temperature constraints are removed.

Eliminating the Q constraint results in undetectable changes in all results when compared to case 01. The Qs constraint elimination enhances some AT field maxima in response to the H constraint, (undesirable) but improves the SST field thereby improving H slightly. It degrades the E field results.

The SST and AT fields are significantly different than case 01 results when the H constraint is removed. AT results are 0.5°C cooler than first guess fields north of 40°N, with additional pockets of ±0.5 to 1.0°C differences located primarily near the west coast of Africa. SST increased by up to 0.5°C in some locations north of 40°N, and cooled off the west coast of Africa. Winds, humidity, and stress are very similar to case 01 results. H results differ dramatically from case 01 in these areas because of the temperature alterations. Large positive magnitude H is evident in this case north of 45°N and in the southern and eastern Atlantic, where small or even negative H is desirable. Additional (objectionable) positive and negative extrema are present. Comparisons of results to OWS-R were degraded when compared to case 01.

Setting the weight on the E constraint to zero affected primarily the Qs field, but only in a minor way. The resulting E field is much smoother, essentially eliminating any of the small-scale features in the VOS E field. Comparison of OWS-R E to resultant E is not as good as in case 01, and numerous very-high magnitude extrema still exist in the resultant E field as a result of extrema in other parameters such as temperature and humidity.

The constraints and associated weights N - R serve as smoothers for the resulting fields. Without them, the results are noisy and uncharacteristic. Lack of UW_c and VW_c smoothness constraints leaves undesired wind field anomalies in the north (high variable wind reports) and in the south (few reports). In the case of no temperature smoothing, temperature anomalies propagate "errors" through all the flux fields eliminating much of the possibility of filtering them. No smoothness constraints on Q and Qs reduces the changes between initial and resultant Q, Qs, and E, which like the lack of wind and temperature smoothing weights, allows noisy extrema to propagate unfiltered readily through the analysis method.

The final weight controls the resultant wind curl to a climatology. Setting this weight to zero has only negligible effects on the direct winds, but the minor changes it does create are most detectable in the curl of the wind. The curl field is qualitatively better with with the inclusion of the curl constraint.

Summing up, temperature results are sensitive to constraints on H as well as on VOS temperature constraints. The heat fluxes are more sensitive to the terms of the vertical differentials in their respective bulk formula than to wind speed. For example, to alter H, the largest change could be brought about by altering the temperatures, or in other words, the gradient of H (E) is largest with respect to temperatures (humidity), not wind speed. The resulting wind speeds are very weak overall, particularly in the north as a result of the averaging process. In order to increase the wind speed, the pseudo-stress must be strengthened. This means the wind component as well as the wind speed will increase. In order to address the shortcomings of the weight selections in these initial cases, several more cases were run.

In order to asses the quantitative 'correctness' of the specific case results, 2 pieces of additional information will be used. First is the set of complete (hourly) OWS observations at OWS R (47°N, 17°W). Differences between the OWS-R means and the analysis results will be used as one selection factor. The second selection criteria is the RMS difference between the VOS means and the results at locations where there were a large number of VOS observations during the period (the assumption underlying this comparison is that the better sampled locations are more accurate). Unfortunately, these locations are located primarily in coastal regions and at the OWS-R location. Coastal regions are for the most part already well sampled by VOS, but not covered by remotely sensed data due to the contamination by land surfaces. Both of these factors are therefore limited in their ability to verify the correctness of the solution.

The last factor in selecting the correct combination of weights is the intangible qualitative assessment based partially on the successful filtering of extraneous extrema and incorrect values. The results should convey generally realistic gradients, i.e. while one expects large north-south gradients of temperature across the Gulf Stream extension, large gradients elsewhere are not always so easily acceptable.

First attempts to improve the results were aimed at increasing the wind speeds, especially in the mid-latitudes where they were particularly anemic. Heat flux results were as a consequence weak, and they were very noisy in the southern half of the basin. Additionally, altimeter winds will be ignored since the preliminary analyses (see section 2) indicated a speed-dependent bias, and its inclusion in the function is detrimental. Through a series of cases where the weights of the wind speeds were increased, vector weights reduced, and flux constraints 'twiddled', it was determined that increasing the ship wind weights

where VOS data was numerous (in coastal and shipping lane regions) led to better wind and flux results. Extrema of various other variables and fluxes were still evident in the south. The RMS wind speed difference between results and VOS means for locations with greater than 250 ship obs was 0.98 m s^{-1} and the temperature RMS differences were approximately 0.8°C.

Further adjustments to the weights using a scheme whereby weights H,K,L,M (AT, stress, H, and E respectively) governing approximation of results to VOS means were made a function of the number of observations in each 2° by 2° box. For grid boxes with less than the basin mean number of observations (NOBS) during the period, the weights were set to one half of the listed weight. If NOBS were less than 5, the weight was one-tenth of the listed weight; and if NOBS were greater than the mean, the full weight is used. The criteria for balancing VOS means to SEASAT means is therefore deemed to simply be a function of the the quantity of VOS reports in each box.

The results of this weight selection improved the results, especially in the fluxes, over that of the case of spatially uniform weights. Winds and AT also improved, and SST degraded slightly.

Additional cases were run in order to further reduce the large wind speed differences and the relatively large temperature differences. The final weight selection, Table 2, shows that the weights are very high on VOS wind speed and SST in order to balance the tendency for the flux constraints to adjust these to incorrect values. The Q and Qs weights I,J, were relaxed to allow for some variation. The smoothing weights for AT, Q and Qs were increased to assure adequate smoothing.

Table 2. Final choice of weights for the functional.

Weight	Functional Term Name	Value
B	SASS Pseudo-stress	1.0
C	VOS wind speed	70.0
D	ALT wind speed	0.0
E	SMMR wind speed	5.0
F	VOS SST	70.0
G	SMMR SST	1.0
H	VOS AT	20.0
I	VOS Q	0.5
J	VOS Qs	0.5
K	VOS wind stress	0.8
L	VOS H	0.6
M	VOS E	2.0
N	Pseudo-stress "smoothing"	1.0
O	SST "smoothing"	1.0
P	AT "smoothing"	5.0
Q	Q "smoothing"	5.0
R	Qs "smoothing"	5.0
S	Pseudo-stress curl	5.0

Adjustable weights were applied only to weights C,F,H,K,L and M (Ship wind speed, SST, AT, and fluxes) and to the initial weights on the ship pseudo-stress components. The final adjustment scheme was if NOBS were less then the basin-mean NOBS, the weight was 0.75 times the original listed weight; if NOBS was greater than 2 times the basin-mean NOBS, the weight was double the listed weight; and if NOBS was less than 5, the weight was set to 0.1 times the listed weight. Otherwise it is the listed weight value. Essentially the quality of the VOS mean input fields were judged by the number of observations that went into the mean values. As shown in Legler (1991) (and as discussed in section 8), this is an approximation to sampling theory and is a reasonable thing to do, but the natural variability should be part of the quality assessment; an aspect not considered here. Accordingly, some qualitative/quantitative evaluation of the SEASAT data would also be beneficial. Weights for VOS SST, wind speed data were much higher than for SMMR data. This does not necessarily lead to zero contribution for SMMR data because it helps to balance the magnitudes of the functional terms.

RMS differences for this final choice of weights, Table 3, indicate that wind speed, SST, Qs, Q, H and E differences are small while RMS values for AT are relatively large. There are fewer constraints on AT than on SST due to the fact that Qs is dependent on SST whereas Q is not dependent so much on AT - without as many constraints, AT is more free to vary without penalty thus accounting for some of the RMS discrepancy between the two temperature results. Stress differences are significant - the mean value of stress magnitude is about 0.02, thus the RMS differences are about 20% of the mean, even at some very well sampled locations. As seen in the next section, the largest wind differences occur in the north portion of the basin.

Table 3. RMS differences between VOS means and results for locations with listed minimum number of VOS observations for the July 7 - August 7, 1978 period. VOS fluxes are calculated from coincident observations. Results are from case with final weight selection.

	Minimum 50 obs.	Minimum 150 obs. (all valid locations except location with largest magnitude difference)
Wind Speed (ms^{-1})	0.39	0.34
SST (°C)	0.35	0.41
AT(°C)	0.54	0.69
Q ($kgkg^{-1}$)	$3.6e^{-4}$	$4.0e^{-4}$
Qs ($kgkg^{-1}$)	$2.8e^{-4}$	$3.0e^{-4}$
Tau-X ($N\ m^{-2}$)	.015	.014
Tau-Y ($N\ m^{-2}$)	.011	.011
H ($W\ m^{-2}$)	1.02	1.67
E ($W\ m^{-2}$)	4.52	6.15

The stress discrepancies can be attributed to the intimate link between wind speed and wind components through the use of pseudo-stress which makes it difficult to alter the wind speed without altering the wind components. The use of pseudo-stress certainly *is* an improvement over the use of wind components because of the fact that the wind speed - wind component correlation information is included in the stress formulation making it possible to get the stress magnitude high enough. However, for cases of highly variable winds (primarily in direction), the mean wind speed calculated using pseudo-stress can still be much too small when compared to mean scalar wind speed and the resulting wind components too large. In future versions of this technique, wind speed will be a separate variable of the functional solution. In the 5-day results discussed in a later section, this small-wind-speed problem is not as prevalent due to the shorter time period over which the pseudo-stress are averaged.

Comparisons of the final results to OWS-R observations confirm that the wind speed is still 1 m s^{-1} too small; SST is $0.5°C$ too high; AT is fine, Q and Qs agree within 3%. Tx and Ty are too big and H and E are small by 0.6 and 14.0 W m^{-2}. However if comparing the results to the VOS means at the nearest grid point to the location of OWS-R, the results appear much better for fluxes, SST, winds and Q. AT and Qs are only slightly worse, thus some deficiencies in these OWS-R comparisons are attributable to insufficient sampling (discussed later).

4.2 Results for July, August, and September Periods

The results and the difference between the July results and the first guess fields (VOS means), Fig. 12, 13, illustrate several interesting changes to the input data. The wind field (derived from pseudo-stress) reflects more the wind speed information than the mean vectors. In the center of the Bermuda High
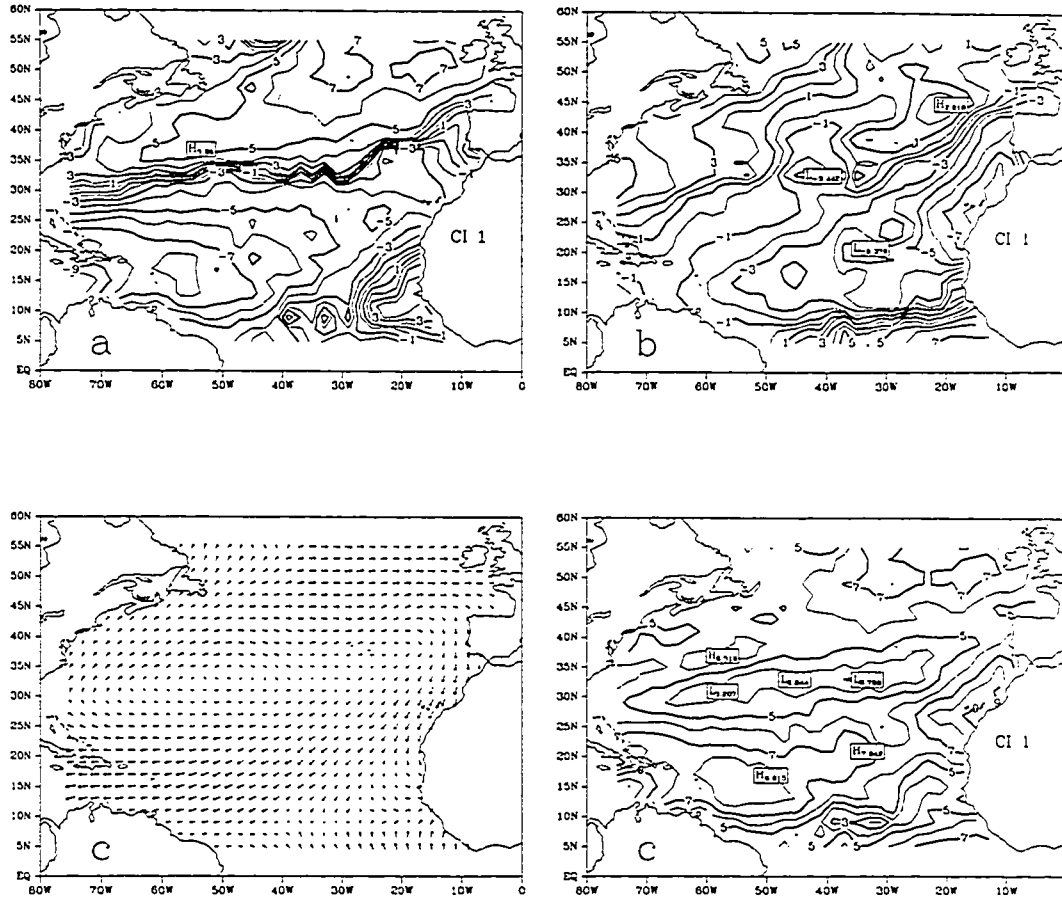
Figure 12.   Resultant fields for the case with final weight selection for July 7 -
August 7, 1978: a) eastward wind, b) northward wind, c) wind
vectors and magnitudes (wind speed), d) SST, e) AT, f) Q, g) Qs, h)
stress vectors and magnitude, i) stress curl (N m^{-3}), j) H, and k) E.
Units are as previously mentioned and contour intervals (CI) are
as listed.

Figure 12.   (Continued)

54
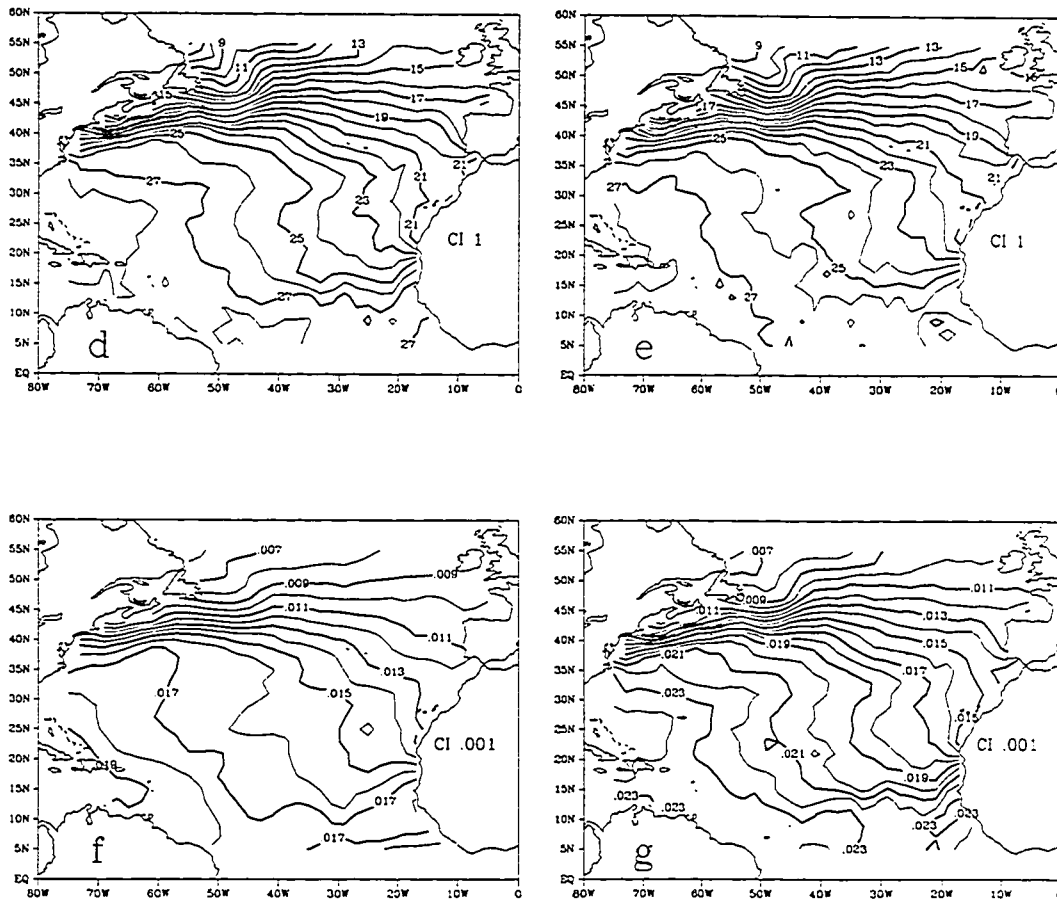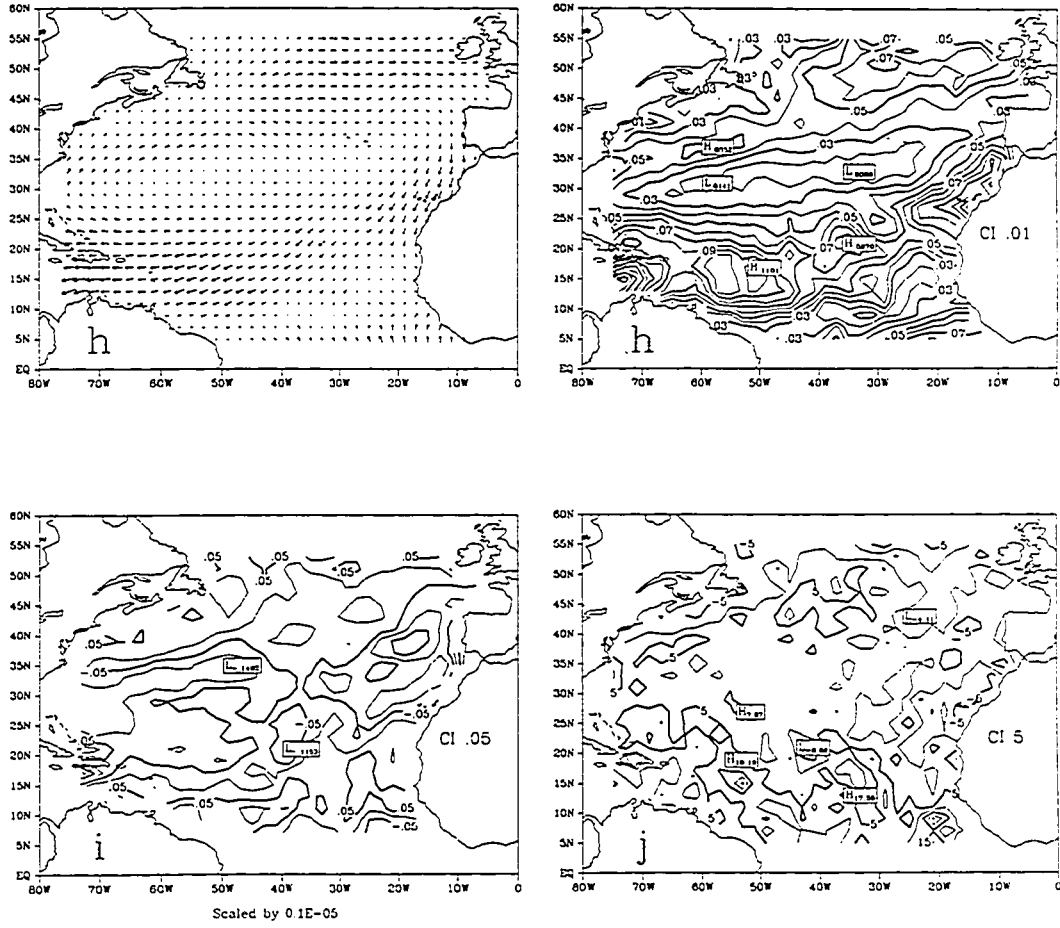
Figure 12.   (Continued)
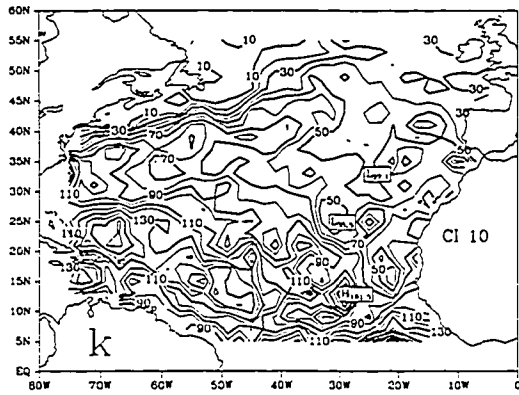
Figure 12.   (Continued)
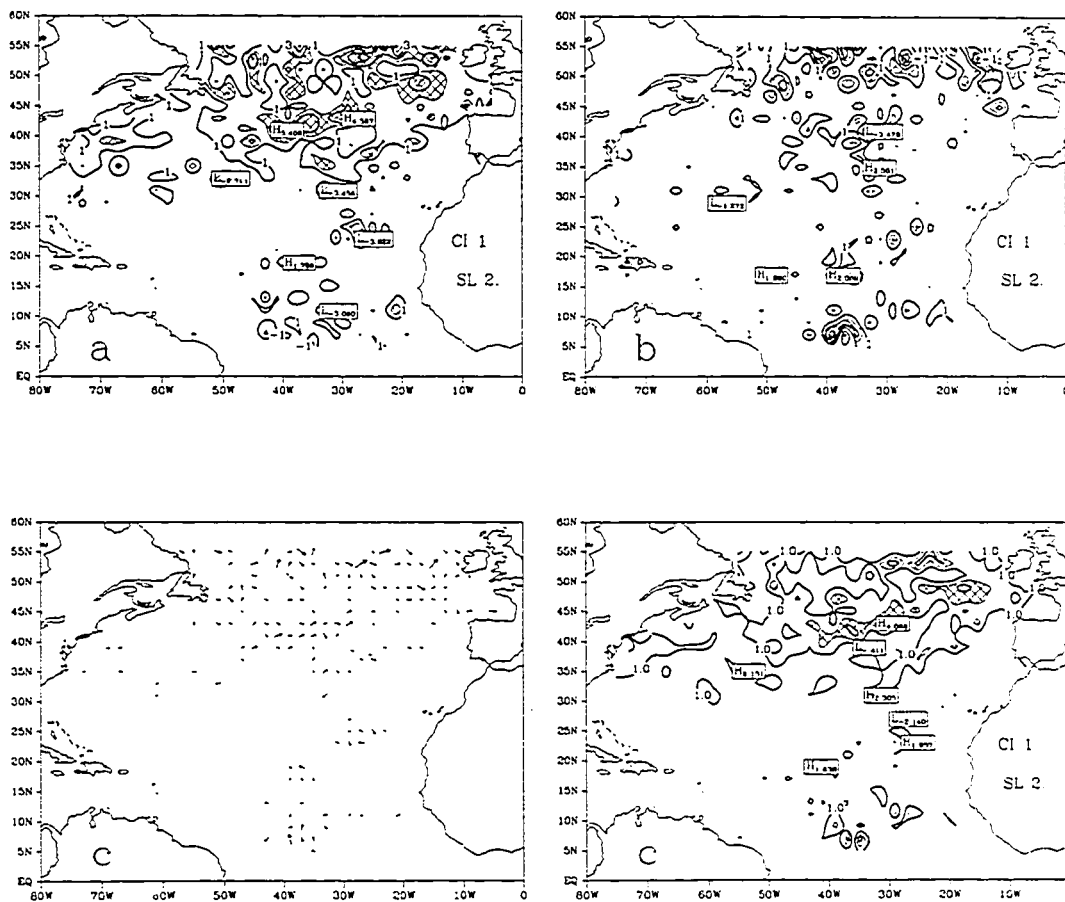
Figure 13. Difference between the resultant fields and the first guess fields for the case with final weight selection for July 7 - August 7, 1978: a) eastward wind, b) northward wind, c) wind vectors and magnitudes (wind speed), d) SST, e) AT, f) Q, g) Qs, h) stress vectors and magnitude, i) H, and j) E. Shading is indicative of negative values (hatching is in one direction only) and positive values (cross-hatching) whose magnitudes exceed the listed shading level. Contour intervals (CI) are as listed with absolute values less than the listed shading level (SI) not shaded. Vectors with magnitude less than 2 m s^{-1} for winds and 0.03 N m^{-2} for the wind stress were not drawn in the vector plots.
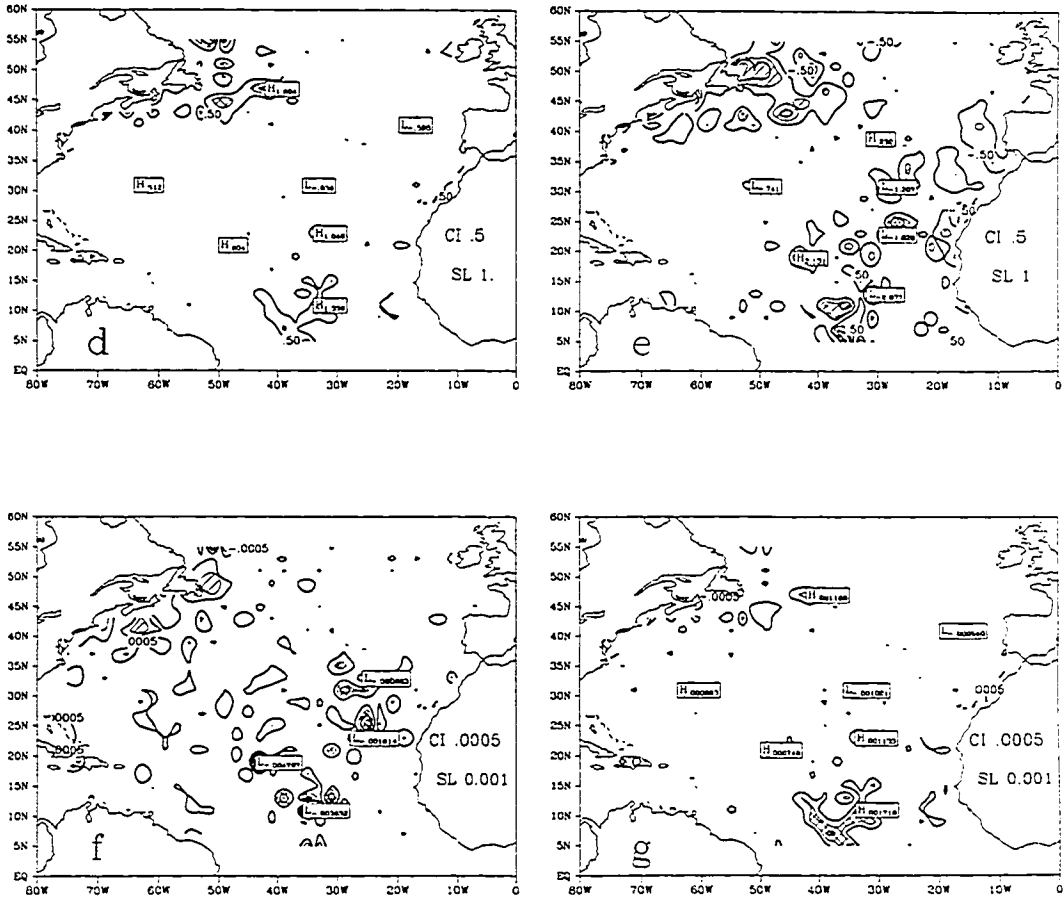
Figure 13.   (Continued)
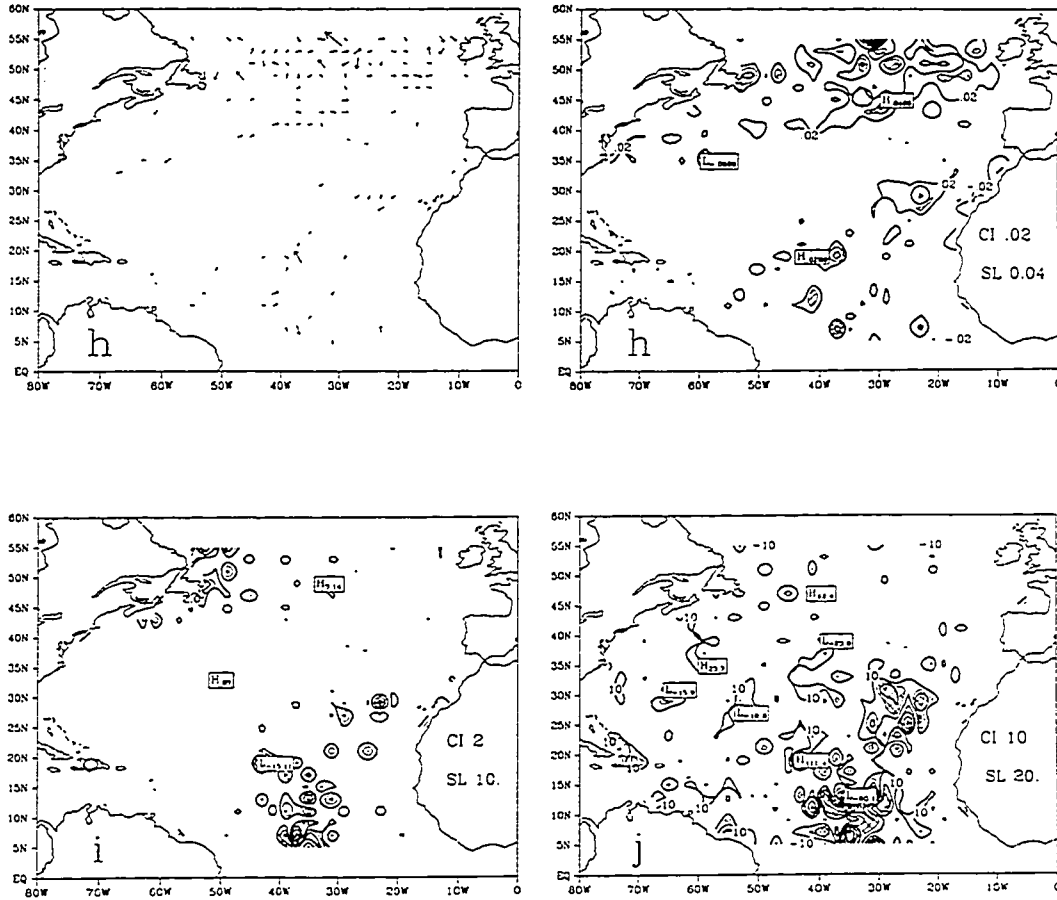
Figure 13.   (Continued)

circulation, mean VOS wind speeds and resultant winds and wind speeds agree; 2-3 m s^{-1}, but the magnitude of the mean VOS vectors is on the order of 0-2 m s^{-1} thus the usual strong wind speeds but weaker mean winds are replaced by equally strong wind speeds **and** strong mean winds. Mean wind vectors north of approximately 35°N were magnified due to the constraint on wind speeds. Although technically, these winds no longer resemble the true mean winds in terms of magnitude, they are more representative of the winds typically encountered there. In the trade wind regions, the mean VOS winds are fairly steady, thus the results better resemble the VOS mean winds in this region.

The result temperature fields are indicative of the typical tight gradient across the Gulf Stream and correctly show a cool tongue stretching to the south west from west Africa. For the vast majority of the Atlantic, the results - VOS mean differences are very small, reflecting good results. The largest SST alterations are east of Newfoundland and to the west and north of west Africa. SST in small patches east of Newfoundland are, in places, 0.5 to 1.0°C warmer than initial estimates from VOS data. For AT, the regions near Newfoundland are cooler by 0.5 to 1.0°C. Likewise, near west Africa there are several large regions adequately sampled by VOS, yet the AT results are 0.5 - 1.0°C cooler than initially observed. Both regions of large SST and/or AT alterations are areas of positive H, and also near land or boundaries.

The difference fields SST-AT and Qs-Q, Fig. 14, dictate the sign as well as partially determine the magnitude of H and E. The resultant fields remained similar to the first guess fields, but distinct differences exist in the northern half of the basin where an area, 35 - 45°W, 45 - 50°N, of (stable conditions) negative SST-AT has been reduced in areal size and even reversed in sign from slightly
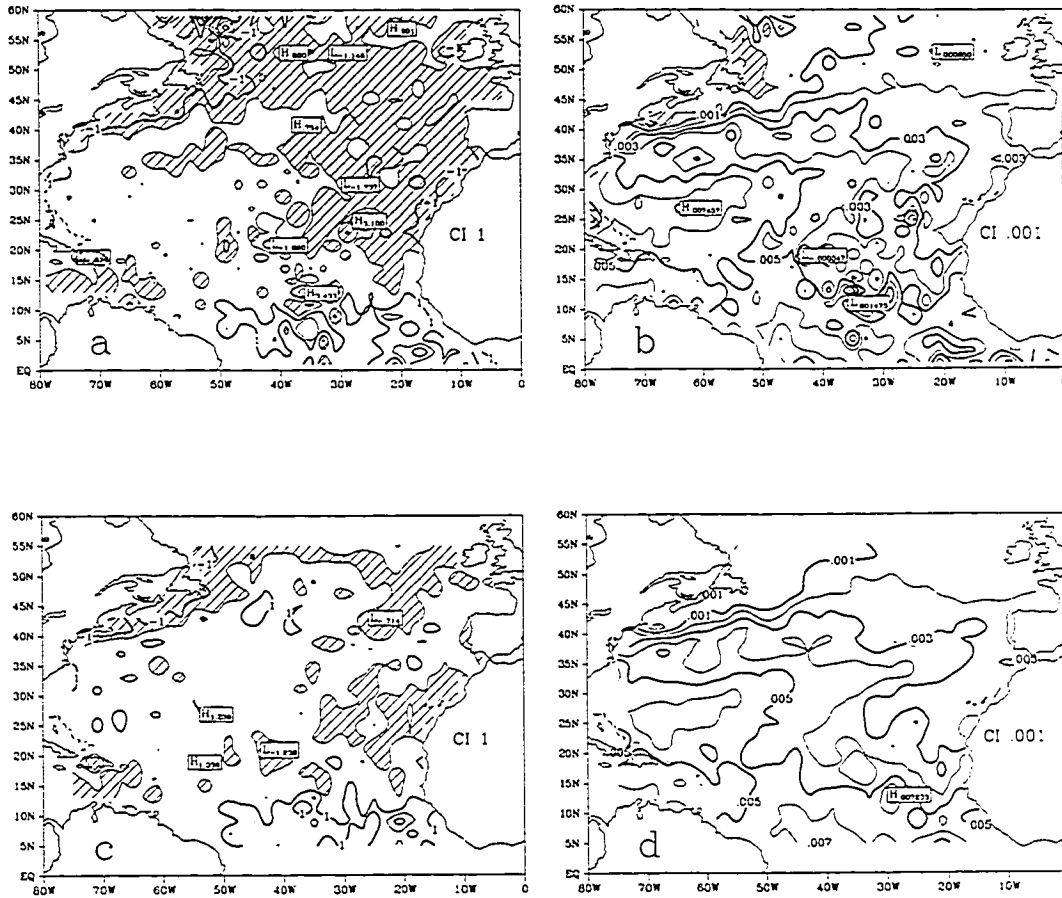
Figure 14. SST-AT for first guess (a) and for results (c). Qs-Q for the first guess (b) and results (d) for the case with final weight selection for July 7 - August 7, 1978. Units are °C and kg kg^{-1} respectively. Data have been smoothed slightly. Shading indicates regions of negative values. Contour intervals (CI) are as listed.

negative to slightly positive. But recall that H is small making these values less critical in relation to the entire heat budget. Additionally, the magnitude of Qs-Q increased north of the western Gulf Stream and north of Newfoundland resulting in larger (positive) E fields, but retained the majority of the established Qs-Q structure. The large-scale characteristics of the original fields are retained in the results and the erroneous extrema located primarily in the southern half of the basin were effectively filtered.

In these July results, the location of the Bermuda High is to the NW of its usual location, Fig. 15. Generally cooler conditions are present in the eastern and northwestern Atlantic. In these same regions, the air is also drier than normal, but only by 1 g kg^{-1} typically. There is one location of warmer moist air at 60°W, 40°N where the wind circulation has brought to the north some tropical air, resulting in smaller H. Wind stress is generally weaker than normal by 0.02 N m^{-2}. H is anomalously weak in the west and north. E is also weak (due to light winds) excepting a small region in the south. There is a southwest - northeast band from Brazil to 35°W, 45°N where E is higher near climatology because of the combination of high Qs and low Q.

The August period (August 7, 00Z - Sep. 7, 00Z) results (see Appendix) indicate the winds since July have broadly strengthened in the north and slightly weakened in the southwest and off northwest Africa. The Bermuda High circulation has shifted southward and slightly eastward. SST and AT were warmer by 0.5 - 1.0°C north of 30°N, but they are still 0.5 - 1.0°C below normal south of 30°N. Q became much higher in the north and west due to the change in atmosphere circulation, and Qs also increased slightly. The tropics were dryer than normal. Stress increased in the north, but were again weaker than normal. They also weakened in the south, but were at or above normal -mirroring the
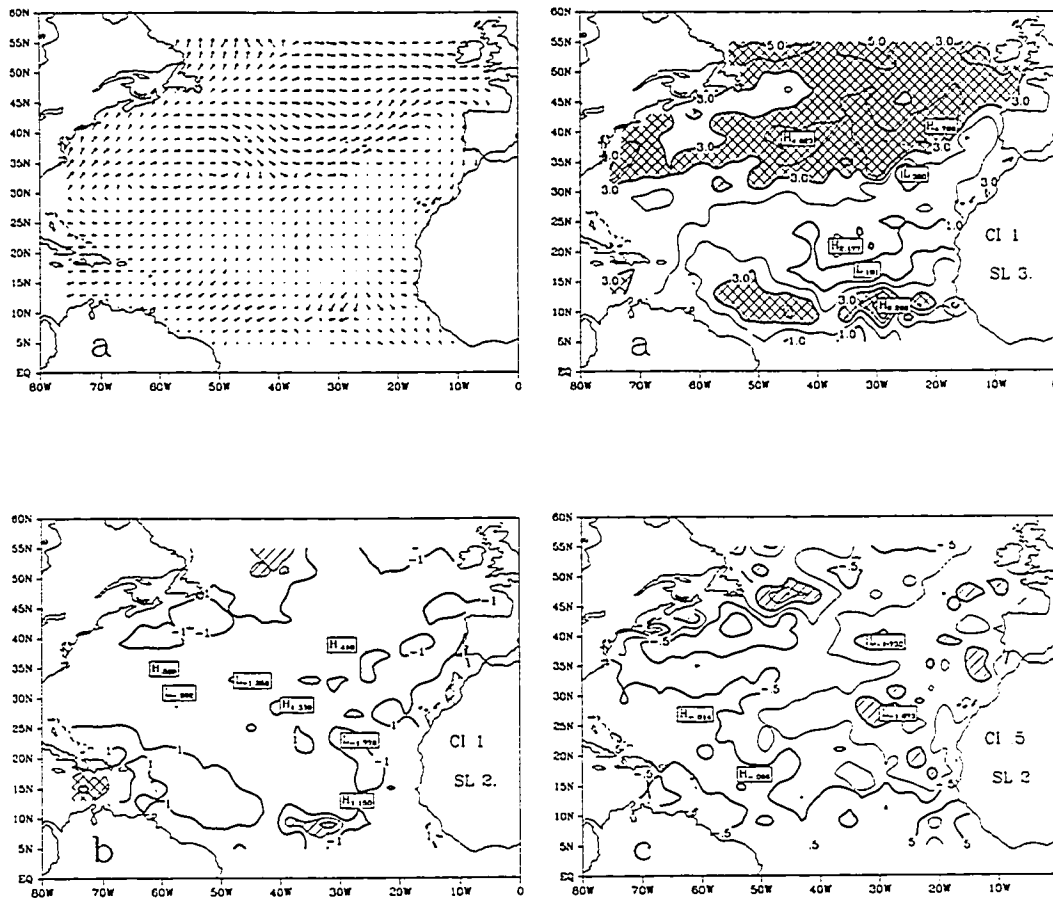
Figure 15. The difference between the July 7 - August 7 analysis results and the Bunker July climatology: a) wind vectors and magnitude, b) wind speed, c) SST, d) AT, e) Q, f) Qs, g) stress vectors and magnitude, h) H, and i) E. Contour intervals (CI) are listed and units are as before. Shading is indicative of negative values (hatching is in one direction only) and positive values (cross-hatching) which exceed the listed shading levels. (SI)
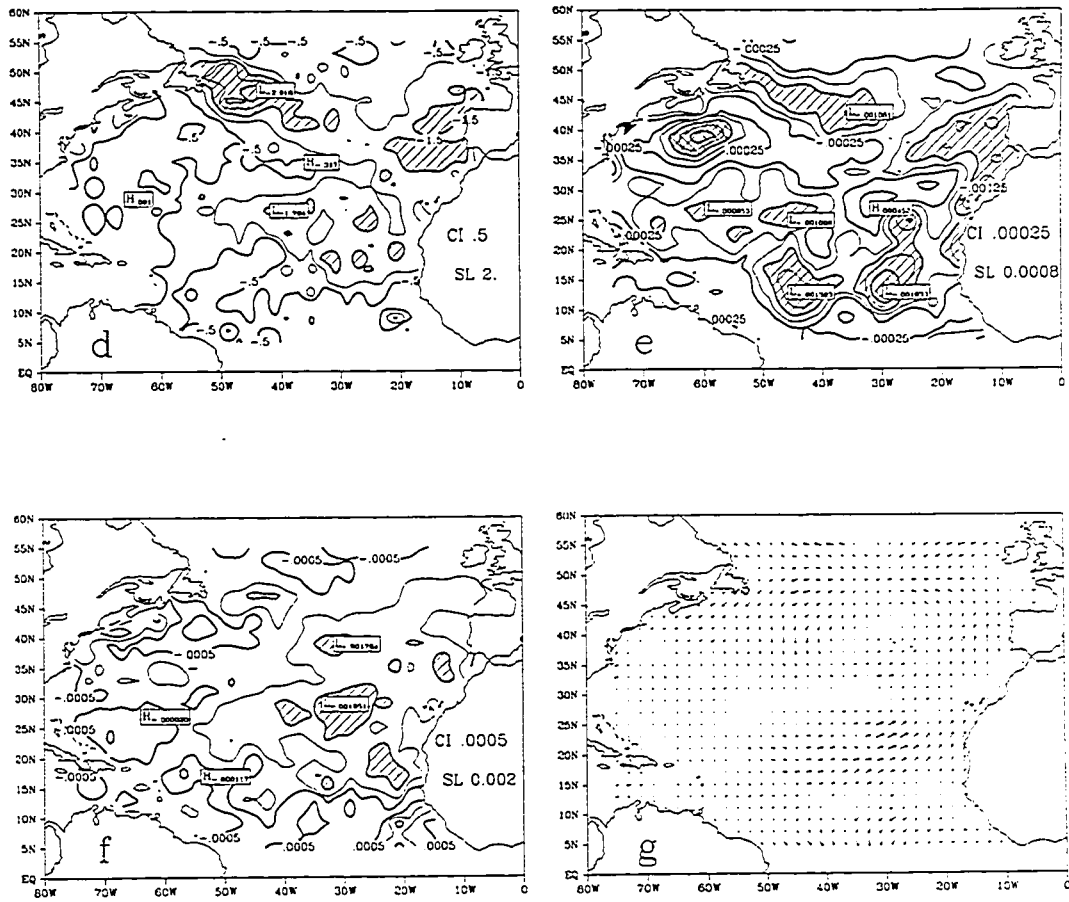
Figure 15.   (Continued)
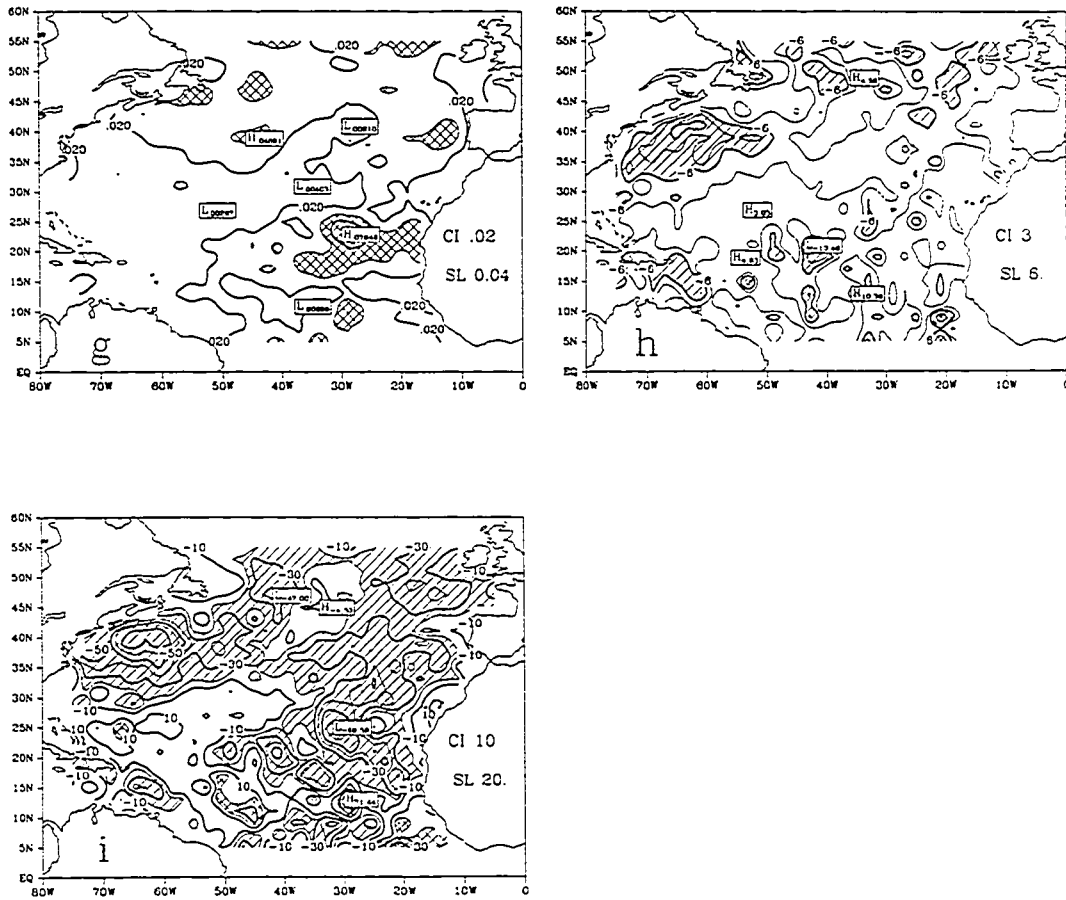
Figure 15.   (Continued)

changes in the winds. H and E increased overall from July (as did the climatological values) particularly in the west, 20-45°N where SST-AT and Qs-Q increased significantly. Again the heat fluxes were broadly weaker than climatology in the north, and marginally larger than climatology in the south. Combined heat flux east of Newfoundland had some particularly high negative anomalies (weaker than climatology), nearing 100 W m^{-2} - principally due to low Qs. The basin average climatology anomaly indicates an underestimation of the climatology of the combined heat flux by 35 W m^{-2}.

The third month of the analyses, Sept. 7, 00Z - Oct. 7, 00Z (Appendix), was marked by the shift in position of the Bermuda High circulation to the northeast, to 18°W, 45°N. Most of the winds north of 25°N are anomalously large as a result, but wind speeds are in general still too small. In the tropics, the winds are nearly normal except in proximity to the African coast where there are anomalous southerlies. Other fields are affected by the circulation change as well; both SST and AT are above normal by up to 2.5°C and 4.0°C respectively in the region of the anomalous wind portion of the anticyclone; north of 30°N and east of 40°W by virtue of the forced ocean and atmospheric circulation. Due to the displaced high pressure circulation and therefore weak southerlies and strong southward intrusion of the cold Labrador Current, northeast of Newfoundland there is a cool anomaly. The tropics have returned to near normal temperatures. The northern two thirds of the basin is still moist except again near Newfoundland, 50 - 60°W, 35 - 45°N where Q is smaller than normal. This area initially had high Q values, but is appears this was reduced by 1 g kg^{-1} during the analysis resulting in higher E. Stress fields follow the wind fields leading again to anomalously weak values in the tropics as well as in the northern half of the basin. Midlatitude H and E increase in magnitude since

August (particularly in the northwest quadrant) following the seasonal norms, and in the tropics, both decrease from August values. Only south of 20°N are there heat flux values larger than climatology. SST-AT and Qs-Q are much larger in September than in August and have a wider range.

4.2 Monthly Results Compared to Servain Data

The 3 analysis months SST results were compared to monthly SST analysis by Servain (Servain (1991)) interpolated to the correct time periods. The differences were primarily in two locations: immediately west of Africa at 22°N, 20 - 30°N and in the areas 30 - 40°W, 5 - 15°N - an area of typically few observations. In each case, the analysis results were cooler than those of Servain's analysis by as much as 1.2°C. RMS errors for the three periods, July, August, and September, were 0.41°C, 0.33°C, and 0.24°C respectively. These differences in the open ocean area may be explained partly by the paucity of VOS observations, but the large differences near the west African coast, a well sampled region, are more puzzling. It should be noted that the SST results agree more closely with the VOS mean SST than with the Servain SST in this region.

4.3 Monthly Results Compared to GLAS Data

The GLAS mean heat fluxes for the monthly analysis periods, Fig. 16, are far larger in magnitude than the heat flux results. GLAS H increases in time from 10 to over 100 W m^{-2} along the northwest Atlantic; Newfoundland to New Jersey. Objective results of H likewise indicate an increase centered in a tongue offshore, but from -5 to 0 W m^{-2} increasing to over 25 W m^{-2}. Near shore results do not change significantly as do the GLAS fluxes where the increase occurs
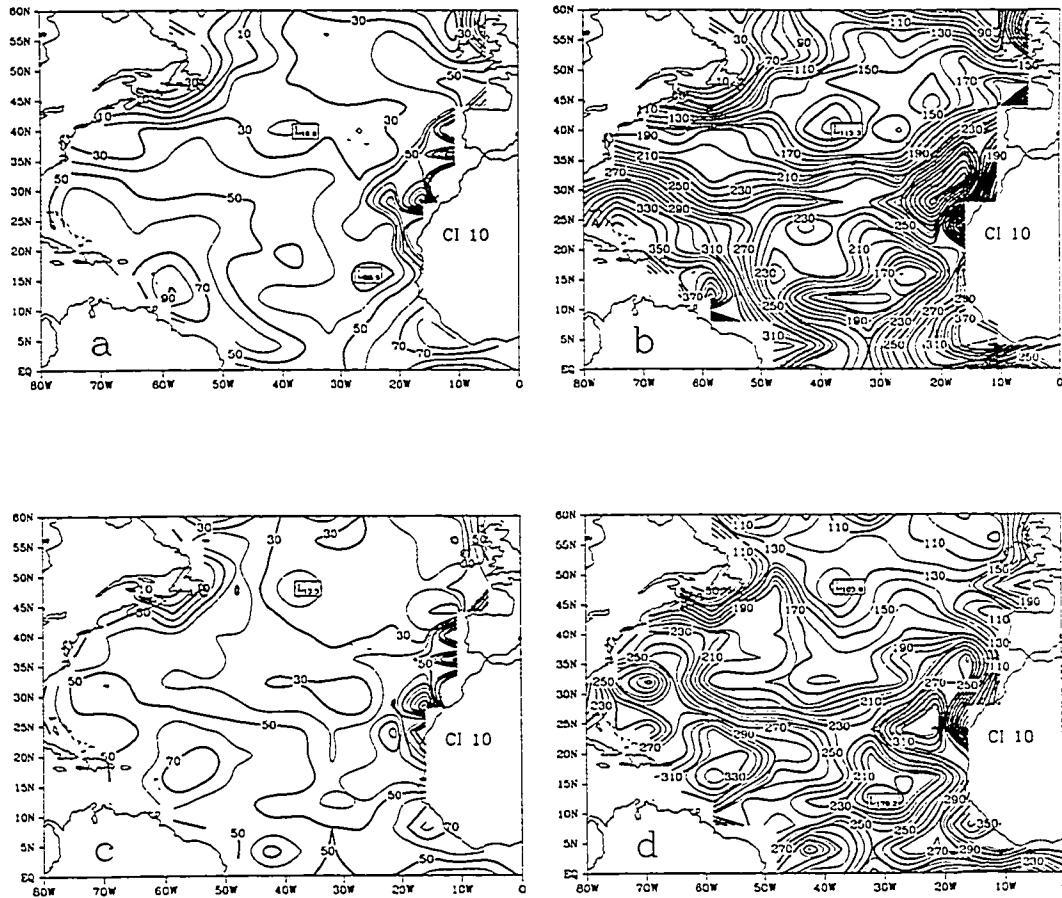
Figure 16.   Sensible and latent heat flux means from the GLAS GCM for July 7
- August 7: (a,b), August 7 - September 7: (c,d), and September 7 -
October 7: (e,f). Units are W m⁻² in both cases. Contour intervals
(CI) are as listed.
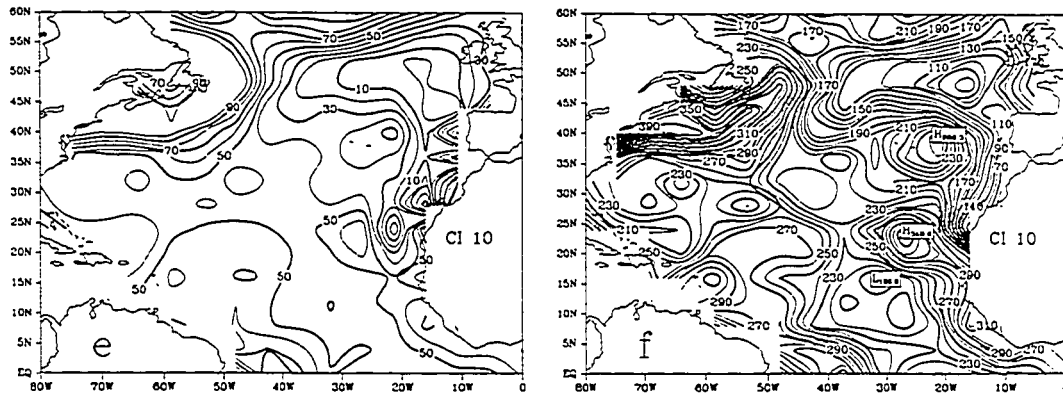
Figure 16.   (Continued)

near-shore and extends uniformly offshore. This discrepancy might be explained by the fact that the GLAS resolution (5° in longitude) is inadequate to resolve this tongue-like detail.

Latent heat values from GLAS are highest in September and lowest in August whereas the results of E generally increased with time. The July maps agree only in the maxima off the northeast coast of S. America and at 10-12°N, 30-40°W. The northern half clearly does not compare structurally. August maps however are more similar. The maximum at 50-60°W, 15°N is reflected in both the GLAS and resultant E fields. The structure in the northern half agrees fairly well; a southwest to northeast oriented tongue of minimum values stretches from the northeast to 50°W, 32°N with generally zonal orientation north of 45°N. Not present in the GLAS values is a high gradient near the North American branch of the Gulf Stream. September maps also compare favorably (structurally) with extrema matching in the south, tight gradients in the northwest and a minima tongue stretching westward from Europe to 35°W.

4.4 5-Day Results

The above experiment for monthly periods was repeated for 5-day periods July 7, 00Z to October 10, 00Z (Appendix). The same technique was applied and the same weights and weight scheme were used (over 50 other weight schemes were also tested but without significant improvement to the results based on the OWS-R and many-VOS location comparison criteria). However, as was not the case for the monthly periods, the 5-day VOS fields had several data void regions for each period. For the first guess, these wind (pseudo-stress) voids were replaced with SASS pseudo-stress and SST voids were filled with SMMR SST values where available. If no SASS and SMMR or

VOS data were available where needed, first guess fields were obtained from the results of the previous 5-day period results (for the first case, from the monthly results of July 7 - August 7). Convergence criteria remained unchanged and the functional converged for each period in under 50 iterations, most often in under 30 iterations.

4.5 Comparison of 5-day Results to OWS-R Data

Comparison of the 5-day results to 5-day means of the separately obtained data from OWS-R was compared for two different cases: the normal analysis results and an additional set of runs of all the 5-day periods, but with no input in-situ information at the OWS-R grid point. This comparison, Table 4, offers insight into the capability of the technique to replicate independently obtained data with no in-situ data used at its location. For almost all the variables, the inclusion of data at the OWS-R grid point is beneficial and increases the correlation and reduces the RMS differences to the independent OWS-R data. There is very good correlation for all variables in both cases, but temperature variability for the 'no OWS-R' results is slightly less well-defined than in the case including the VOS OWS-R data. The RMS differences are smaller when the analysis method has in-situ information, but the temperature RMS differences reduce only marginally indicating a level of uncertainly in the full OWS-R measurements that is not being resolved by the available in-situ and remotely-sensed data. The high correlation and the relatively high magnitudes of the heat flux RMS differences are partly due to the underestimation of the wind speed. Magnitudes of the flux RMS differences are smaller than those general uncertainly estimates for seasonal means given by Lambert and Boer (1988).

Table 4.   Correlation and RMS differences between 5-day objective results (run normally and without any information at OWS-R grid point) and 5-day means of separately obtained OWS-R data (calculations performed with 85% of points (eliminates 3 of 19 points) with smallest difference values).

	Analysis w/ VOS OWSR		Analysis w/ no in-situ, no OWS-R data at OWS-R location	
	Correlation	RMS difference	Correlation	RMS difference
U	0.96	1.6 m s^{-1}	0.97	1.17 m s^{-1}
V	0.97	0.90 m s^{-1}	0.94	1.26 m s^{-1}
W	0.99	0.87 m s^{-1}	0.98	1.75 m s^{-1}
SST	0.91	0.65 °C	0.89	0.68 °C
AT	0.87	0.56 °C	0.79	0.62 °C
Q	0.96	0.22 g kg^{-1}	0.93	0.34 g kg^{-1}
Qs	0.99	0.10 g kg^{-1}	0.94	0.26 g kg^{-1}
Tx	0.97	0.013 N m^{-2}	0.96	0.019 N m^{-2}
Ty	0.95	0.012 N m^{-2}	0.88	0.018 N m^{-2}
H	0.99	0.8 w m^{-2}	0.78	4.5 w m^{-2}
E	0.98	11.9 w m^{-2}	0.84	22.3 w m^{-2}

Correlations of the 5-day results of H and E to 5-day means of GLAS H and E that were interpolated to the same grid as the results were very poor. The mean correlation for both H and E was near 0. There were a few isolated points where correlations were greater than 0.50, but there were also a few with negative correlations of the same magnitude. The poor spatial resolution and old age of the GLAS GCM clearly are conditions leading to these poor correlations.

5. ANALYSIS OF RESULTS

An additional method whereby the technique can be assessed is comparison of the mean of the results over the entire analysis period to the same mean from VOS observations. If there is a systematic deficiency in the objective analysis technique, this type of comparison should identify it. The monthly and 5-day results long term mean (hereafter referred to by MRM - Monthly Result Mean and WRM - Weekly Result Mean, respectively) when compared to the VOS means for the entire analysis period (VM) showed westerlies were 2-3 m s^{-1} and 1-2 m s^{-1} stronger north of 30°N respectively. This is no doubt due to the nature of wind means being very small in areas of variable winds and the treatment in this technique of winds as pseudo-stress. As already discussed, the monthly wind results overestimate the magnitude of these winds, while the 5-day wind results were more realistic. In the tropics, each wind result mean is at or slightly weaker than VM except for the eastern branch of the ITCZ where the results again overestimate VOS means. Wind speed differences are relatively small, with largest values ~0.5 m s^{-1} in the northern half of the basin.

The SST result means are more similar to each other than were the two wind mean results. The SST result means are both broadly warmer than VOS means, but by less than 0.5°C, with the largest difference values east and south of Newfoundland - an area of high SST variability. The mean difference between results mean and VM over the entire basin was less than 0.1°C.

73

AT results were generally cooler for both WRM and MRM. The difference between them and VM indicates a broad cool bias for the results of again less than 0.5°C. AT results are especially cooler east and south of Newfoundland. Note that the larger differences were mostly found along coastal and boundary areas, particularly for the 5-day results.

The WRM of Tx and Ty are closer to VM than are the MRM. The largest differences are in the north and off northwest Africa. The 5-day results did a poorer job than the monthly results of accurately depicting the mean heat fluxes. Both WRM and MRM were higher than VM for H in the northwest - in some locations, H result means had the wrong sign, but when considering the entire basin, VM H was larger. The mean of results for E were higher than VM. The differences were distributed primarily over the western and southern parts of the Atlantic basin. The largest discrepancies against the 5-day mean E were in the tropical Atlantic, while for the monthly mean, the largest differences were in the tropical and northwest Atlantic.

The RMS differences, Table 5, demonstrate that the 95-day mean of temperatures, humidity, H, and E are fairly well represented by both the 5-day and monthly results. For mean winds and stress though, using 5-day results is better due to the use of pseudo-stress and the tendency for the longer time periods to have smaller mean winds. The MRM heat flux values have marginally better agreement with VM probably because of the better results for monthly temperatures and humidities. In all cases except for the winds, the RMS differences are substantially lower than the natural variability during this time period - a good indication of the quality of the results. Overall, this indicates the 5-day results are comparable to monthly

Table 5.   RMS differences between overall 95-day mean of VOS data, and mean of all results.

	95-day VOS mean and mean of 5-day results	95-day VOS mean and mean of monthly results
U (m s^{-1})	0.99	2.1
V (m s^{-1})	0.66	1.1
Wind Spd (m s^{-1})	0.63	0.58
SST (°C)	0.34	0.29
AT (°C)	0.42	0.38
Q (g kg^{-1})	0.37	0.39
Qs (g kg^{-1})	0.32	0.26
Tx (N m^{-2})	0.014	0.015
Ty (N m^{-2})	0.011	0.012
H (W m^{-2})	2.1	1.7
E (W m^{-2})	11.1	8.77

results and if monthly means are needed, it may be advantageous to average the 5-day results.

The variability of the 5-day results, Fig. 17, is similar to climatological estimates (Isemer and Hasse (1987);Bunker (1976)) in structure, but are smaller (as expected since this is a comparison between variabilities over two vastly different time spans). Maximum wind component variability is concentrated north of 45°N where the movement of the semipermanent Bermuda high pressure systems occurs, and in the region of the ITCZ (extends from the African coast at 15°N westward and southward to Brazil at 5°N) where winds are light, but highly variable. The north-south wind variability has a maximum in the ITCZ region which envelops the position of the ITCZ during the analysis period. Zonal wind component variability is slightly more variable than that for the meridional component. SST variability is centered in the Gulf Stream; from Cape Hatteras north and then south and east of Newfoundland. The SST variability maximum in the eastern Atlantic indicates variations in the southward return flow of the N. Atlantic Current, but may also be influenced by upwelling along the northwest African coast, and variability of the Canary current. The minima running north-south, from 50°W, 30°N to 30°W, 55°N is a feature not seen in climatologies and is the result of specific circulation patterns during the analysis period. Variability in AT is much larger overall than for SST, particularly in the northern half of the basin where advection around the shifting location of the the high pressure anti-cyclonic circulation pattern is to blame. In the tropics, it is comparable to SST variability, but according to climatological estimates, tropical AT variability is ordinarily greater than tropical SST variability. Humidity variability is maximum over the Gulf
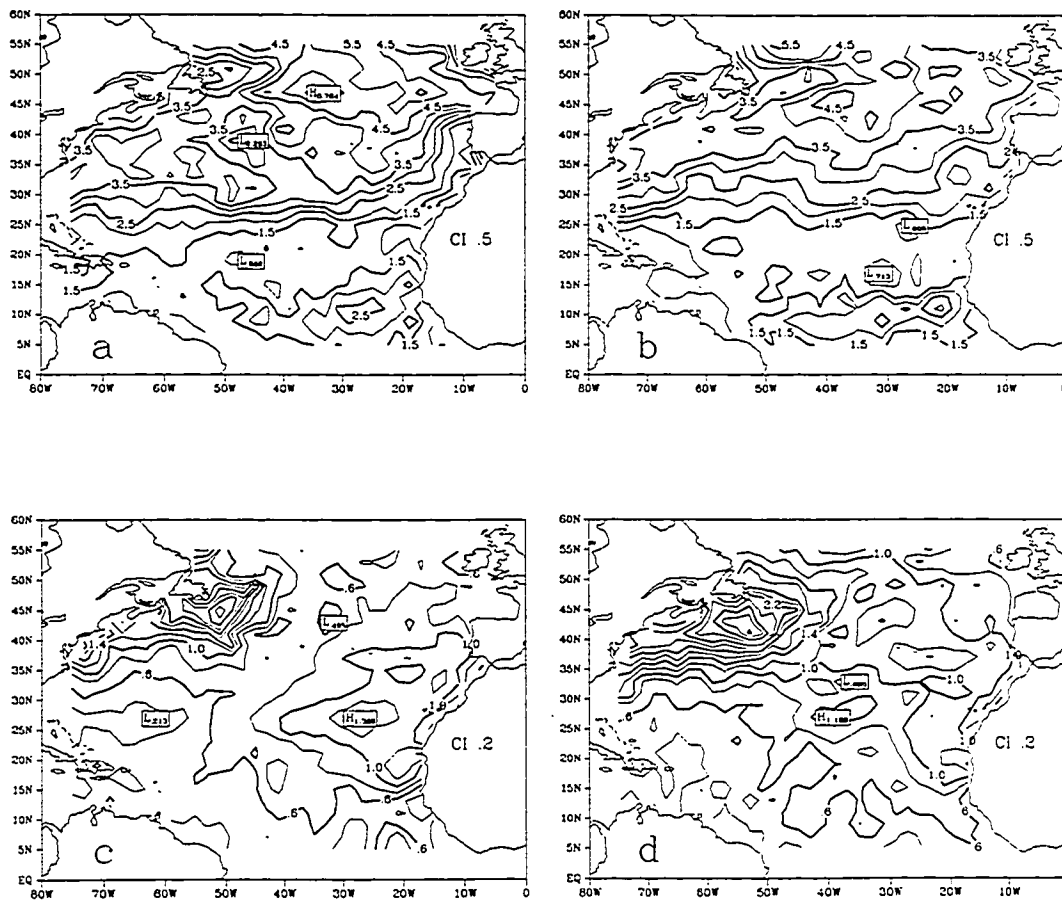
Figure 17.   Standard deviation of the 5-day results over the 95-day analysis
             period for a) eastward wind, b) northward wind, c) SST, d) AT,
             e) Q, f) Qs, g) Tx, h) Ty, i) H, j) E, k) SST-AT (°C), and l) Qs-Q (kg
             kg⁻¹). Contour intervals (CI) are as listed.
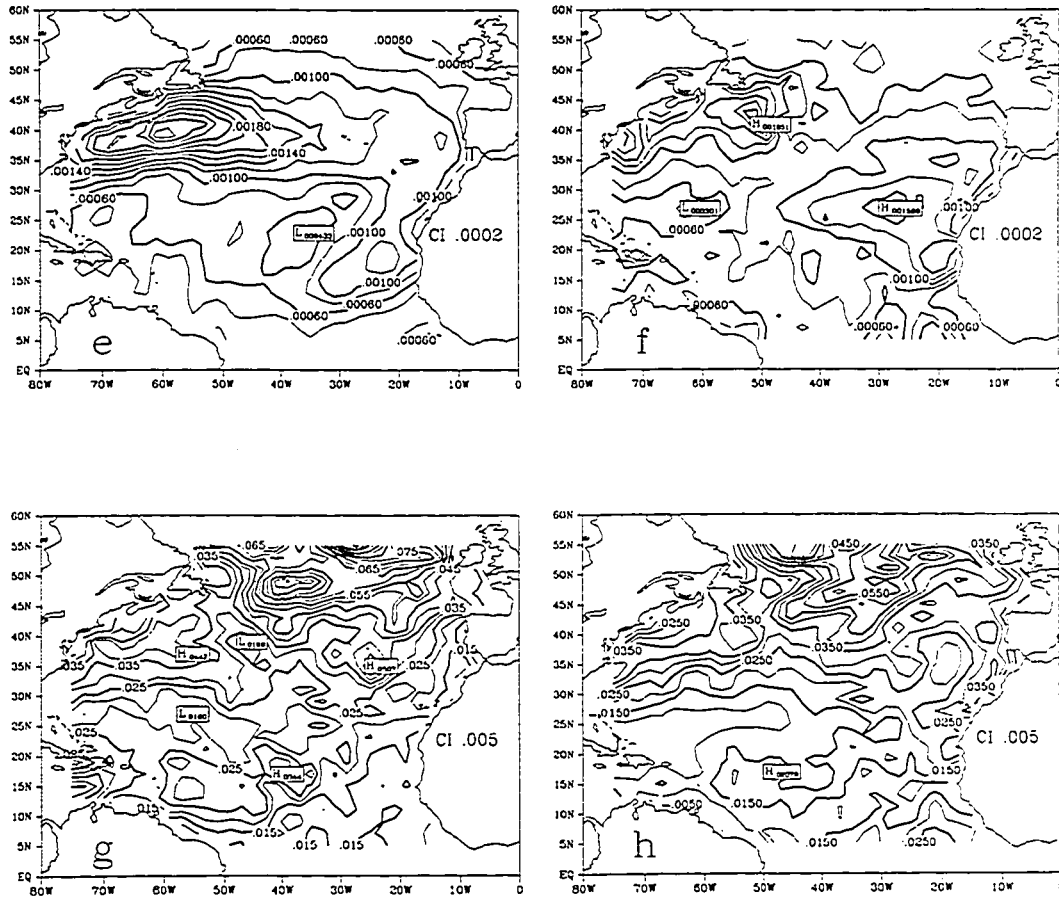
Figure 17. (Continued)
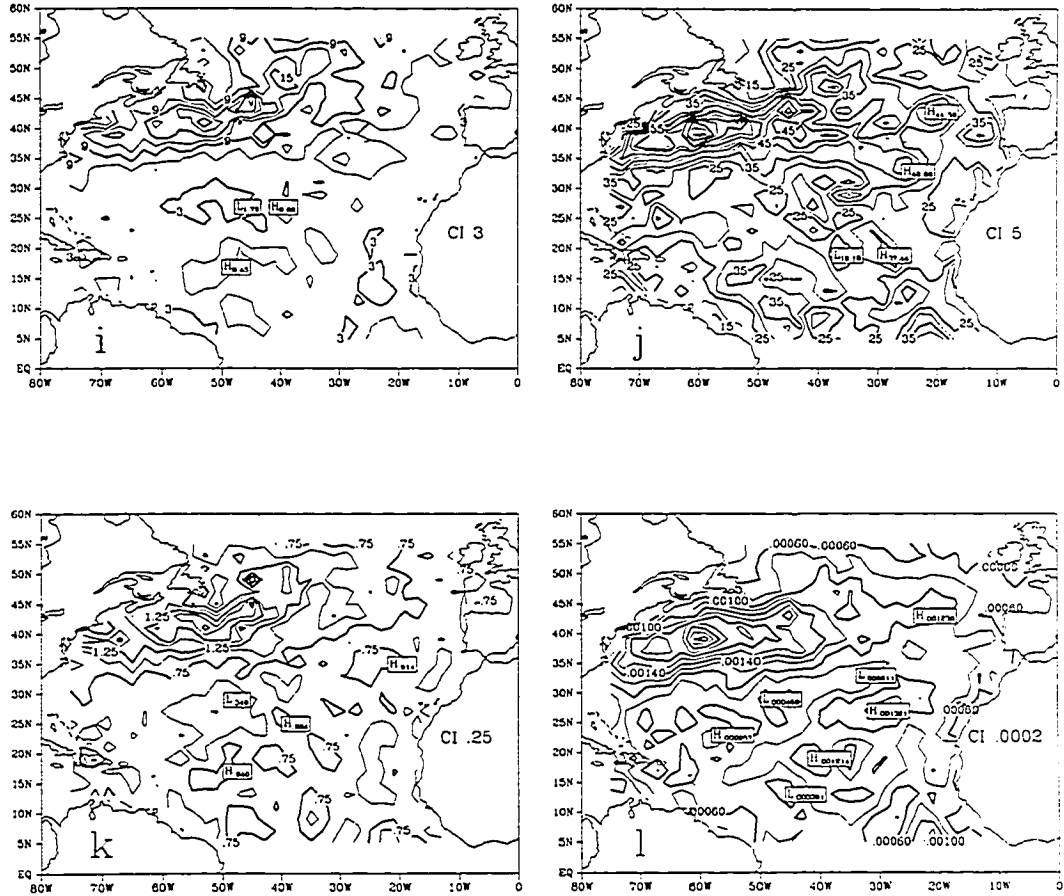
Figure 17.   (Continued)

Stream with maximums of over 2 g kg^{-1}. This maximum straddles the position of the North Atlantic current and likewise follows the general circulation of the mean wind field turning south west of Europe and extending into the tropics at 20°N. The advection of cooler/dryer air over the Atlantic from North America and the subsequent southwestward advection in the eastern Atlantic is highly variable as are the synoptic conditions that generate these patterns. The stress variability follows that of the wind in the north, but unlike the wind pattern in the tropics, stress variability is higher in the vicinity of the trades than in the region of the ITCZ; something found in the interannual time scales as well (Cayan (1990)). Wind speed, temperature, and humidity variabilities are all slightly higher in the trades than in the ITCZ; these affect the variability of the drag coefficient, and therefore possibly contributing to the creation of this high stress variability. H is most variable where the variability of the temperatures is maximum; over the Gulf Stream and North Atlantic currents, and where SST-AT variability is highest. The eastern and southern regions of the Atlantic have variabilities of less than 6 W m^{-2} which is sometimes higher than the typical magnitude of H itself. Latent heat variability is similar to Q - Qs variability in the north, but in the southern half, there is more deviation from this agreement.

Correlations between the 5-day results and the VOS 5-day means for SST, AT, U,V, Q, Qs, Tx, Ty, H, and E are very high (exceeding 0.75) in areas corresponding to the availability of plentiful VOS observations (i.e. north of 35°N; in the southwest, and along the coastal regions). East of Newfoundland at 30°W to 50°W and in the southeast Atlantic (southeast of a line from 55°W, 15°N to 20°W, 35°N) the correlations are not as high (or

nonexistent) because of the lack of VOS data from which to make a correlation calculation.

Correlation of 5-day results to 5-day means of remotely sensed winds and SST were also calculated. In the southeast, SASS correlations to wind results were better than VOS correlations to wind results (no doubt due to availability and dependence on SASS data in this region), but the SASS correlations were generally less than 0.75. The north-south SASS wind to resultant north-south wind had smaller correlations than the east-west component correlations. The best correlation between both northward and eastward SASS and result winds was in the southwest and the northeast, both regions where wind speed is relatively high, but not all areas of high wind speed had high correlations. SMMR wind speed to result wind speed correlations were mild and generally positive with highest values (exceeding 0.75) in the northeast and southwest again; SMMR SST correlates very well with the results except in the Gulf Stream extension (North Atlantic Current) where the SST results correlate better with VOS SST. In the southeast Atlantic, where there are relatively few data, results correlated much better (0.5 to 0.75) with SMMR SST than with VOS SST.

5.1 Heat Fluxes for 5-day Periods

The latent and sensible fluxes for the 5-day period are well correlated during the analysis period meaning the impact of these fluxes is most often additive. Correlations are generally greater than 0.5, and north of 30°N, exceed 0.75. The mean correlation, 0.71, is slightly higher than some previous estimates (Siegel (1977)). In the vicinity of the northwest African coast, upwelling reduces evaporation in a very narrow region, which in turn

reduces both H and E close to zero and creates a weak and even negative correlation between H and E.

Correlations between H and SST and also H and AT show that in most of the Atlantic north of 30°N, there is high negative (~-0.75) correlation between H and AT, but that little exists between H and SST. In general, wind speed is not correlated to H anywhere, but from H-V correlations it is clear northerly winds that generally occur in the band 25°W to 35°W, 35°N to 45°N advect cooler temperatures into more moderate regimes and likewise increase H. Likewise in the eastern Atlantic, southerly winds bring warm tropical air north, decreasing H. In the east Atlantic there is decreased correlation between H and AT but increased correlation with SST. In this eastern Atlantic region off northwest Africa, northerly wind correlates to cooler SST and demonstrates that wind driven circulation (i.e. coastal upwelling, North Atlantic current) is determining H. In the tropical region, correlation between H and SST is comparable to that between H and AT demonstrating that tropical H has no definite dependence on a specific thermal condition of the air or sea. Thus, in the northern Atlantic, H is primarily determined by the temperature of the air being advected by north-south winds over the ocean. However in the eastern Atlantic, this is not so, rather H is coupled to wind-driven SST variability.

Latent heat flux variations are primarily driven by Qs - Q north of 35°N and this is due mostly to a negative relationship between Q and E, i.e. the advection of cooler and dryer air in the north to the south and east enhances evaporation/latent heat capability (Fig. 18, 19). In the area of largest values of E, i.e. the Gulf Stream, E is best correlated to Q and V - advection of warm wet air into this extra-tropical region. In the southwest Atlantic where
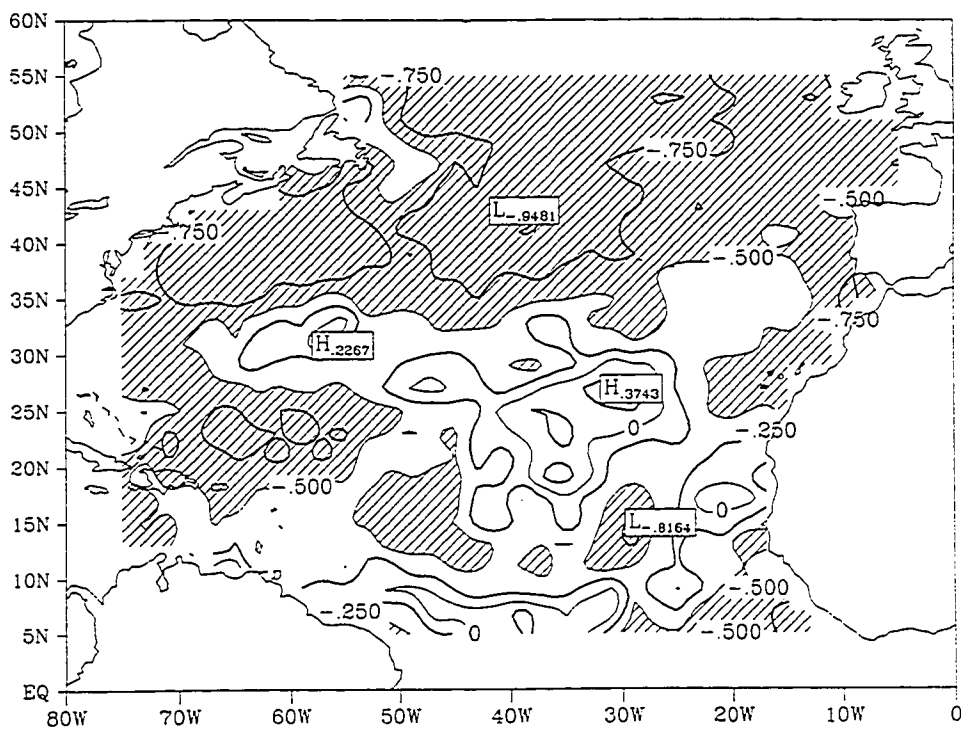
Figure 18.   Correlation between 5-day results of E and Q. Contour interval
is 0.25, and shading highlights areas of negative correlation
with magnitudes exceeding 0.5.

Figure 19.   Correlation between 5-day results of E and V (northward wind).
Contour interval is 0.25. Shading represents negative
correlation with magnitude exceeding 0.5, cross-hatching is for
positive correlations with magnitudes exceeding 0.5.

E is de-coupled from Qs - Q , E is better correlated with the wind speed (primarily the easterlies) than with differential humidity. Easterlies are advecting dryer African air westward, creating larger E. In the southeast, E is correlated to both the differential humidity as well as to winds.

North-south winds determine H and E in the northern half of the basin because the orientation of the temperature and humidity fields are zonal, i.e. cross gradient winds advect relatively cool/dry or warm/wet air into the relatively opposite climatological regimes. The north-south oriented structure of the correlation of V with AT, Q and SST, Fig. 20, 21, and 22, is consistent with expected anti-cyclonic, high pressure general circulation patterns found in the north Atlantic during summer. At the center of the circulation pattern there is little correlation between the winds, temperatures, and humidity. There is zonal circulation north of the center which has little or no effect, since the temperatures and humidity are oriented zonally. Northward (southward) advection of AT and Q which results in anomalous H and E occurs east (west) of the circulation center generating relatively lower (higher) heat flux values. In the southern half of the basin where gradients are meridional in the east and zonal in the west, E is determined in the west by easterlies which are in the southernmost area of the high pressure circulation.

The relationship between surface fluxes and SST has its roots in the bulk formula as well as in atmospheric feedback. In the tropics, the incoming solar radiation is responsible for much of the variation in SST on seasonal time scales. For intraseasonal time scales, local variations in SST can directly affect the solar input at the ocean surface (and associated changes in cloudiness) (Chertock, et al. (1991)). Likewise in the tropics, latent heat
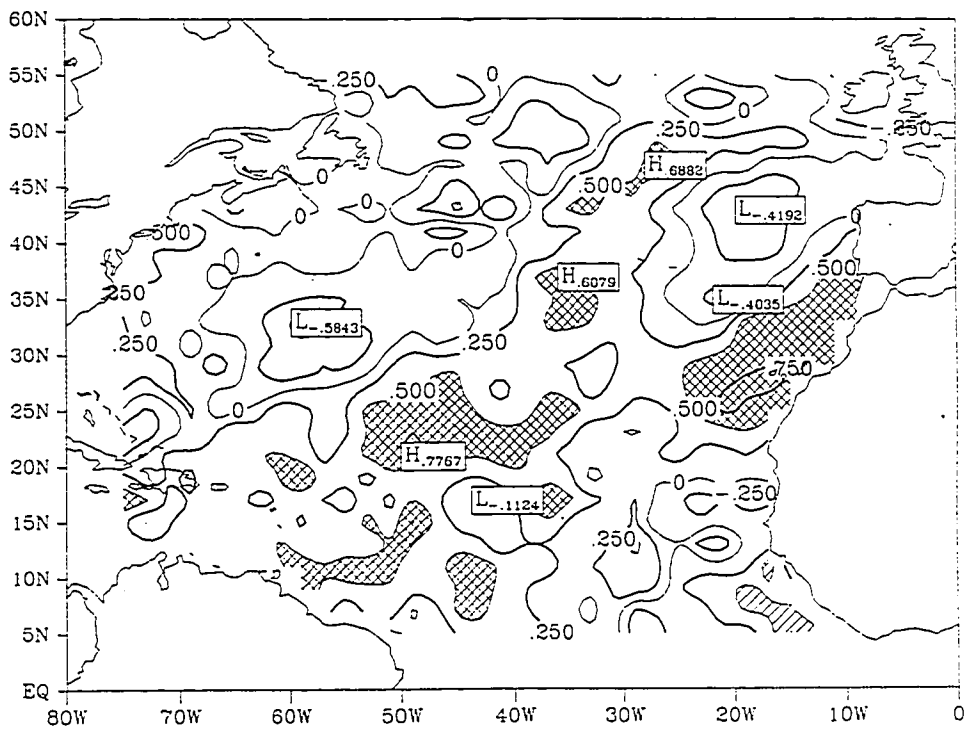
Figure 20. Correlation between 5-day results of SST and V (northward wind). Contour interval is 0.25. Shading represents negative correlation with magnitude exceeding 0.5, cross-hatching is for positive correlations with magnitudes exceeding 0.5.
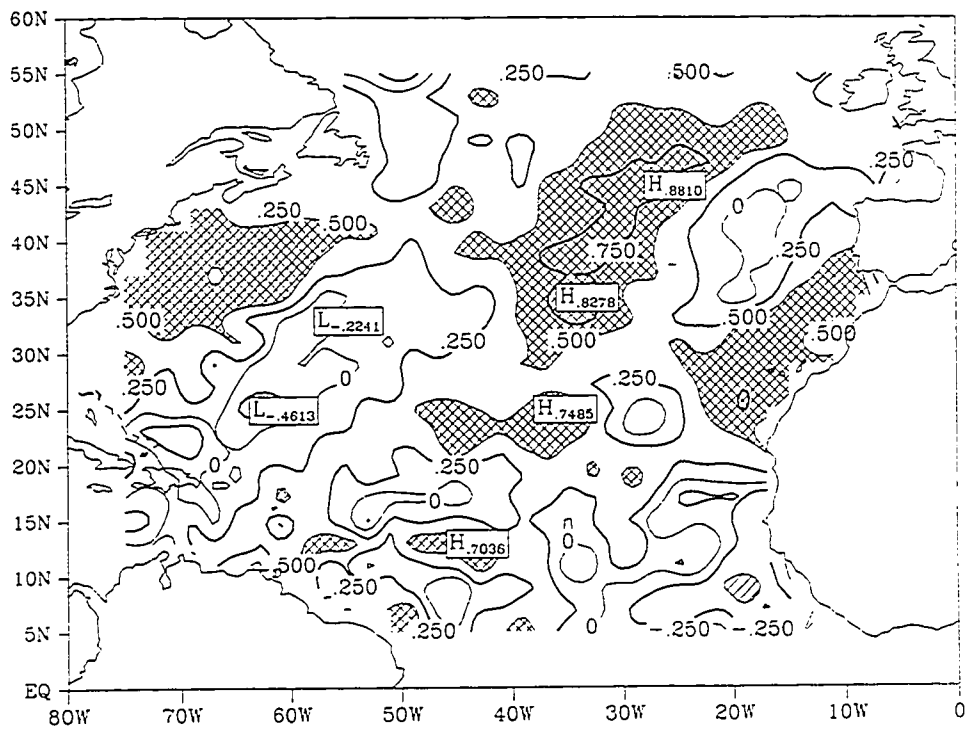
Figure 21. Correlation between 5-day results of AT and V (northward wind). Contour interval is 0.25. Shading represents negative correlation with magnitude exceeding 0.5, cross-hatching is for positive correlations with magnitudes exceeding 0.5.
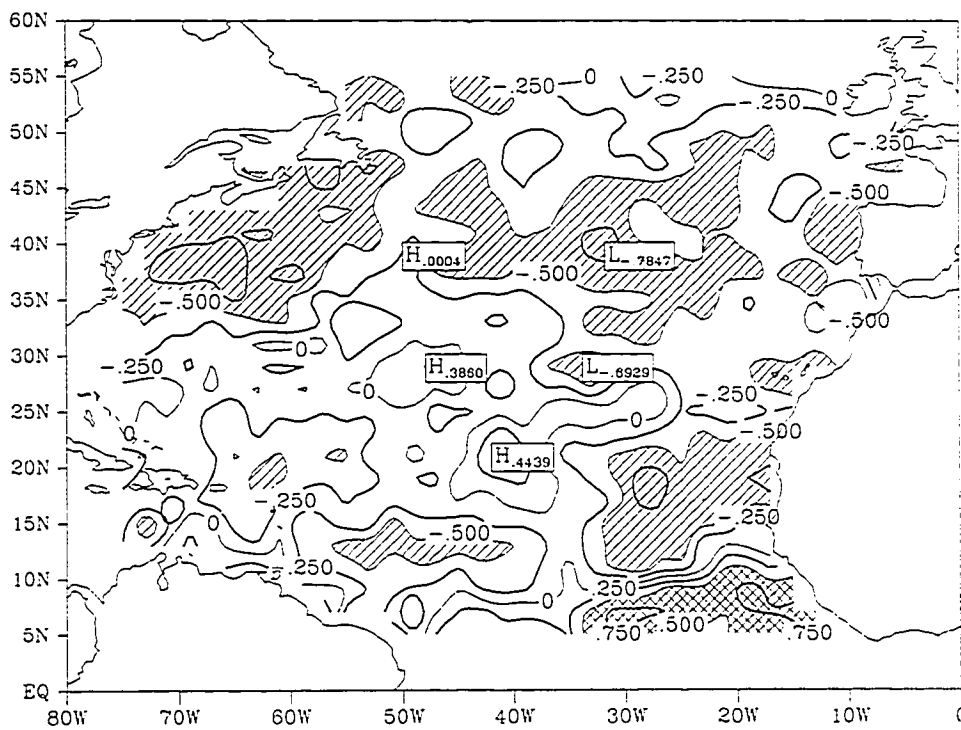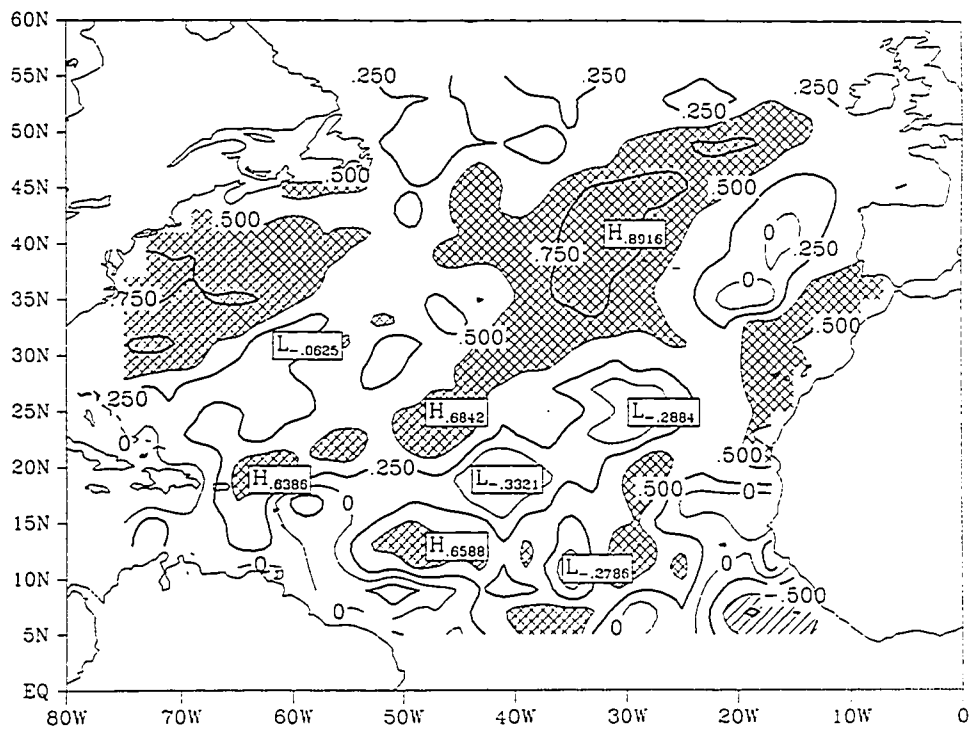
Figure 22.   Correlation between 5-day results of Q and V(northward wind).
Contour interval is 0.25. Shading represents negative
correlation with magnitude exceeding 0.5, cross-hatching is for
positive correlations with magnitude exceeding 0.5.

flux is a major contributor to SST variability in the tropical Pacific during ENSO events (Liu and Gautier (1990)). Driving of the heat fluxes by SST is marked by the strong correlation between SST and heat fluxes at zero lag. The highest such correlations from the 5-day period results are, as expected, in the tropics. Warm SST generates larger H and E values by virtue of the smaller dependence of H and E on winds, as well as the given direct relation of SST to H and the indirect relation of SST to E through Qs. The correlations are greater, 0.5 - 0.85 between SST and H, than between SST and E, but neither is consistent throughout the tropical region. Correlations between SST change in time to H at the earlier time (i.e. SST change lags H) are insignificant, but correlations between SST change and E at the earlier time, show significant negative values (when E is large, SST decreases). These correlations are maximum off the North American coast from Cape Hatteras to Newfoundland. Smaller regions of negative correlation also exist in the eastern Atlantic, just west of Spain. The negative correlation off N. America is in a region where both SST and E are highly variable, ruling out the possibility of a persistence driven correlation. These correlations never exceeded 0.75 in magnitude and must be considered with caution since there are only 19 flux and temperature fields from which to calculate a correlation.

6. ERROR ANALYSIS

There are numerous terms in the error budget for any derived product: measurements are never exact and they may be biased or contaminated in like fashions, the results may be skewed by the particular technique, etc. There are also errors in calculating average quantities if the number of samples in those calculations are insufficient to result in statistically confident average (Legler (1991)). This sampling error is the focus of this section.

The VOS means used as input into the objective technique described in this research are not derived from uniformly dense observations. This makes these means subject to errors by inadequate sampling. A quantitative estimate, statistical sampling confidence intervals, of this type of error can be calculated. We will assume the VOS observations are independent and stationary as required by the sampling theory. The remotely sensed data fields are also averaged quantities, but the individual remotely sensed data are not as statistically independent as VOS data owing to the fact that in any given 2° by 2° box, the average of remotely sensed data is a combination of multiple observations per swath overpass, and therefore, are not generally separated by sufficient time or distance to be considered independent. This is true for SMMR and SASS winds, however SMMR SST have such coarse resolution that they might be considered independent.

We will assume the observations that comprise the mean have normal distributions. Previous research (Legler (1991)) has shown this

assumption results in little error for winds and temperatures at fixed measuring platforms. It will be further assumed that the observations are randomly distributed in each grid box. Weare and Strub (1981) showed the effects of non-random spatial and temporal averaging to sometimes contribute significantly to the errors in calculating mean fluxes. The statistical confidence intervals of the means used as input for the 3 monthly cases presented in this study are calculated using sampling theory:

$$\pm Z_c \frac{\sigma}{\sqrt{N}}$$

where Z_c is the critical value (taken to be 1.96, indicating 95% confidence level), σ is the population standard deviation, and N is the number of observations used in calculating the mean. If N is too small ($N < 30$), the statistical soundness of this particular expression for confidence intervals is compromised and small sampling theory is suggested (which gives wider confidence limits results). Most locations in the Atlantic have at least 30 observations in any given month, but those that don't (mostly in tropics) will not be discussed in detail. Since σ is generally unknown and/or not well defined for many locations in each analysis month, and given that σ for monthly means is both a function of location and the particular averaging period, a climatological estimate of σ is used - the *monthly* standard deviation values available from COADS, for each calendar month in the period 1970 - 1989 were averaged. These values, Fig. 23, are considerably less than climatological estimates of standard deviation values for each variable (Bunker (1976)), which are estimates of σ for the entire data record of several decades, not monthly mean σ's. Climatological estimates
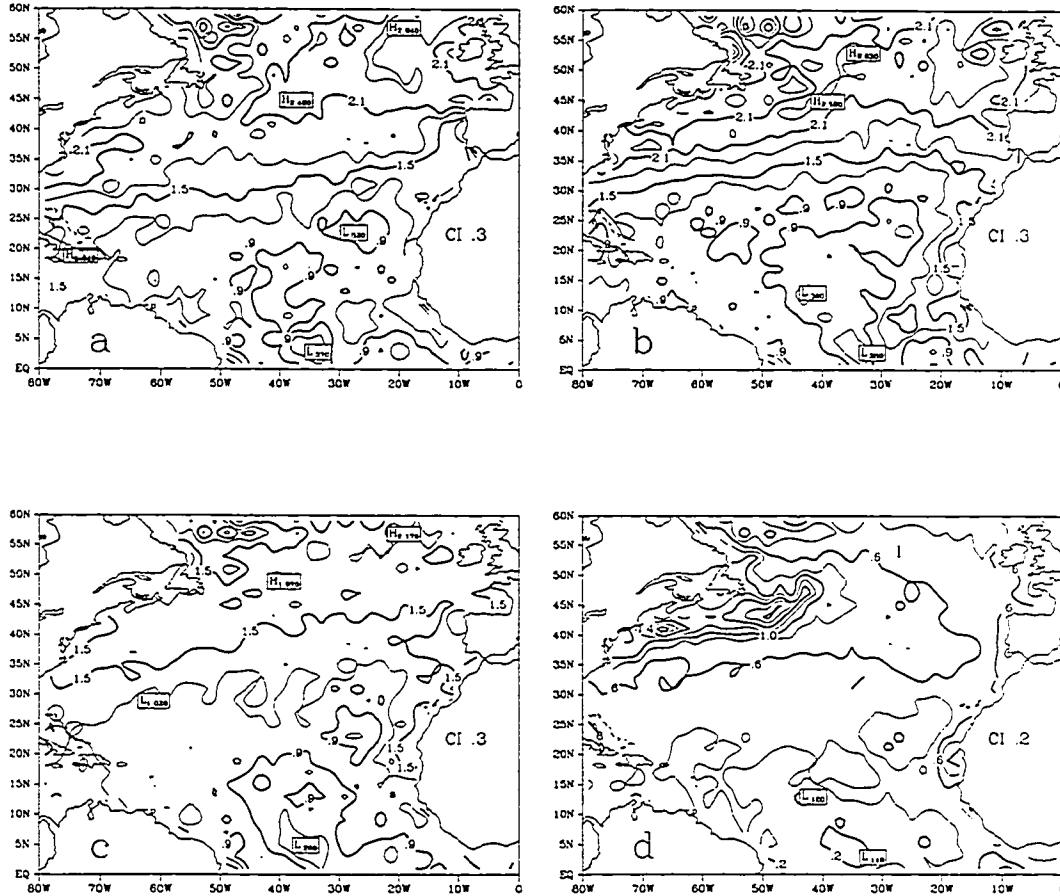
Figure 23.   Mean of monthly standard deviation values from January 1970 - December 1989 from COADS data for a) eastward wind, b) northward wind, c) wind speed, d) SST, e) AT, and f) Q. Contour intervals (CI) are as listed and units are as previously listed except for Q which is in g kg⁻¹.
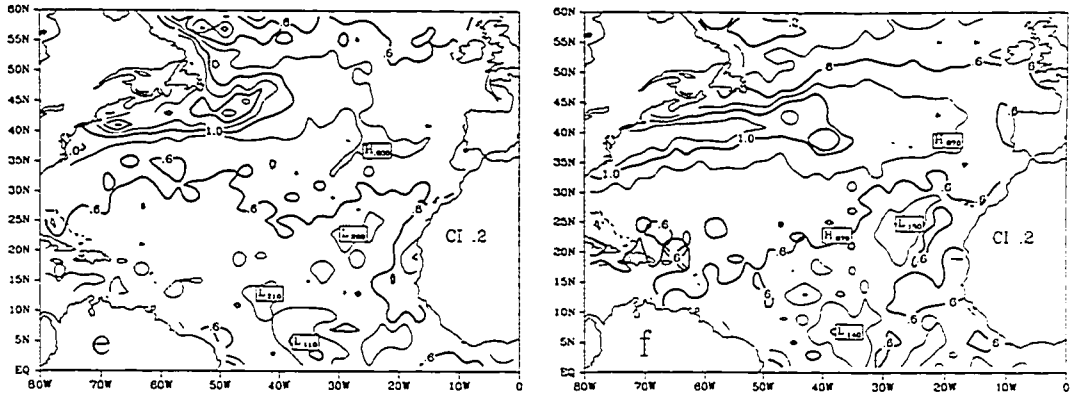
Figure 23.   (Continued).

of monthly σ compare favorably in structure to both the Bunker maps and to the standard deviation maps for the variables during the analysis period. However, the magnitudes are about one half of the climatological standard deviation values and are comparable to the standard deviation values of the analysis period.

Confidence intervals were calculated for SST, AT, U, V, wind speed, and Q for each of the monthly periods on the same grid as the results using the VOS number of observations data. Means for these quantities are shown in Table 6. Smaller confidence intervals for Spd as compared to the vector components agrees with findings by Legler (1991) and demonstrates that because wind speed has naturally less variability than the wind components, there is more inherent accuracy in mean wind speed than in the mean wind components. Confidence intervals for winds and humidity increase in time due to their increasing variability (this rise in confidence intervals should also be considered relative to the increase in mean values of the winds and humidity). An example of the spatial distribution of the confidence limits for this July period is shown in Fig. 24 (a minima in confidence interval indicates a relatively statistically significant mean). Minima are located in the mid-section of the north Atlantic and along the coastal regions, corresponding to the areas of densest VOS coverage (see Fig. 1). For winds, the confidence intervals in the north are generally only slightly higher than those in the south (ignoring extremely large values in the south which are due to poor data density). Wind variability is higher in the north, but there are also heavy concentrations of VOS observations. On the other hand, wind variability is smaller in the south, but availability of VOS data is also less. The confidence intervals for winds and temperatures are considerably less

Table 6. Mean confidence intervals over the analysis region for monthly analysis periods considering VOS data only.

	U (m s⁻¹)	V (m s⁻¹)	Spd (m s⁻¹)	SST (°C)	AT (°C)	Q (g kg⁻¹)
July	0.59	0.57	0.50	0.22	0.25	0.28
August	0.64	0.63	0.54	0.21	0.25	0.30
September	0.73	0.72	0.59	0.21	0.26	0.33
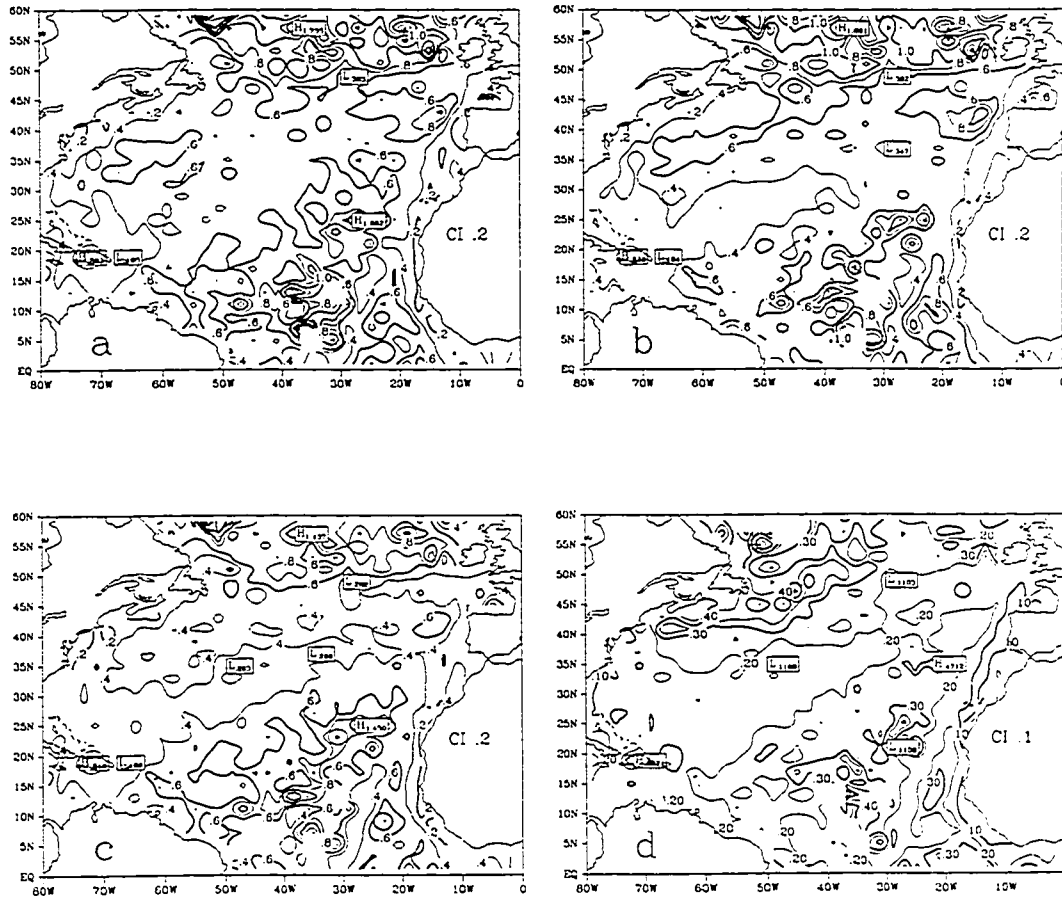
Figure 24. Confidence intervals for the July analysis period using VOS
number of observations data: a) eastward wind, b) northward
wind, c) wind speed, d) SST, e) AT, and f) Q. Units are as
previously mentioned for these variables. Contour intervals
(CI) are as listed. Data void regions indicate where no VOS data
were available.
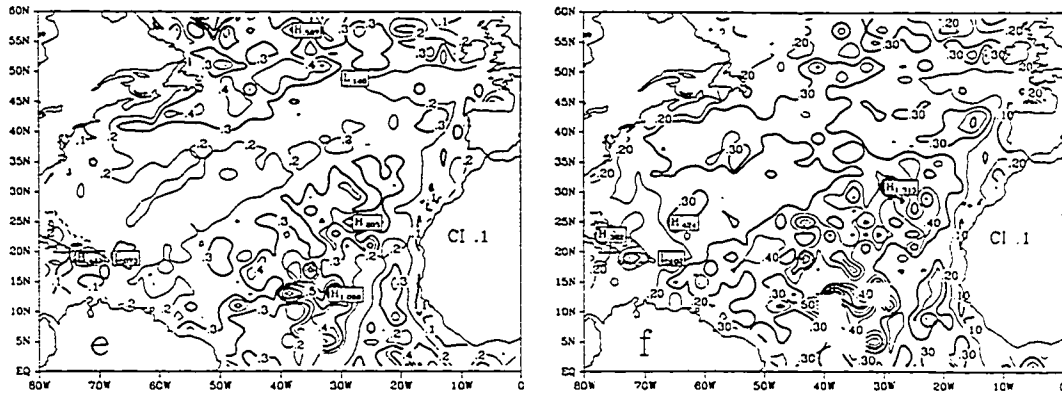
Figure 24.   (Continued).

than the generally accepted accuracies of 1-2 m s^{-1} and 0.5 - 1°C respectively (see Wilkerson and Earle (1990)) indicating the sampling errors for these variables is probably less important than other errors. Humidity confidence intervals are fairly uniform, (about 0.3 g kg^{-1}), except near coastal regions (more NOBS). The increased variability in the north is balanced by increased availability of observations. Note that even though the confidence intervals are fairly consistent over most of the Atlantic, the mean values for the months in question generally decrease to the north making the confidence intervals more significant there, i.e. less accurate.

Confidence intervals for the remotely sensed data, Fig. 25, are more suspect on account of the remotely sensed data possibly breaking the statistical assumptions one must make in computing these characteristics. These data are more uniformly distributed over the Atlantic region, but there are a few locations where the VOS observations outnumber the SEASAT data. The largest improvement over VOS confidence intervals is in the tropics where the remotely sensed data availability reduces the confidence intervals to less than those in the north because of the naturally reduced variability encountered in the tropics. SST from SMMR has very low confidence intervals overall, but north of 30°N and west of 30°W, the VOS SST have less sampling errors due to higher availability of VOS observations. SMMR SST data in this area likely are reduced in number due to rain/fog. SMMR wind speed confidence intervals have a small range between 0.2 and 0.4 m s^{-1}. Basin wide they are one half of VOS confidence limits.
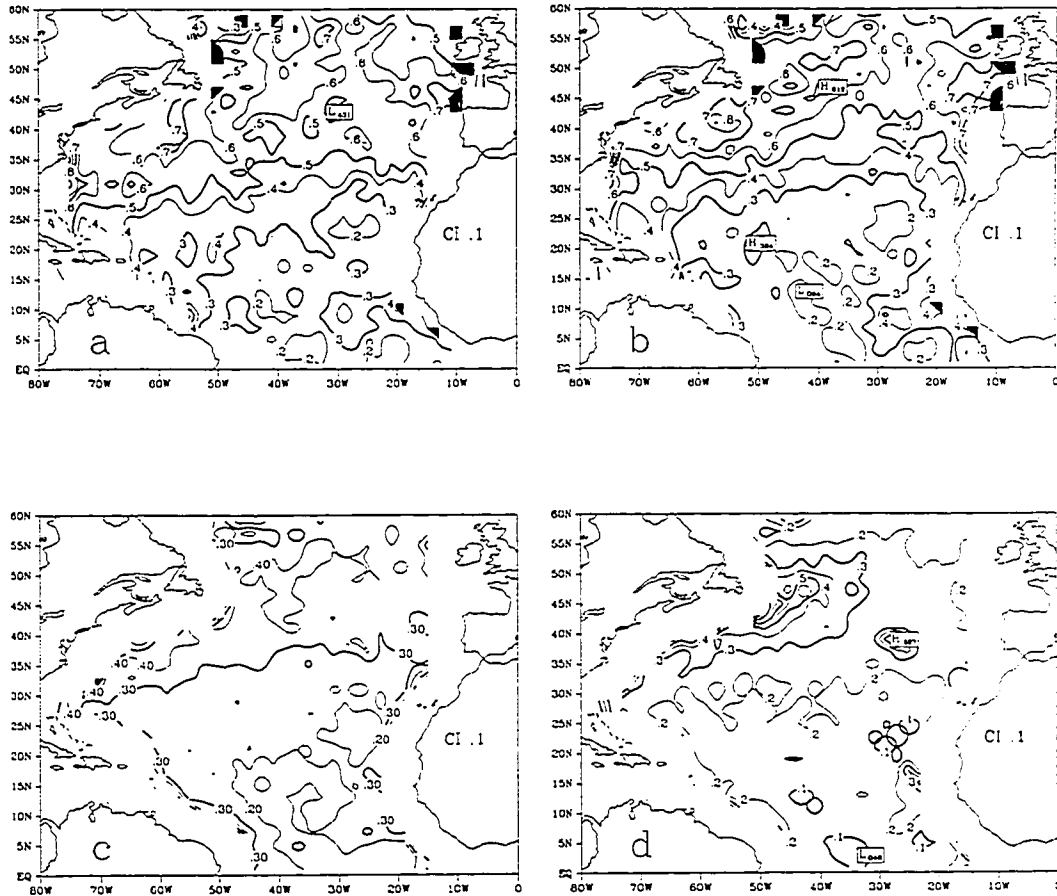
Figure 25. Confidence intervals for the July analysis period using the remotely sensed number of observations data for: a) eastward wind (SASS), b) northward wind (SASS), c) wind speed (SMMR), and d) SST (SMMR). Units are as previously mentioned for these variables. Contour intervals (CI) are as listed. Data void regions indicate where no remotely sensed data were available.

Confidence intervals were also calculated for the fluxes for each analysis month. Since the fluxes are a derived quantity, the same sampling theorem could not be used. Instead, a Monte Carlo scheme was used. The monthly wind, temperature, and humidity resultant values $\pm$ some randomly chosen value in the range of previously calculated confidence intervals considering VOS observations were inserted into the bulk formula. All other parameters in the bulk formula such as density, C_p, and L were held constant introducing minimal error into the calculation. The fluxes were calculated many times using this bulk formula, thus the effects of both the mean values of winds, temperatures, and humidity as well as the confidence intervals of those mean values were included in the confidence limit for each resultant flux field (note; since a confidence interval for Qs was not available, the confidence interval for Q was used). For each grid box in the monthly results, the Monte Carlo experiment was repeated 100 times. For this repeated flux calculation, the flux confidence interval was taken to be two times the standard deviation of the 100 flux values. According to standard statistical norms, this would account for nearly 95% of that flux distribution.

Flux confidence intervals, Fig. 26, follow much the same pattern as the confidence intervals of the wind and temperatures; minimum along the coastal regions and in the mid-Atlantic, but higher in the north and south. The most accurate stresses occur where the NOBS are maximum and the stresses are smallest, 20-40°N, across most of the Atlantic. The confidence interval in this area is about 10% of the resulting stress; north and south of this band, the error is roughly 25% of the resultant stress values, or about .01 N m^{-2}. Confidence intervals for H, ~ 2-4 W m^{-2}, are frequently larger than

Figure 26. Confidence intervals calculated for the July fluxes using the Monte Carlo experiment with VOS number of observations as described in the text: a) Tx, b) Ty, c) H, and d) E. Units are as previously mentioned for these variables. Contour intervals (CI) are as listed. Data void regions indicate where no VOS data were available.

the magnitude of H, particularly in the north. This makes the sign of H very suspect. In the south, these confidence intervals are not as large because of the smaller variabilities of the winds, temperatures, and humidity. The confidence intervals for E are in the range of 10-12 W m^{-2} north of 35°N, but in the south, they are double those in the north - because there are so few observations. Note that in the vicinity of the Gulf Stream and North Atlantic current, E has maximum variability, but the confidence intervals are not significantly higher even though the variability of humidity is maximum. The natural variability for wind, temperatures, and humidity are all smaller in the tropics than in the north, thus better estimates of the fluxes could be calculated there if VOS were uniformly distributed over the Atlantic.

Flux errors decrease from July to August, but increase again in September, Table 7. In contrast, the confidence intervals for the component fields increased in time. Confidence intervals for Ty are smaller than those for Tx due to the smaller magnitudes of Ty variability as previously discussed. The stress confidence intervals are both well below the implied accuracy of the results as well as the variability of the stress during the analysis period indicating the sampling errors are small in relation to other types of errors. On the other hand, H and E confidence intervals are relatively larger in the same comparisons. This is not unexpected since the heat fluxes involve the difference of two variables, thus a small random error on the two variables will result in a wider range of these flux values.

Adding SASS U and V, SMMR wind speed, and SMMR SST observations to the VOS observations increases the available numbers of observations, hence decreases the flux confidence intervals (increases the

Table 7.   Mean flux confidence intervals for each analysis month considering only the VOS data reports.

	Tx (N m⁻²)	Ty (N m⁻²)	H (W m⁻²)	E (W m⁻²)
July	.0067	.0055	2.5	11.8
August	.0040	.0034	2.3	11.6
September	.0092	.0078	3.0	15.1

accuracy), Fig. 27. For stress, the additional data are especially effective at reducing the confidence interval in the tropical Atlantic as there were previously few observations in that region. Coastal regions did not improve as no SASS data were available. Reductions ranged from one third to one half on average - this stress confidence interval is now ~ 10% of the mean stress values - basin wide. For H and E, the additional temperature information was not so plentiful given the coarse resolution of SMMR SST. Combined with the additional wind speed data, confidence intervals for H decreased typically by less than 1 W m^{-2}. The improvement for E was also slight since there were no additional information on Q, about 1 W m^{-2}.

As previously mentioned, these sampling errors are only a portion of the total error budget. To simulate the effects of random errors being a part of the results, the flux Monte Carlo experiment was repeated using the resultant winds, temperatures, and humidity plus random 'errors' of up to 0.5 m s^{-1} for wind components and speed, 0.5°C for temperatures, and 0.5 g kg^{-1} for humidity variables in the bulk formula. Magnitude of the randomness added to the resultant values reflects the typical "error" of monthly VOS means (see Woodruff et. al, 1991).

The error fields then for July, Fig. 28, show more uniformity since the inherent monthly variability as well as the sampling are not a factor in these error estimates. The only factor is the spatial structure of the objective analysis results and the sensitivity of the flux formulation to specific ranges of wind, temperature, and humidity values.

Stress error fields tend to correlate with component magnitudes and the heat flux error fields correlate to some degree with wind speed. In regions of high wind speeds, random errors in temperatures and humidity
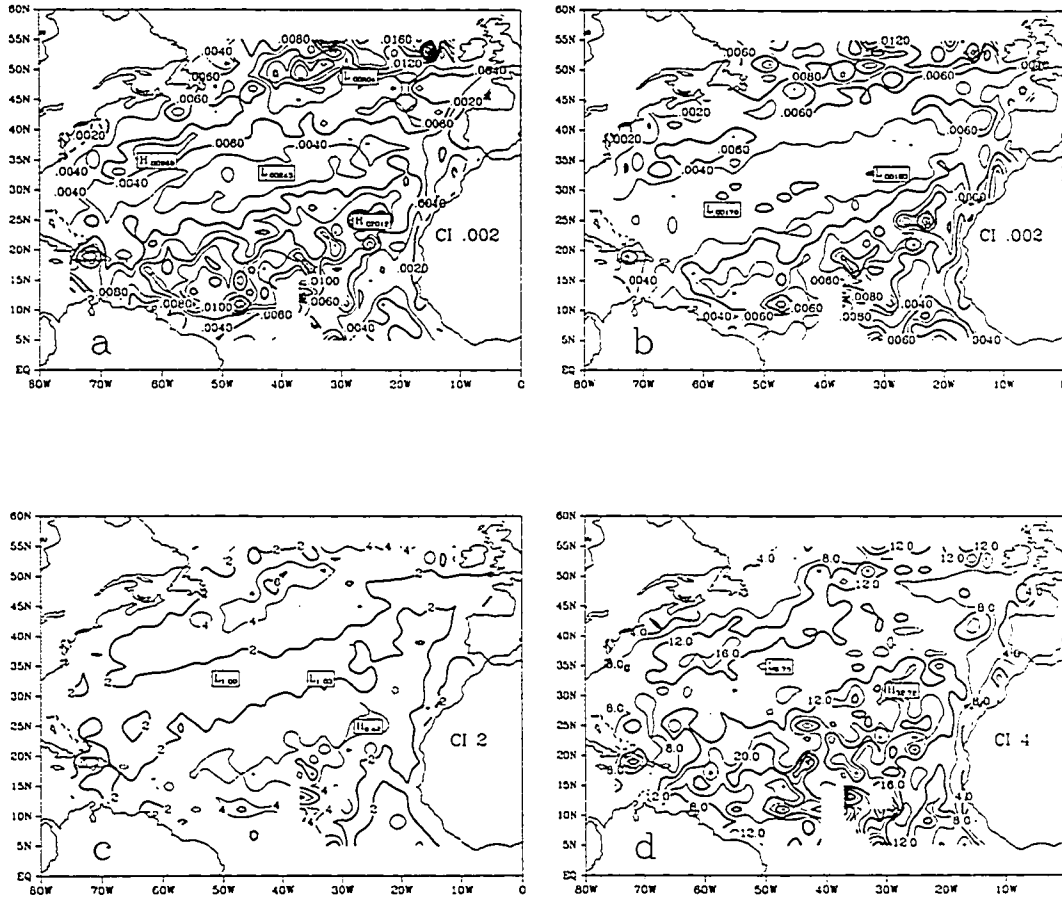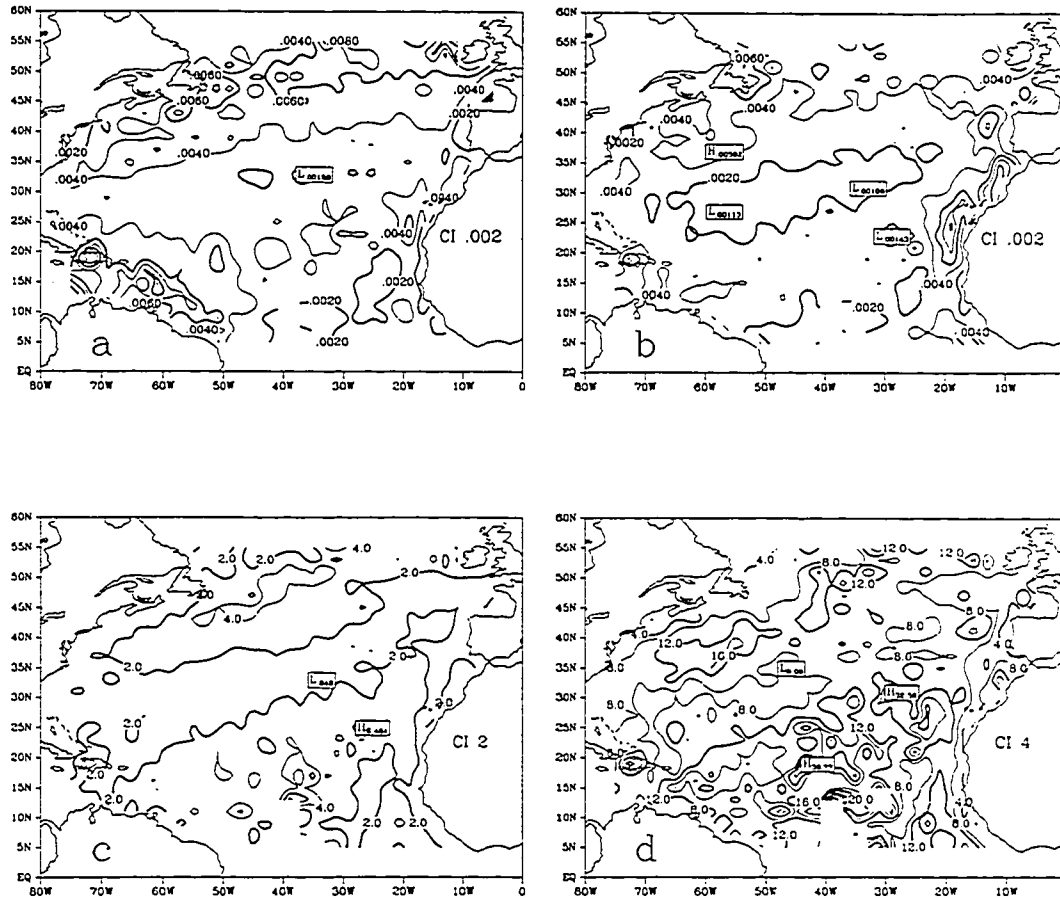
Figure 27.   Confidence intervals calculated for the July fluxes using the Monte Carlo experiment with VOS plus remotely sensed number of observations as described in the text: a) Tx, b) Ty, c) H, and d) E. Units are as previously mentioned for these variables. Contour intervals (CI) are as listed.
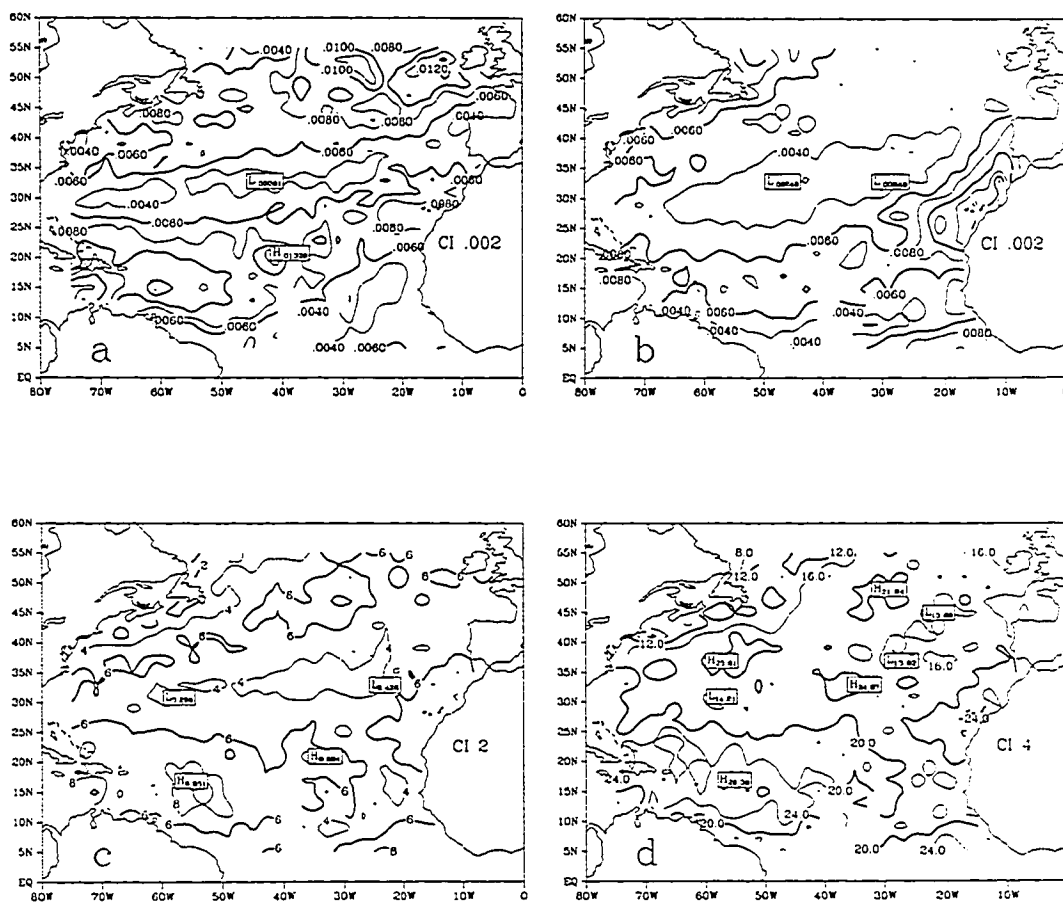
Figure 28.   Confidence intervals calculated for the July fluxes using only additional random errors added to winds, temperatures, and humidity as described in the text: a) Tx, b) Ty, c) H, and d) E. Units are as previously mentioned for these variables. Contour intervals (CI) are as listed.

are amplified in the bulk formula as compared to lower wind speeds. Better accuracy in temperatures and humidity is more beneficial to the heat flux calculation in these regions than improvements in winds. For example, when repeating this Monte Carlo experiment with the random magnitude of the added winds were reduced from 0.5 m s^{-1} to 0.1 m s^{-1}, the stress error fields are halved in magnitude, but the decrease in H and E error fields are only on the order of 5% or less. These conclusions are dependent of course on the particular temperatures, humidity. Thus in locations where the temperature and humidity differences were large, an increase in their accuracy may be less critical.

Compared to the confidence intervals by sampling theory, the random error fields are comparable for stress. Thus even with perfect data, if there are not enough data, the baseline error for these months using VOS data will be on the order of that found in Fig. 28. For H and E, the randomness error is twice as large as the error from under-sampling, underscoring the need for more accurate observations and good analysis schemes to reduce the random errors even further. If SEASAT observations and VOS obs. are considered jointly, random error for the heat fluxes, then the random errors in the data are dominant for heat fluxes and stress because the North Atlantic will be sufficiently sampled.

Confidence intervals for the 5-day periods were not calculated as no good estimate of the population variability for 5-day means could be found. It is noted that there would be obvious reduction in the NOBS available, but likewise, there would also likely be a reduction in variability which might balance this reduction in data.

7. SUMMARY AND CONCLUSIONS

An objective technique which produces regularly spaced fields of winds, temperatures, humidity, wind stress and sensible and latent heat fluxes is developed. It combines in-situ Volunteer Observing Ship (VOS) data and remotely sensed data from SEASAT during July 7 - October 10, 1978 for the north Atlantic. The objective technique is a variational method which reduces a set of several constraints expressing closeness to input data, climatology and some kinematics according to an a priori chosen set of weights. The bulk formula, which include parameterizations for both wet and dry vertical stability and wind speed, are used to calculate and update the fluxes at each iteration in order to force the winds, temperatures, and humidity to comply within the bulk formulation to some degree. Results were computed for the 3 monthly and for the 19 5-day periods.

Results of temperatures, humidity, and fluxes for both the monthly and 5-day cases were comparable to both well sampled VOS locations as well as to other independent data sources. For monthly means, SST and AT results were typically accurate to within 0.5°C, but were suspect near continental boundaries though these boundary locations were often centers of high temperature variability. The monthly results for winds were overall representative of the mean wind conditions, i.e. less than 1 m s⁻¹ RMS difference between VOS means and the results, but were too strong in the north by 1 m s⁻¹. The treatment of the winds as pseudo-stress and the tendency for mean winds to be near zero limited somewhat the resulting

108

correctness of the wind component results in areas of highly variable winds, particularly for the monthly results. The 5-day results correlated well to independent OWS data (for both analysis results using in-situ data at the independent OWS data site, and without), but correlation of the temperatures and hence H were less (~0.8). For most of the Atlantic, the 5-day results of winds, temperatures, and humidity correlated well to VOS means, but in the southeast where there were relatively few VOS observations, there was a better correlation to the remotely sensed data. RMS difference values indicate that without any in-situ information, the RMS error for the fluxes (wind stress, sensible and latent heat) are 0.02 N m^{-2}, 2-5 W m^{-2}, and 10-25 W m^{-2} respectively. These values are well below uncertainties given previously.

Comparison of the analysis period long-term VOS mean to the mean of all the results indicates the systematic overestimation of the winds and the stress in the north portion of the basin, particularly by the monthly results. Otherwise, the winds were comparable. Temperature means all agreed to within 0.5°C except near Newfoundland, where temperatures are highly variable. Because of this temperature uncertainty, the sign of H is suspect in this area because typical mean values are small. The monthly heat flux results displayed less difference to the VOS means than did the 5-day results, but neither showed significant systematic differences that could be attributed to any specific technique or data deficiency.

Variability of the 5-day results shows the expected high values in the vicinity of the Gulf Stream for the temperatures, humidity, and heat fluxes. SST variability is surprisingly high in the eastern Atlantic indicating the importance of both coastal upwelling along northwest Africa and the return

flow of the North Atlantic current. Variability of humidity follows the mean wind circulation, with maximums in areas where there was advection of dry/wet air into relatively opposite climatological regimes.

From the results, it was determined that the heat fluxes were coupled to and dependent on various parameters. For the north and west Atlantic, H is best correlated to the north-south wind and AT due to advection of cooler and warmer air by the relative position of the high and low pressure systems. In the east, it is primarily the SST and V which is driving H, i.e. wind driven coastal upwelling and North Atlantic current. Similarly, in the north, the (primarily north-south) advection of wet or dry air into the opposite climatological regimes is coupled to changes in E. These variations for both H and E in the north are determined by the position and strength of the anti-cyclonic circulation of the semi-permanent Bermuda High system. In the tropics where this high pressure system is not as influential, the determination of H and E is driven by a combination of factors, although in some places such as the western tropical Atlantic, E is best correlated to zonal advection of dry African air into the region. Moreover, when determining the relationship between SST and the heat fluxes, the SST usually determines E in several regions in the tropics. Lagged correlations between SST and E (E leading by one 5-day period) showed that there were some areas in mid-latitudes, primarily near the N. American coast and in the eastern Atlantic west of Spain, where E was negatively correlated with SST meaning that SST is dependent on E.

An analysis of the errors associated with insufficient sampling of the natural variability in each part of the Atlantic is also presented. Confidence intervals were calculated based on sampling theory which considers both the

natural variability and the number of observations that went into the gridded mean values used as input for the objective analysis. This was done for the VOS data, remotely sensed data, and a combination of these. The sampling errors were surprisingly uniform between the mid-latitudes and the tropics due to the relatively large number of VOS obs balancing the relatively higher variability in the north and the relatively small variability, but poorer sampling in the tropics. Since the remotely sensed observations were uniformly distributed, the sampling error when using this type of data was smaller in the tropics than in the north. Typical sampling errors for wind, temperatures, and humidity were 0.6 m s^{-1}, 0.25°C, and 0.3 g kg^{-1} respectively and are functions of space and time.

Errors attributed to inadequate sampling for the fluxes are calculated using a Monte Carlo scheme whereby the component data (winds, temperatures, and humidity) plus some value in the range of ± their respective confidence intervals is used in the bulk formula repeatedly. The spread of those multiple flux values is deemed to be the sampling error. Using VOS data only, the stress error is a minimum of about 10% of the mean stress values in the mid-Atlantic; in the north and south it approaches 20%. The error in H and E is 2-4 W m^{-2} and 10-15 W m^{-2} respectively. Adding remotely sensed data reduces the stress sampling error by 40%, and H and E by 1 W m^{-2}. The scheme used in this research (and many objective analysis schemes) attempts to reduce these sampling errors by using neighboring grid box information and known correlation structures to bet better estimates of the mean values. The results of the various comparisons tend to verify the errors of H and E are generally about 2-5 and 5-20 W m^{-2} respectively, dependent on the analysis period length. These estimates are below

estimates of random error (but then again some of the accuracy assessment is based on VOS data - itself a non-accurate value). For stress, the errors are about 0.02 N m^{-2}, which is a little higher than estimates of random noise for wind stress.

When considering VOS data only, the sampling errors for stress are generally the same magnitude as those errors contributed by random errors in the mean VOS values. For the heat fluxes, the sampling errors are about half of those attributable to random errors. Heat fluxes are found to be more sensitive to the accuracies of temperatures and humidity than accuracies of winds because of the subtraction operator in the flux formula and the close proximity between the two subtracted values. Even with near perfect winds, uncertainty in H and E due to random errors are on the order of 5 and 18 W m^{-2} respectively. Reducing the random error by obtaining more accurate observations and by using some type of analysis scheme which reduces the random part of the error budget is critical for obtaining reasonable estimates of wind stress and the sensible and latent heat fluxes. The technique used in this research is a step towards that goal.

In the future, ERS-1 ocean surface data much like that available from SEASAT will be available for analysis. It is hoped that this technique will aid in examining this data and will extend our knowledge of the interaction between the upper ocean and atmospheric boundary layer.

8. Appendix

Analyses results for the August 7 - September 7, 1978 and the September 7 - October 7, 1978 cases are shown in Figures 29 - 30. An example of results for a 5-day period, July 7 - July 12, 1978 are shown in Figure 31.
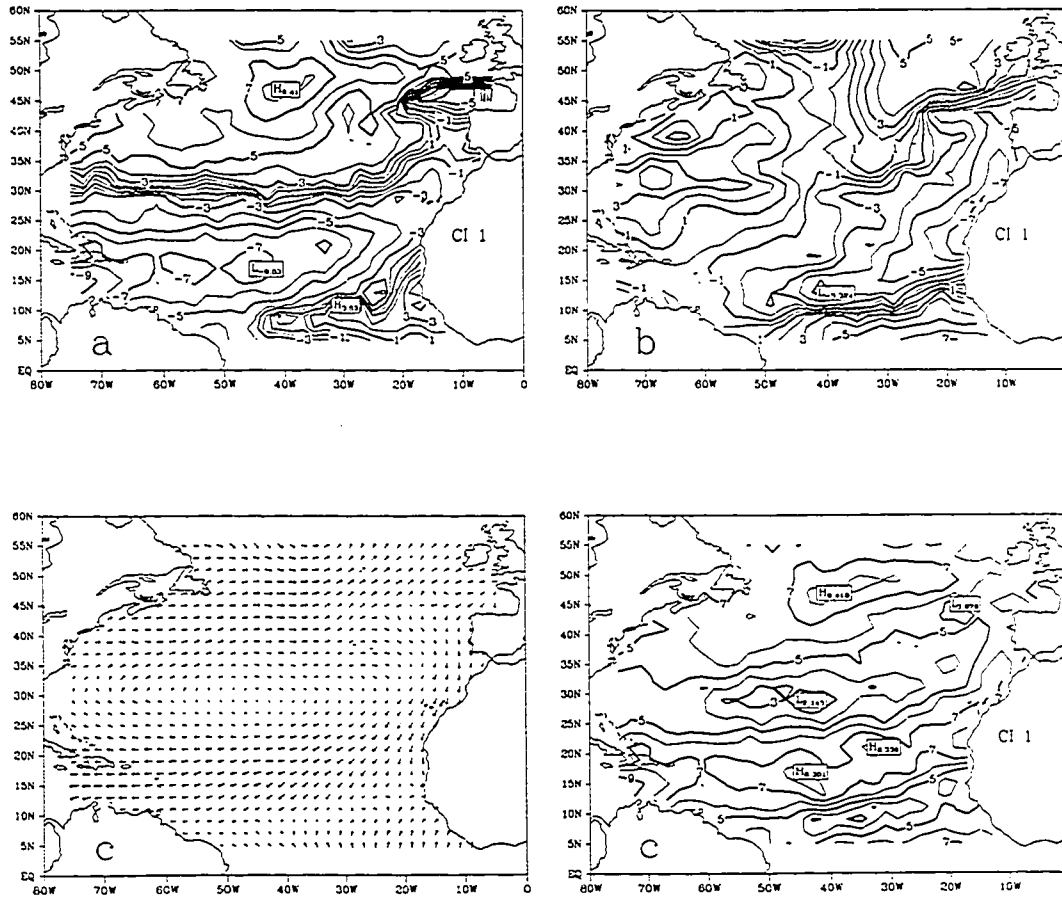
Figure 29. Resultant fields for the case with final weight selection for August 7 - September 7, 1978: a) eastward wind, b) northward wind, c) wind vectors and magnitude (wind speed), d) SST, e) AT, f) Q, g) Qs, h) stress vectors and magnitude, i) stress curl (N m^{-3}), j) H, and k) E. Units are as previously mentioned and contour intervals (CI) are as listed.

Figure 29.   (Continued)

Figure 29.   (Continued)

Figure 29.   (Continued)
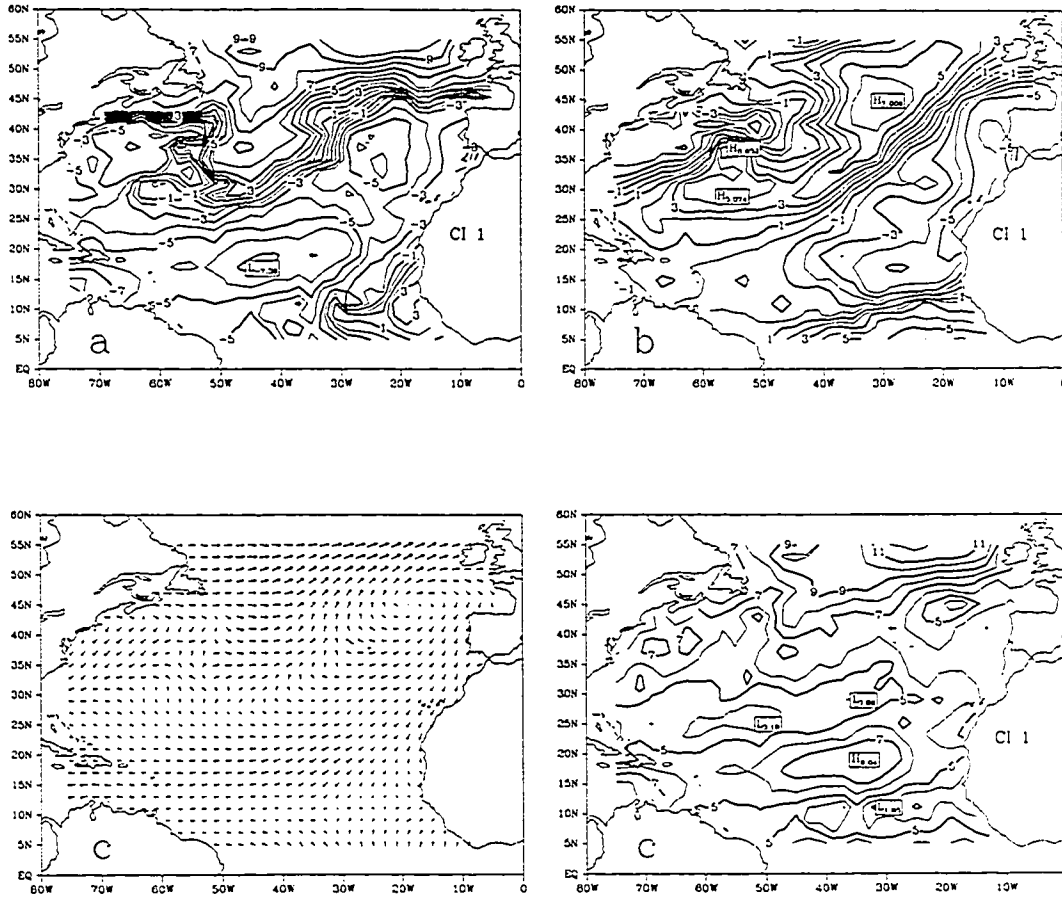
Figure 30. Resultant fields for the case with final weight selection for September 7 - October 7, 1978: a) eastward wind, b) northward wind, c) wind vectors and magnitude (wind speed), d) SST, e) AT, f) Q, g) Qs, h) stress vectors and magnitude, i) stress curl (N m⁻³), j) H, and k) E. Units are as previously mentioned and contour intervals (CI) are as listed.

Figure 30. (Continued)

Scaled by 0.1E-05

Figure 30.   (Continued)

Figure 30.   (Continued)

Figure 31. Resultant fields for the case with final weight selection for the 5-day period July 7 - July 12, 1978: a) eastward wind, b) northward wind, c) wind vectors and magnitude (wind speed), d) SST, e) AT, f) Q, g) Qs, h) stress vectors and magnitude, i) stress curl (N m⁻³), j) H, and k) E. Units are as previously mentioned and contour intervals (CI) are as listed.
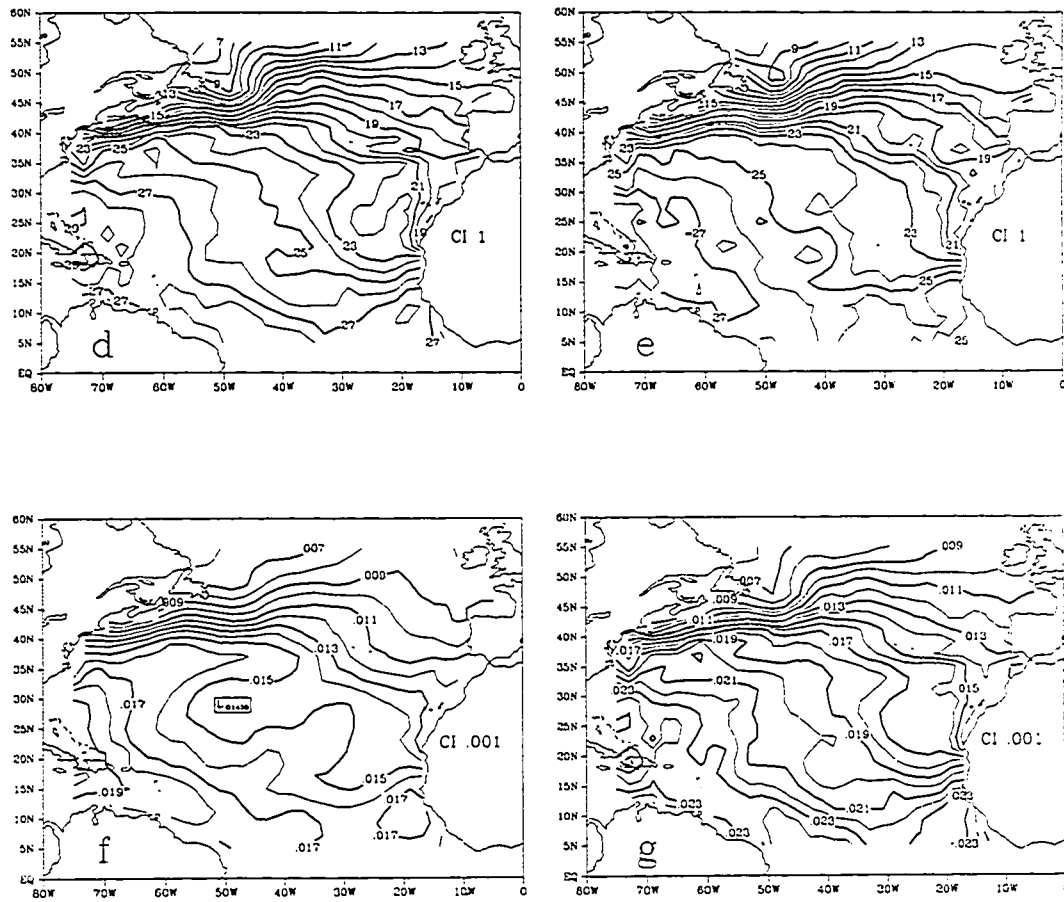
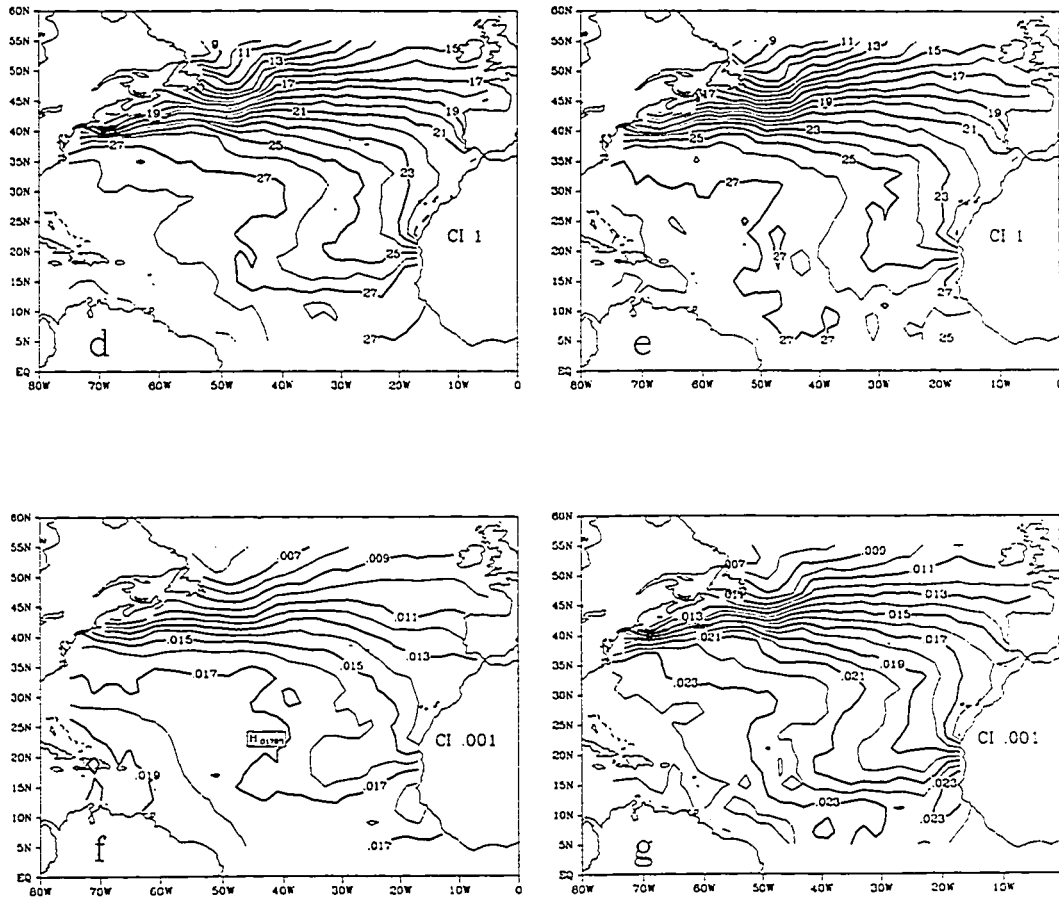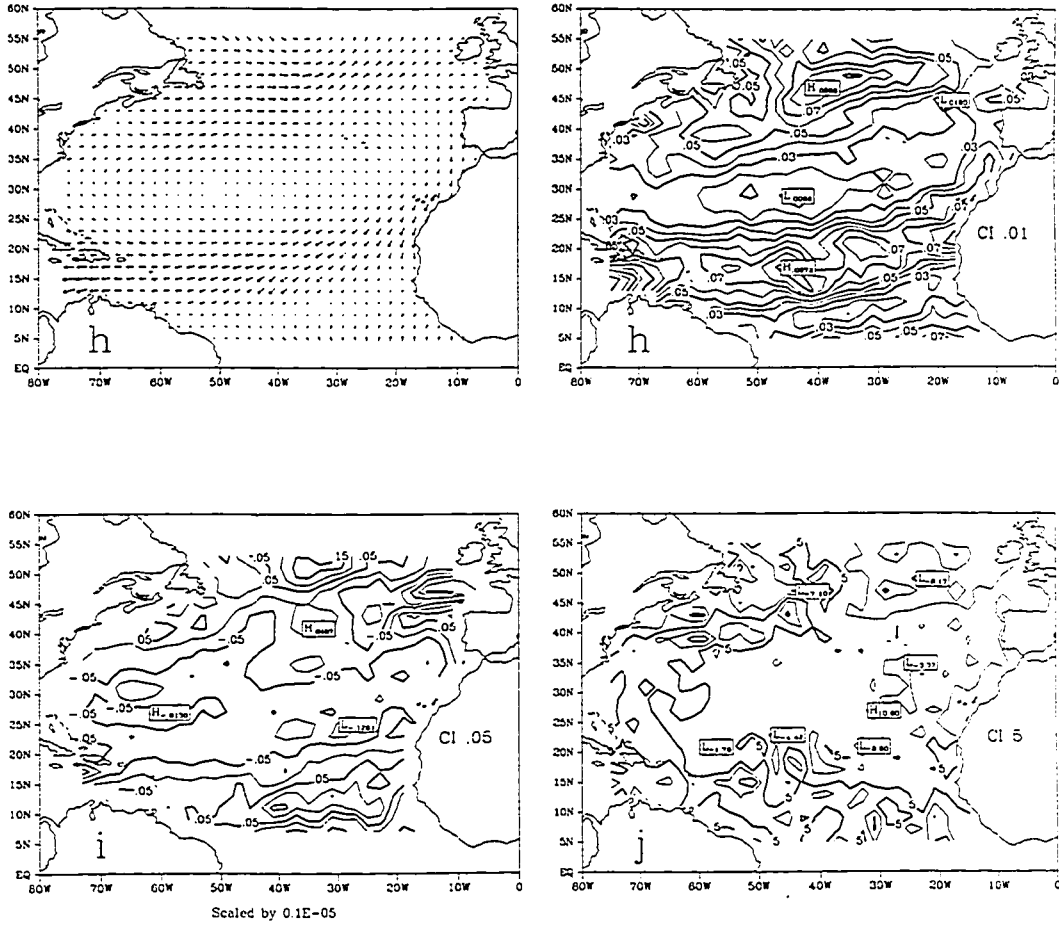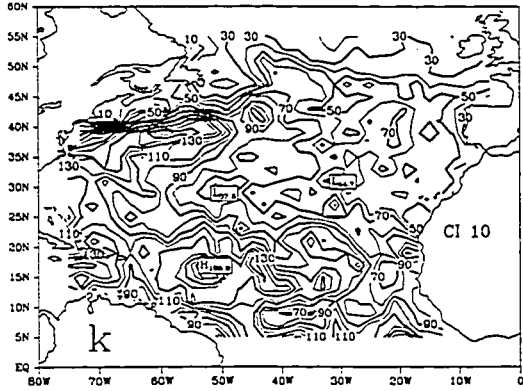Figure 31.   (Continued)
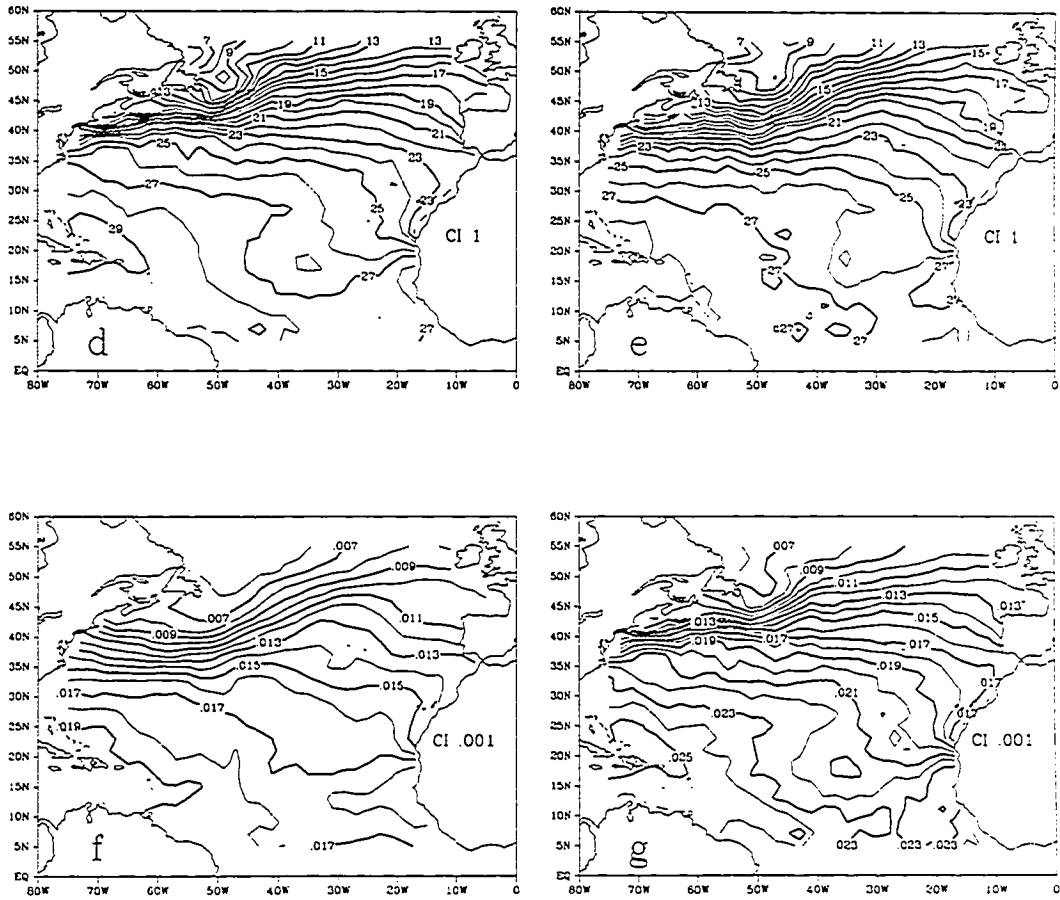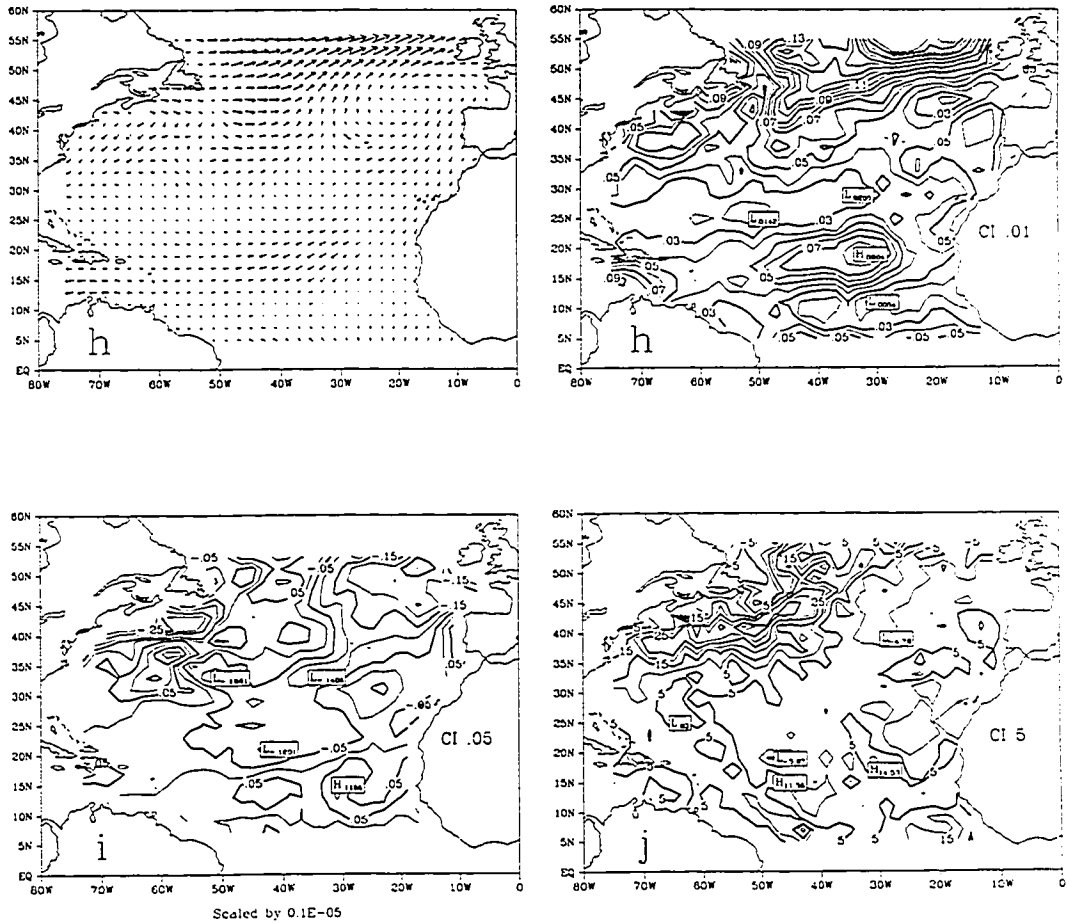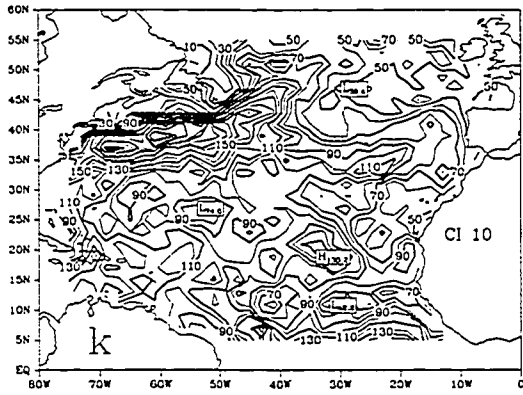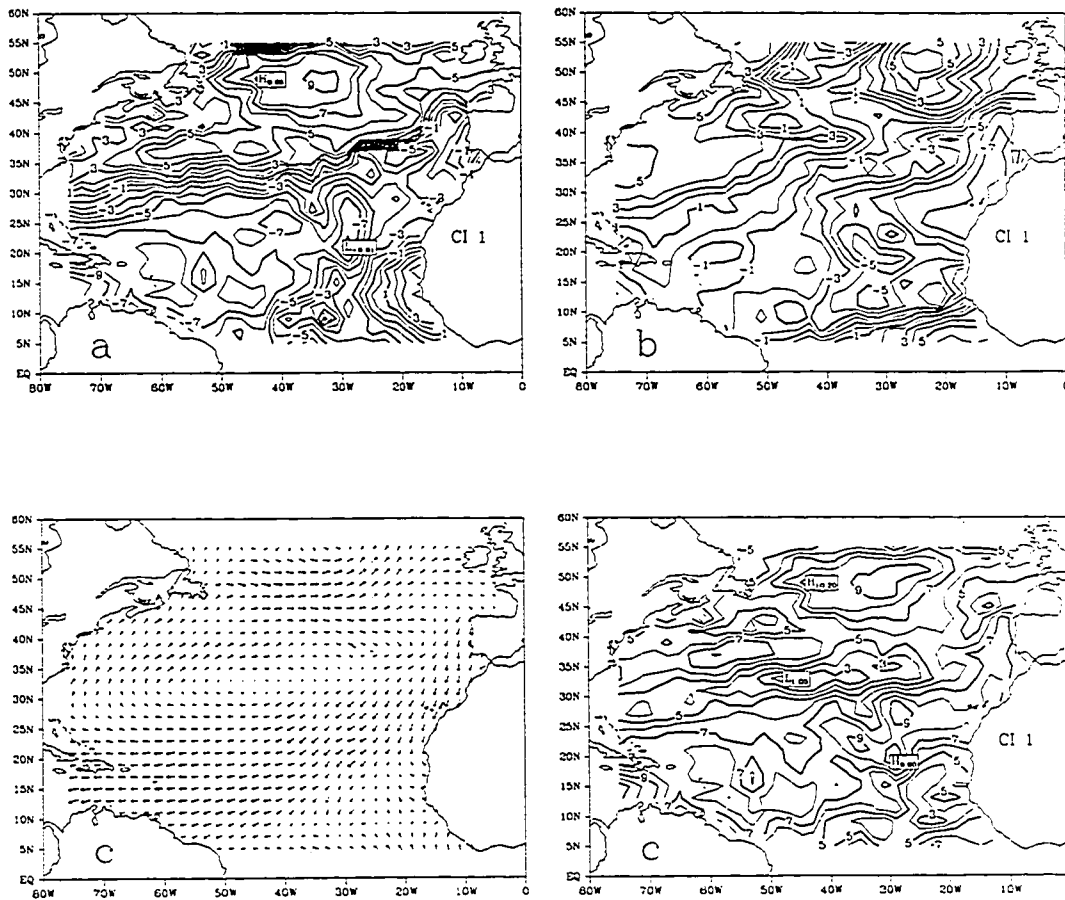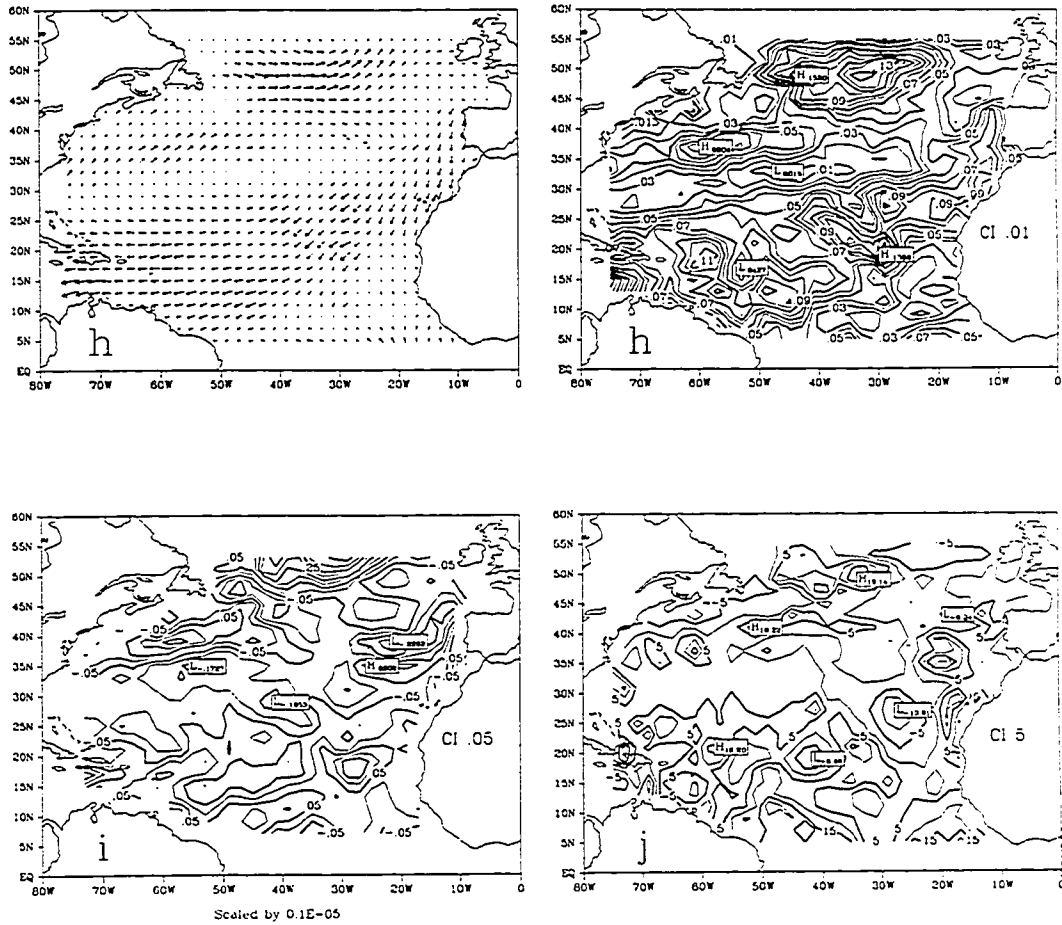
Figure 31. (Continued)
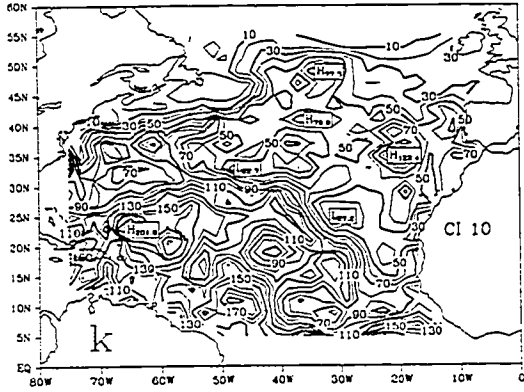
Figure 31.   (Continued)

9. References

Anderson, D., A. Hollingsworth, S. Uppala, and P. Woiceshyn, 1991: A study of the use of scatterometer data in the European Centre for Medium-Range Weather Forecasts operational analysis-forecast model 2. Data impact. *J. Geophys. Res.*, **96**, 2635-2647.

Atlas, R., S. C. Bloom, R. N. Hoffman, J. V. Ardizzone, and G. Brin, 1991: Space-based surface wind vectors to aid understanding of air-sea interactions. *EOS Trans. Amer. Geophys. Soc.*, **72**, 201-208.

Barnier, B., 1986: Investigation of the seasonal variability of the wind stress curl over the North Atlantic ocean by means of EOF analysis. *J. Geophys. Res.*, **91**, 863-868.

Barnier, B., M. Crépon, J. Y. Simonot, and M. Boukthir, 1989: Evaluation des flux de surface du Centre Européen de Prédiction Météorologique à Moyen Terme. Institut de Mecanique de Grenoble. Report No. 87/CNES/1255, 90 pp.

Bean, B. R., and R. F. Reinking, 1978: Marine turbulent boundary layer fluxes of water vapor, sensible heat and momentum during GATE. *Turbulent fluxes through the sea surface , wave dynamics, and prediction*, A. Favre and K. Hasselmann, Eds., Plenum Press, pp. 21-34.

Bernstein, R. L., 1982: SST mapping with Seasat. *J. Geophys. Res.*, **87**, 7865-7872.

Bernstein, R. L., and D. B. Chelton, 1985: Large-scale sea surface temperature variability from satellite and shipboard measurements. *J. Geophys. Res.*, **90**, 11619-11630.

Bernstein, R. L., and J. H. Morris, 1983: Tropical and midlatitude north Pacific sea surface temperature variability from the Seasat SMMR. *J. Geophys. Res.*, **88**, 1877-1891.

Blanc, T. V., 1985: Variation of bulk-derived surface flux, stability, and roughness results due to use of different transfer coefficient schemes. *J. Phys. Oceanogr.*, 15, 650-669.

Bunker, A. F., 1976: Computations of surface energy flux and annual air-sea interaction cycles of the North Atlantic Ocean. *Mon. Wea. Rev.*, 104, 1122-1140.

Busalacchi, A. J., and J. J. O'Brien, 1980: The seasonal variability in a model of the tropical Pacific. *J. Phys. Oceanogr.*, 10, 1929-1951.

Busalacchi, A. J., and J. J. O'Brien, 1981: Interannual variability of the equatorial Pacific. *J. Geophys. Res.*, 86, 10901-10907.

Busalacchi, A. J., K. Takeuchi, and J. J. O'Brien, 1983: Interannual variability of the equatorial Pacific-revisited. *J. Geophys. Res.*, 88, 7551-7562.

Cayan, D. R., 1990: Variability of latent and sensible heat fluxes over the oceans. *PhD. Dissertation*, University of California, San Diego, 199 pp.

Chelton, D. B., K. J. Hussey, and M. E. Parke, 1981: Global satellite measurements of water vapor, wind speed and wave height. *Nature*, 294, 529-532.

Chelton, D. B., and P. J. McCabe, 1985: A review of satellite altimeter measurement of sea surface wind speed: with a proposed new algorithm. *J. Geophys. Res.*, 90, 4707-4720.

Chertock, B., R. Frouin, and R. C. J. Somerville, 1991: Global monitoring of net solar irradiance at the ocean surface: climatological variability and the 1982-1983 El Niño. *J. Climate*, 4, 639-650.

Diaz, H. F., C. S. Ramage, and S. D. Woodruff, 1987: Climatic summaries of ocean weather stations. NOAA/ERL/Univ. of Colorado. 350 pp.

Ehret, L. L., and J. J. O'Brien, 1989: Scales of North Atlantic wind stress curl determined from the Comprehensive Ocean-Atmosphere Data Set. *J. Geophys. Res.*, 94, 831-842.

Esbensen, S. K., and Y. Kushnir, 1981: The heat budget of the global ocean: an atlas based on estimates from surface marine observations. Climate Research Institute, Oregon State University. Report No. 29, 133 pp.

Esbensen, S. K., and R. W. Reynolds, 1981: Estimating monthly averaged air-sea transfers of heat and momentum using the bulk aerodynamic method. *J. Phys. Oceanogr.*, 11, 457-465.

Frankignoul, C., and R. W. Reynolds, 1983: Testing a dynamical model for mid-latitude sea surface temperature anomalies. *J. Phys. Oceanogr.*, 13, 1131-1145.

Geernaert, G. L., 1990: Bulk parameterizations for the wind stress and heat fluxes. *Surface Waves and Fluxes*, G. L. Geernaert and W. J. Plant, Eds., Kluwer Academic Publishers, pp. 91-172.

Goldenberg, S. B., and J. J. O'Brien, 1981: Time and space variability of the tropical Pacific wind stress. *Mon. Weather. Rev.*, 109, 1190-1207.

Han, Y., and S. Lee, 1981: A new analysis of monthly mean wind stress over the global ocean. Department of Atmospheric Sciences, Oregon State University. Report No. 26, 148 pp.

Hanawa, K., and Y. Toba, 1987: Critical examination of estimation methods of long-term mean air-sea heat and momentum transfers. *Ocean-Air Interactions*, 1, 79-93.

Haney, R. L., 1985: Midlatitude sea surface temperature anomalies: a numerical hindcast. *J. Phys. Oceanogr.*, 15, 787-799.

Hantel, M., 1971: Wind stress curl - the forcing function for oceanic motions. *Studies in Physical Oceanography, a tribute to Georg Wust for his 80th birthday*, A. H. Gordon, Ed., Gordon and Breach, pp. 124-136.

Harlan, J., Jr., and J. J. O'Brien, 1986: Assimilation of scatterometer winds into surface pressure fields using a variational method. *J. Geophys. Res.*, 91, 7816-7836.

Hastenrath, S., and P. Lamb, 1977: *Climatic Atlas of the Tropical Atlantic and Eastern Pacific Oceans*. Univ. of Wisconsin Press, 97 pp.

Hoffman, R. N., 1982: SASS wind ambiguity removal by direct minimization. *Mon. Wea. Rev.*, 110, 434-445.

Hoffman, R. N., 1984: SASS wind ambiguity removal by direct minimization, II, use of smoothness and dynamical constraints. *Mon. Wea. Rev.*, 112, 1829-1852.

Hsiung, J., 1986: Mean surface energy fluxes over the global ocean. *J. Geophys. Res,* **91,** 10585-10606.

Inoue, M., and J. J. O'Brien, 1984: A forecasting model for the onset of a major El Niño. *Mon. Wea. Rev.,* **112,** 2326-2337.

Isemer, H. J., and L. Hasse, 1987: *The Bunker Climate Atlas of the North Atlantic Ocean,.* Springer-Verlag, 218 pp.

Kalnay, E., and R. Atlas, 1986: Global analysis of ocean surface wind and wind stress using a general circulation model and Seasat scatterometer winds. *J. Geophys. Res.,* **91,** 2233-2240.

Kalnay, E., R. Balgovind, W. Chao, D. Edelmann, J. Phaendtner, L. Takacs, and K. Takano, 1983: Documentation of the GLAS fourth order general circulation model. Volume I: model documentation. Laboratory for Atmospheric Sciences. Global Modeling and Simulation Branch. Report No. 86064, 381 pp.

Lambert, S. J., and G. J. Boer, 1988: Surface Fluxes and Stresses in General Circulation Models. Canadian Climate Center. Report No. 88-1; CCRN18, 183 pp.

Large, W. G., and J. A. Businger, 1988: A system for remote measurements of the wind stress over the ocean. *J. of Atmos. and Oceanic Tech.,* **5,** 274-285.

Leetma, A., and A. F. Bunker, 1978: Updated charts of the mean annual wind stress, convergences in the Ekman Layers, and Sverdrup transports in the North Atlantic. *J. Mar. Res.,* **36,** 311-322.

Legler, D. M., 1991: Errors of 5-day mean surface wind and temperature conditions due to inadequate sampling. *J. Atmos. Ocean. Technol.,* **8,** 705-712.

Legler, D. M., I. M. Navon, and J. J. O'Brien, 1989: Objective analysis of pseudo-stress over the Indian ocean using a direct-minimization approach. *Mon. Wea. Rev.,* **117,** 709-720.

Legler, D. M., and J. J. O'Brien, 1985: Atlas of Tropical Pacific Wind-Stress Climatology 1971-1980, Florida State University, Tallahassee, Florida, 187 pp.

Legler, D. M., and J. J. O'Brien, 1988: Tropical Pacific wind stress analysis for TOGA. Intergovernmental Oceanographic Commission, Technical Series. Volume 4, 7 pp.

Levitus, S., 1982: Climatological atlas of the world ocean. U.S. Government Printing Office. *NOAA Prof. Pap. 13*, 173 pp.

Levitus, S., 1984: Annual cycle of temperature and heat storage in the world ocean. *J. Phys. Oceanogr.*, 14, 727-746.

Lipes, R. G., 1980: SEASAT scanning multichannel microwave radiometer mini-workshop III report. Jet Propulsion Lab. Publ. 622-224, 55 pp.

Lipes, R. G., 1982: Description of SEASAT radiometer status and results. *J. Geophys. Res.*, 87, 3385-3395.

Lipes, R. G., R. L. Berstein, V. J. Cardone, K. B. Katsaros, E. G. Njoku, A. L. Riley, D. B. Ross, C. T. Swift, and F. J. Wentz, 1979: Seasat scanning multichannel microwave radiometer: Results of the Gulf of Alaska workshop. *Science*, 204, 1415-1417.

Liu, W. T., 1986: Statistical relation between monthly mean precipitable water and surface-level humidity over global oceans. *Mon. Wea. Rev.*, 114, 1591-1602.

Liu, W. T., and C. Gautier, 1990: Thermal forcing on the tropical Pacific from satellite data. *J. Geophys. Res.*, 95, 13209-13217.

Liu, W. T., K. B. Katsaros, and J. A. Businger, 1979: Bulk parameterization of air-sea exchanges of heat and water vapor including the molecular constraints at the interface. *J. Atmos. Sci.*, 36, 1722-1735.

Liu, W. T., and P. P. Niiler, 1984: Determination of monthly mean humidity in the atmospheric surface layer over oceans from satellite data. *J. Phys. Oceanogr.*, 14, 1451-1457.

Mac Veigh, J. P., B. Barnier, and C. Le Provost, 1986: Spectral and eof analysis of four years of ECMWF wind stress curl over the North Atlantic ocean. *J. Geophys. Res.*, 92, 13141-13152.

Navon, I. M., and D. M. Legler, 1987: Conjugate-gradient methods for large-scale minimization in meteorology. *Mon. Wea. Rev.*, 115, 1479-1502.

Njoku, E. G., J. M. Stacey, and F. T. Barath, 1980: The SEASAT scanning multichannel microwave radiometer (SMMR): Instrument description and performance. *IEEE J. Oceanic Eng.*, OE-5, 100-115.

O'Brien, J. J., R. Kirk, L. McGoldrick, J. Witte, R. Atlas, E. Bracalente, O. Brown, R. Haney, D. E. Harrison, D. Honhart Cdr., H. Hurlburt, R. Johnson,

L. Jones, K. Katsaros, R. Lambertson, S. Peteherych, W. Pierson, J. Price, D. Ross, R. Stewart, and P. Woiceshyn, 1982: Scientific opportunities using satellite wind stress measurements over the ocean. Nova University/NYIT Press. 153 pp.

Oberhuber, J. M., 1988: An atlas based on the COADS data set: the budgets of heat, buoyancy and turbulent kinetic energy at the surface of the global ocean, Max-Plank -Institut für Meteorologie, Hamburg, Germany, 100 pp.

Picaut, J., J. Servain, P. Lecomte, M. Séva, S. Lukas, and G. Rougier, 1985: Climatic Atlas of the Tropical Atlantic Wind Stress and Sea Surface Temperature 1964-1979, Université de Bretagne Occidentale-University of Hawaii, Honolulu, Hawaii, 467 pp.

Pierson, W. J., Jr., 1990: Examples of, reasons for, and consequences of the poor quality of wind data for the marine boundary layer: implications for remote sensing. *J. Geophys. Res.*, **95**, 13313-13340.

Rienecker, M. M., and L. L. Ehret, 1988: Wind stress curl variability over the north Pacific from the Comprehensive Ocean-Atmosphere Data Set. *J. Geophys. Res.*, **93**, 5069-5077.

Schluessel, P., W. J. Emery, H. Grassl, and T. Mammen, 1990: On the bulk-skin temperature difference and its impact on satellite remote sensing of sea surface temperature. *J. Geophys. Res.*, **95**, 13341-13356.

Schmitz, W. J., Jr., W. R. Holland, and J. F. Price, 1983: Mid-latitude mesoscale variability. *Rev. Geophys. Space Phy.*, **21**, 1109-1119.

Schopf, P. S., and M. A. Cane, 1983: On equatorial dynamics, mixed layer physics and sea surface temperature. *J. Phys. Oceanogr.*, **13**, 917-935.

Schott, F. A., and C. W. Böning, 1991: The WOCE model in the western equatorial Atlantic: upper layer circulation. *J. Geophys. Res.*, **96**, 6993-7004.

Seguin, W. R., and K. B. Kidwell, 1979: Influence of synoptic scale disturbances on surface fluxes of momentum and latent and sensible heat. *Deep-Sea Res.*, **GATE Supplement I to Vol 26**, 51-64.

Semtner, A. J., and R. M. Chervin, 1989: A simulation of the global ocean circulation with resolved eddies. *J. Geophys. Res.*, **93**, 15502-15522.

Servain, J., 1991: Simple climatic indices for the tropical Atlantic Ocean and some applications. *J. Geophys. Res.*, **96**, 15137-15146.

Shanno, D. F., and K. H. Phua, 1980: Remark on algorithm 500- a variable method subroutine for unconstrained nonlinear minimization. *ACM Tran. Math. Softw.*, **6**, 618-622.

Siegel, A. D., 1977: Oceanic latent and sensible heat flux variability and air-interaction. Colorado Satate University. 31 pp.

Simonot, J. Y., and H. LeTreut, 1987: Surface heat fluxes from a numerical weather prediction system. *Climate Dynamics*, **2**, 11-28.

Slutz, R. J., S. J. Lubker, J. D. Hiscox, S. D. Woodruff, R. L. Jenne, D. H. Joseph, P. M. Steurer, and J. D. Elms, 1985: COADS Comprehensive Ocean-Atmosphere Data Set Release 1. CIRES University of Colorado. 300 pp.

Smith, S. D., 1988: Coefficients for sea surface wind stress, heat flux, and wind profiles as a function of wind speed and temperature. *J. Geophys. Res.*, **93**, 15467-15472.

Thompson, K. R., R. F. Marsden, and D. G. Wright, 1983: Estimation of low-frequency wind stress fluctuations over the open ocean. *J. Phys. Oceanogr.*, **13**, 1077-1083.

Townsend, W. F., 1980: An initial assesment of the performance achieved by the SESAT-1 radar altimeter. *IEEE J. Oceanic Eng.*, **OE-5**, 80-92.

Trenberth, K. E., and J. G. Olson, 1988: An evaluation and intercomparison of global analyses from the National Meteorological Center and the European Centre for Medium Range Weather Forecasts. *Bull. Amer. Meteor. Soc.*, **9**, 1047-1057.

Weare, B. C., and P. T. Strub, 1981: The significance of sampling biases on calculated monthly mean oceanic surface heat fluxes. *Tellus*, **33**, 211-224.

Wentz, F. J., 1986: User's Manual SEASAT Scatterometer Wind Vectors. Remote Sensing Systems. RSS Technical Report 81586, 21 pp.

Wentz, F. J., V. J. Cardone, and L. S. Fedor, 1982: Intercomparison of wind speeds inferred by the SASS, altimeter, and SMMR. *J. Geophys. Res.*, **87**, 3378-3384.

Wentz, F. J., S. Peteherych, and L. A. Thomas, 1984: A model function for ocean radar cross sections at 14.6 GHz. *J. Geophys. Res.*, **89**, 3689-3704.

133

Wilkerson, J. C., and M. D. Earle, 1990: A study of differences between environmental reports by ships in the voluntary observing program and measurements from NOAA buoys. *J. Geophys. Res.*, 95, 3373-3386.

Willebrand, J., 1978: Temporal and spatial scales of the wind field over the North Pacific and North Atlantic. *J. Phys. Oceanogr.*, 8, 1080-1094.

Woodruff, S. D., S. J. Lubker, R. G. Quayle, U. Radok, and E. D. Doggett, 1991: Differences within and among surface marine datasets. NOAA/ERL. 216 pp.

10. Abbreviated Biography

David M. Legler is currently a Research Associate in the Mesoscale Air-Sea Interaction Group at Florida State University. He obtained his B.S. and M.S. in Meteorology in May 1982 and 1984 respectively from Florida State University. Past honors include winner of the 1982 Father James B. Macelwane Award for undergraduate research papers from the American Meteorological Society; NASA Trainee (1982-1984); Science Definition and Working Team for NASA NSCAT, NASA EOS-A STIKSCAT, and ERS-1 Altimeter projects; member of organizing committee for 1988 INO, WOCE, and US-TOGA Workshop on Atmospheric Forcing of Ocean Circulation; NASA Graduate Student Researchers Program (1989-1992); and invited speaker, IGOSS Ocean Products Seminar, April 1991 in Tokyo, Japan.

He has presented papers at major meetings since 1983 and has also published the following papers:

"Empirical Orthogonal Function Analysis of Wind Vectors Over the Tropical Pacific Region", 1983, *Bull. Amer. Meteor. Soc.*, 64, 234-241.

Comments on "Empirical Orthogonal Function-Analysis of Wind Vectors Over the Tropical Pacific Region", 1984, *Bull. Amer. Meteor. Soc.*, 65, 162.

"EOF Analysis of Western Pacific Winds", Tropical Ocean-Atmosphere Newsletter, September, 1983.

"Development and Testing of a Simple Assimilation Technique to Derive Average Wind Fields from Simulated Scatterometer Data" with J. J. O'Brien, 1985, *Monthly Weather Review*, 113, 1791-1800.

"Atlas of Tropical Pacific Wind Stress Climatology, 1971-1980", with J. J. O'Brien, 1985.

"Empirical Orthogonal Function Analyses of Tropical Atlantic Sea Surface Temperature and Wind Stress: 1964-1979", with J. Servain, 1986; *Journal of Geophysical Research-Oceans*, 91, 14181-14191.

"Analysis of Near Real-Time Wind-stress data from the Tropical Pacific", with J. J. O'Brien, Tropical Ocean-Atmosphere Newsletter, February 1986.

"Tropical Wind Stress Analysis for TOGA", with J. J. O'Brien, 1986, TOGA Topics, 2, 3-6.

"Conjugate-Gradient Methods for Large Scale Minimization in Meteorology", with I. M. Navon, 1987, *Monthly Weather Review*, 115, 1479-1502.

"Prediction of the El Niño of 1986-1987" with T. P. Barnett, N. Graham, M. Cane, S. Zebiak, S. Dolan, J. O'Brien, 1987, *Science*, 241, 192-196.

"Verification of a numerical ocean model of the Arabian Sea", with R. C. Simmons, M. E. Luther and J. J. O'Brien, 1988, *Journal of Geophysical Research*, 93, 15437-15454.

"Objective Analysis of pseudo-stress over the Indian Ocean using a direct minimization approach", with I. M. Navon and J. J. O'Brien, 1989, *Monthly Weather Review*, 117, 709-720.

"Tropical Pacific wind stress analysis for TOGA" with J. J. O'Brien, 1988, *IOC Time Series on Ocean Measurements 4*, IOC Tech. Series, 33, UNESCO, 11-17.

"VARIATM - A FORTRAN program for objective analysis of pseudo-stress with large-scale conjugate-gradient minimization" with I. M. Navon, 1991,*Computers and Geosciences*, 17, 1-21.

"Errors of 5-day mean surface wind and temperature conditions due to inadequate sampling", 1991, *Journal of Atmospheric and Oceanic Technology*, 8, 705-712.